STUDYING THE EFFECTS OF COMPOSITION AND SINTERING PARAMETERS ON DIELECTRIC PROPERTIES OF TANTALUM OXIDE DOPED BARIUM TITANATE.

BY

ADNAN MOUSHARRAF
STUDENT NUMBER 0411112011
August 3, 2013

THIS THESIS PAPER IS SUBMITTED TO THE DEPARTMENT OF MATERIALS AND METALLURGICAL ENGINEERING IN PARTIAL FULFILLMENT OF THE REQUIREMENTS FOR THE DEGREE OF MASTER OF SCIENCE IN MATERIALS AND METALLURGICAL ENGINEERING

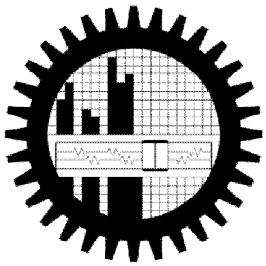

DEPARTMENT OF MATERIALS AND METALLURGICAL ENGINEERING
BANGLADESH UNIVERSITY OF ENGINEERING AND TECHNOLOGY

CANDIDATES' DECLARATION

IT IS DECLARED HEREBY THAT THIS THESIS PAPER OR ANY PART OF IT HAS NOT BEEN SUBMITTED TO ANYWHERE ELSE FOR THE AWARD OF ANY DEGREE

.....

Adnan Mousharraf
M.Sc. Engg., MME, BUET.

The thesis titled "Studying the effects of composition and sintering parameters on dielectric properties of Tantalum Oxide doped Barium Titanate" submitted by Adnan Mousharraf, student no 0411112011 F, session April 2011 has been accepted as satisfactory in partial fulfillment of the requirements for the degree of Master of Science in Materials and Metallurgical Engineering on August, 2011.

Board of Examiners

.....

Chairman
Dr. Md. Fakhrul Islam
Professor, GCE, BUET.

.....

Member (Ex-Officio)
Dr. Md. Mohar Ali
Professor &Head, MME, BUET.

.....

Member
Dr. A. K. M. Bazlur Rashid
Professor, MME, BUET.

.....

Member (External)
Dr. M. Rezwan Khan
Professor & Vice-Chancellor, United International University

Dedicated to

THE THREE SPECIAL PEOPLE WHO MEAN EVERYTHING TO ME

MY PARENTS
&
MY LOVELY WIFE (Peony)

ACKNOWLEDGEMENT

The Department of Materials and Metallurgical Engineering (MME)and Department of Glass and Ceramic Engineering (GCE)has given me the opportunity to work with some of the finest equipment in modern times through this thesis. Despite various limitations the department ensured me consistent access to all these facilities. This not only helped me carry out the research efficiently but also acquainted me with some of the most modern facilities and their functions. Firstly, I pay my utmost gratitude to the Department of Materials and Metallurgical Engineering and secondly, to the Department of Glass and Ceramic Engineering.

I am eternally grateful to my advisor, my research supervisor and my revered mentor Professor Dr. Md. Fakhrul Islam. He provided me with the technical base needed to undertake the research, always pointed me to the right direction and corrected my mistakes. Being a very busy person he spared me his valuable time regarding my work. I thank him from the bottom of my heart for his sincere cooperation, priceless advices and consistent encouragements and motivation. Had he not been in there, the research could not be completed.

I am very thankful to Dr. Hasan(Lecturer of GCE, BUET) for his priceless assistance with FE-SEM. For the same reason I owe special thanks to Mr. Rubbayat (Lecturer, GCE, BUET) and Mr. Mehdi (Lecturer, GCE, BUET) for their assistance with the microscopy. With or without any schedule I bothered them for help and they provided the best of their assistance.

I am also grateful to Mr. Tan, representative of JEOL, Singapore for his support with FE-SEM.

I am also grateful to Dr. Gafur, Senior Scientific Officer, BCSIR and Mr. Rakib, Engineer, BCSIR for their support with the XRD.

I pay my gratitude to Mr. Maksud for helping me with the operation and handling of variousequipment.

I am deeply grateful to Mr. Shahjalal for his kind assistance with the laboratory works.

I express thanks to all my revered teachers and friends for helping me either directly or indirectly with wisdom and motivation.

ABSTRACT

The research aimed at optimizing the composition and sintering parameters of Ta_2O_5 doped $BaTiO_3$ ceramics to enhance its dielectric properties. For conducting the research, $BaTiO_3$ was dopedwith Ta_2O_5 in the range of 0.5-1.5 mole %.

At first, nano sized pure $BaTiO_3$ and Ta_2O_5 were milled, dried and pressed into pellets to prepare the green samples. Then the green samples were fired in a high temperature furnace for densification. Both single and double stage sintering was used for densification of the samples. Thereafter SEM and XRD techniques were used to examine the structure of the sintered samples with particular focus on the incorporation of Ta^{5+} ions into the $BaTiO_3$crystal lattice. During XRD analysis, the X-ray diffraction peaks of (111), (200) and (002) planes of $BaTiO_3$ and (220) plane of Ta_2O_5 were investigated. The SEM analysis was focused on measuring grain size andinvestigating grain size distribution of the sintered samples. Following the SEM analysis, EDX analysis was conducted for elemental analysis and to understand the diffusion process of Ta^{5+} in the $BaTiO_3$crystallattice. Finally, dielectric properties of the samples were measured using an impedance analyzer. Finally, a correlation was established between the dielectric properties of the sintered samples and their microstructure.

From the research, it can be concluded that single stage sintering in the range of 1250^0C to 1300^0C for 2hrs proved insufficient for diffusion of Ta^{5+} ion into the lattice. As a result, $Ta2O_5$ gave strong pinning effect and resulted in poor dielectric properties of doped $BaTiO_3$ ceramics. However, double stage sintering proved to be effective for diffusion of Ta^{5+} ion into the latticeand enhancing the dielectric properties of Ta_2O_5 doped $BaTiO_3$ ceramics. The best room temperature dielectric constant of 22,000-23,000 was obtained for 1.5 mole% Ta_2O_5 doped $BaTiO_3$ sintered at 1310^0C for zero hours and 1280^0C for six hours. Such high dielectric constant was achieved due to the combination of high %theoretical density and optimum grain size at this sintering condition.At a temperature range of 30^0 to 60^0C, this combination of composition and sintering parameters yielded dielectric constant of around 21,000.In addition to enhancing dielectric constant, 1.0-1.5 mole % Ta_2O_5 stabilized the cubic phase of $BaTiO_3$. However, at certain sintering condition, even 0.5mole% Ta_2O_5 stabilized the cubic phase of $BaTiO_3$.

CHAPTER 1
INTRODUCTION

1.1 Scope of Barium Titanate based materials

Barium titanate ($BaTiO_3$) has been of practical interest in the field of electronic materials for more than 60 years because of its attractive properties.Firstly, it is chemically and mechanically very stable. Secondly, it exhibits ferroelectric properties at and above room temperature, and finally because it can be easily prepared and used in the form of ceramic polycrystalline samples. Due to its high dielectric constant and low loss characteristics, barium titanatehas been used in applications, such as capacitors, multilayer capacitors (MLCs)and other energy storage devices [1].

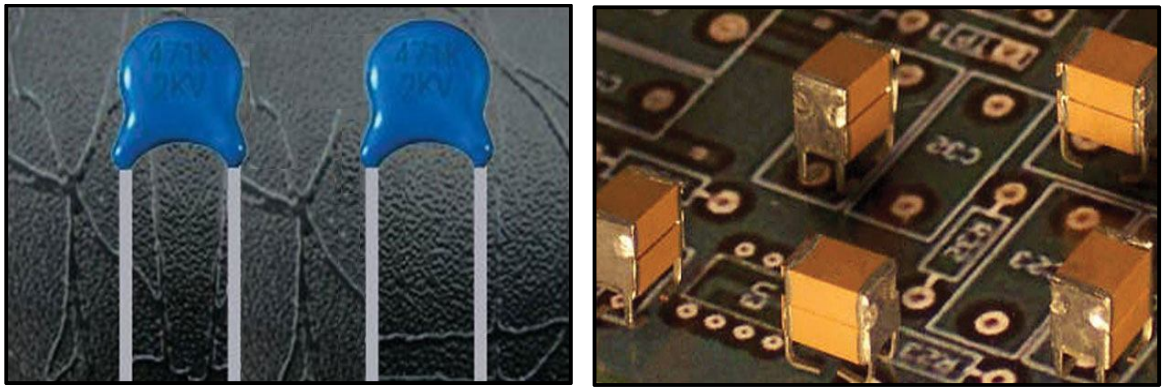

Fig. 1.1: Use of Barium titanate as (a) capacitors, (b) MLCs.

Dopedbarium titanate has found wide application in positive temperature coefficient resistors, ultrasonic transducers, piezoelectric devices, and has become one of the most important ferroelectric ceramics [2].

Fig. 1.2: Use of Barium titanate as (a) transducers, (b) actuators.

1.2 Review of experimental work on pure BariumTitanate

It is true that $BaTiO_3$ has attracted considerable interest for applications in a variety of fields. However, pure $BaTiO_3$ shows very poor dielectric properties. Pure $BaTiO_3$ with coarse grained microstructure shows dielectric constant in the range of 1000-1500. Fine-grained pure $BaTiO_3$ with an average grain size of 1-2µm exhibits dielectric constant in the range of 3500-5000 at room temperature [3-5].Since pure $BaTiO_3$exhibits poor dielectric properties, itsapplication is somewhat limited.

Dielectric properties ofpure $BaTiO_3$dependon many factors such as particle size and morphology; density, grain size and porosity percentage of the sintered microstructure. Many researchers have worked really hard to improve the dielectric properties of pure$BaTiO_3$by applying variousnano powder synthesis techniques, different densification methods and optimizing the microstructure of the densified samples [5-9].

1.2.1 Application of new powder synthesis techniques

Miclea and his colleagues used mechanochemical synthesis techniqueto directly produce fine grained powder of barium titanateinstead of using conventional way to synthesize barium titanate by the solid state reaction between barium carbonate and titanium dioxide which is a simple and lowcost process [5].Then theysintered the synthesized powders at a temperature range of 1200-1450^{0}C. According to them,the samples were fully densifiedbetween 1350 and 1400^{0}C and the density reached maximum values of about 98% of theoretical density(Figure.1.3).

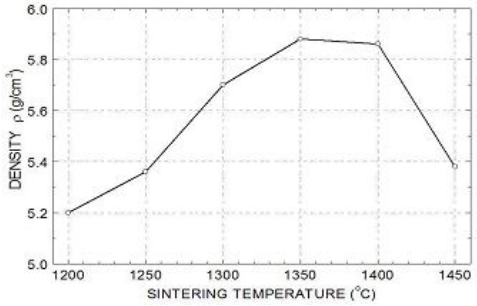

Fig. 1.3: Density vs. sintering temperature for $BaTi0_3$. [5]

From their observation, the grain size increased rather steadily with increasing sintering temperature (Figure.1.4).

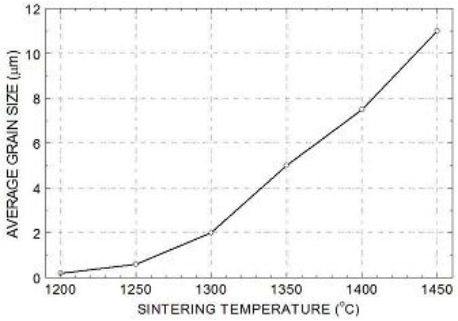

Fig. 1.4: Grain size behavior of $BaTi0_3$ as a function of sintering temperature. [5]

They have also showed the behavior of relative dielectric constant as a function of the grain size. From Figure 1.5it is visible that there is an optimum grain size of 2µm for which the dielectric constant showed a maximum value of 5, 800. For samples with smaller or greater grain size the dielectric constant decreased, this process being more pronounced for coarse grained samples. Thus for samples with grains of 12µm the dielectric constant decreased to 1, 000.

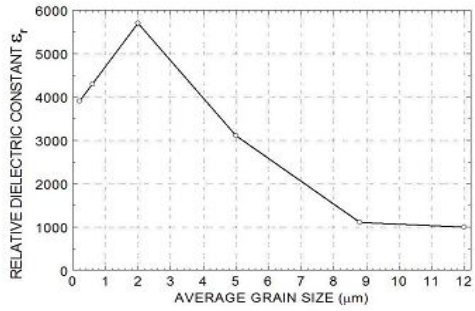

Fig. 1.5: Dielectric constant for $BaTi0_3$ sintered samples with different grain size. [5]

1.2.2 Application of new sintering techniques

Weiling and his colleagues used a new sintering method- spark plasma sintering (SPS) to producehighly dense and fine-grained $BaTi0_3$ ceramics. The specimens attained high density at low temperature and in a very short time. Theyinvestigated the dielectric properties of these superfine ceramics (Figure.1.6).

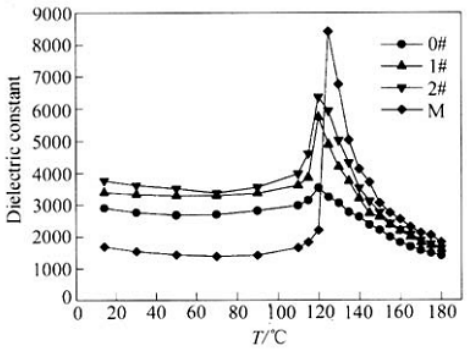

Fig.1.6: Temperature dependence of dielectric constant at various grain size of $BaTi0_3$. [6]

1.2.3 Application of different densification techniques

Arlt and his colleagues used hot isotactic pressing to prepare $BaTi0_3$ceramics withgrain sizes in the range 1-7µm. These samples showed decent dielectric properties (Figure.1.7).

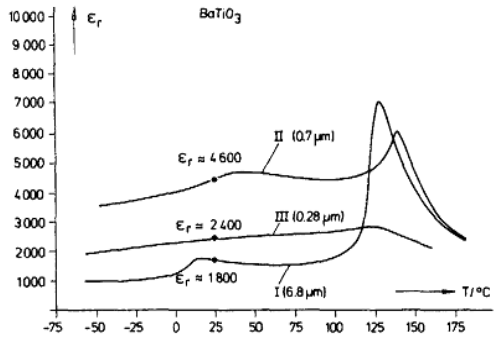

Fig.1.7: Temperature dependence of dielectric constant.[7]

1.3 Review of experimental work on doped Barium Titanate

In one hand, researchers have worked relentlessly to improve dielectric properties of pure $BaTiO_3$, On the other hand, theyhave doped $BaTiO_3$with several dopants like MgO, ZrO_2, Ta_2O_5, Nb_2O_5 etc. to improve dielectric properties of doped $BaTiO_3$[10-14].

1.3.1 Effect of doping with MgO

Magnesium ion from the oxide MgOhas an atomic radius of .086nm and 2+ charge. So, substitution of Ti^{4+} ion by Mg^{2+} ion results in charge imbalance and formation of oxygen vacancies.Since it has low charge density, substitution with Mg^{2+}ion doesn't improve the dielectric properties a great deal. It broadens and depresses the transition peak of lower phase transformation of $BaTiO_3$ and shifts the curie temperature to higher temperature [11]. However, it cannot broaden the transition peak.

Toru Nagai and his colleagues, revealed the existence of orthorhombic phase of $BaTiO_3$solid solution at room temperature with 0.5 mole% or more MgO [11]. Moreover,they showed the effect of MgO doping on the microstructure of $BaTiO_3$by sintering the samples at 1350^0C for 2hrs. According to them, for 1.0 mole% MgO doping, there was a decrease in grain size of sample due to pinning effect. However, at 2mole% MgO doping, the grain size of the sintered sample started to increase as a result of inhomogeneous distribution of MgO in the Matrix, which is clearly visible from Figure 1.8.

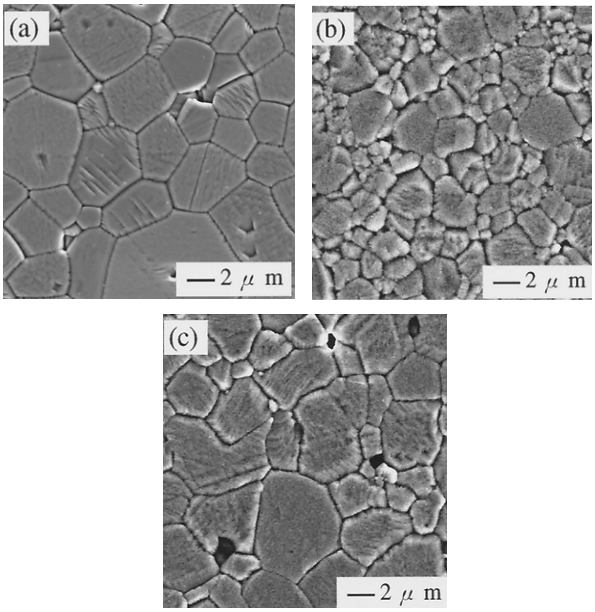

Fig. 1.8: SEM images and EDX mappings of MgO doped $BaTiO_3$ solid solution: (a) SEM for x=0, (b) SEM for x=1, (c) SEM for x=2.[11]

They also showed the effect of MgOdoping on the dielectric properties of $BaTiO_3$. According to them,MgO doped $BaTiO_3$showed dielectric constant in the range of 1000-1500 at room temperature.

With increased doping level, Curie temperature shifted to lower temperature. Moreover, MgO doping suppressed peaks of lower phase transformation (Figure.1.9).

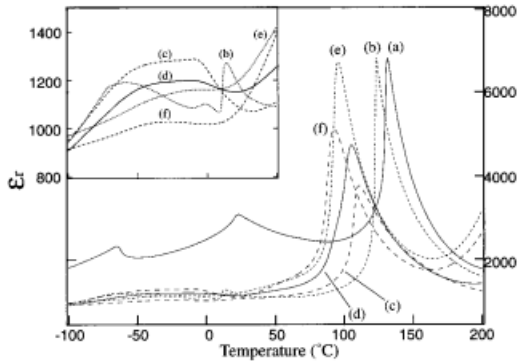

Fig. 1.9 Change in the relative dielectric constant of (1-x/100) BaTiO3– (x/100)MgO with temperature: (a) x=0, (b) x=0.2 (c) x=0.5, (d) x=1, (e) x=2, and (f) x=5 mole%. The inset shows the change at a different range of the dielectric constant.[11]

1.3.2 Effect of doping with ZrO_2

Zirconium ion from the oxide ZrO_2has an atomic radius of .079nm and 4+ charge.Since Ti and Zr ions both have same valence, substitution by Zr^{4+} ion does not produce any charge imbalance.Zr^{4+}ion doesn't improve the dielectric properties a great deal. However, it is known to shift the curie point of barium titanate to lower temperatures; even a shift as low as to room temperature is possible [12].

During sintering it tries to get into barium titanate grains through diffusion where it replaces titanium ion from the crystal. However this diffusion is a limited process since zirconia itself is a very stable compound and only zirconium ion could go through the crystal. Therefore a significant amount of zirconia particles remain at grain boundaries and cause inhibition to the movement of grain boundary of barium titanate during sintering.

According to Armstrong and his colleagues [12], the densities of the sintered $BaTiO_3$ compacts increased with sintering temperature up to 1320°C, where maximum density was achieved for samples containing 0 and 2 wt% ZrO_2(Figure.1.10).

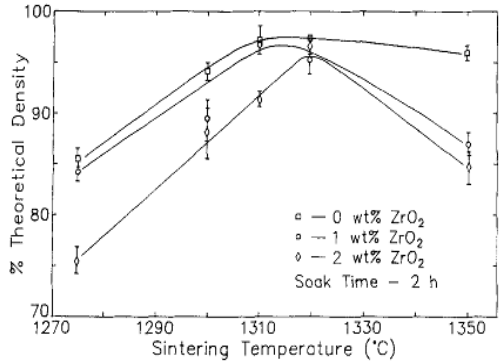

Fig. 1.10: % theoretical density as a function of sintering temperature of $BaTiO_3$ doped with 0 to 2 wt%ZrO_2. [12]

They have also shown the effect of ZrO_2doping onthe microstructure of $BaTiO_3$. With no ZrO_2 added to the $BaTiO_3$, a dense microstructure consisting essentially of large grains (average grain size 32 micron) was observed. With 1.0wt% ZrO_2 addition the fraction of large grains decreased significantly, resulting in a bimodal distribution of large grains in a fine-grain matrix. In contrast, with 2.0 wt% ZrO_2 added, a microstructure consisting entirely of uniform small grains (average GS 0.8 micron) was obtained (Figure.1.11).

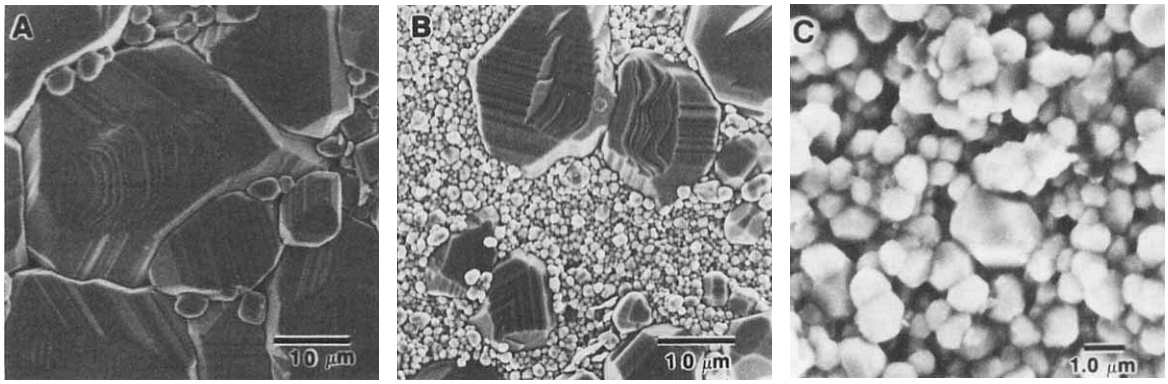

Fig. 1.11: SEM images of ZrO_2 doped $BaTiO_3$ solid solution sintered at 1320^{0}C for 2hrs: (a) 0.0 wt%, (b) 1.0 wt%, (c) 2.0 wt%. [12]

Moreover, they have shown the effect of ZrO_2on the dielectric properties of $BaTiO_3$. The samples sintered at 1320 and 1350°C showed dielectric response and Curie peak characteristics similar to those of the unmodified $BaTiO_3$, over the temperature range 50 to 150°C. However, the Curie temperatures were 8 to 10°C below that of undoped $BaTiO_3$ reflecting some ZrO_2 solubility in the perovskite lattice.The samples sintered at 1300 and 1310°C showed increased permittivity and suppressed Curie peaks, the 1300°C sample displaying an essentially flat permittivity response between 30 and 125°C (Figure.1.12).

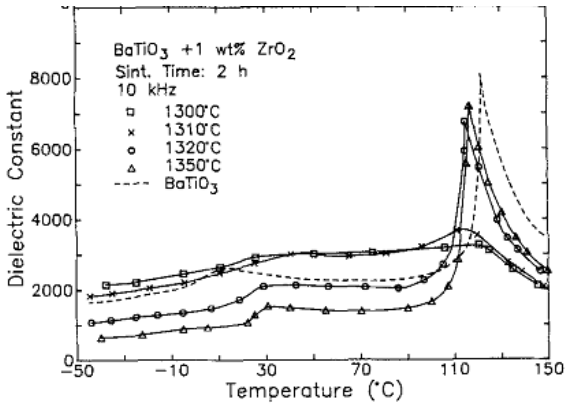

Fig. 1.12: Dielectric constant as a function of temperature for $BaTiO_3$ and 1-wt%-Zr02-modified samples sintered in the range of 1300 to 1350°C.[12]

1.3.3 Effect of doping with Nb_2O_5

Niobium ion from the oxide Nb_2O_5has an atomic radius of .069nm and 5+ charge.Niobium ion is a donor dopantand substitution by Niobium produces a charge imbalance and charge compensation requires that electron, electron holes, or vacancies be produced.This situation can raise the mobility of charged species inside the material and therefore yield high capacitance values.

Nb^{5+} ion improves dielectric properties. Unlike other dopants, Nb_2O_5 is known to shift the curie point of barium titanate to higher temperatures [12-13].

Yuan and his colleagues, showed the effect of Nb_2O_5 doping on the microstructure of $BaTiO_3$by sintering the samples at 1280^0C. SEM micrographs for samples showed thatdoping with 0.3–2.4 mole% Nb_2O_5 resulted in homogeneous fine grained and rather porous microstructure (Figure.1.13a–d). As Nb_2O_5concentration increased further, significant grain growth occurred and the proportion of pores decreased (Figure.1.13e-f). This phenomenon occurred because whenNb_2O_5content was increased to 1.2 mole%, secondary phase began to occur.

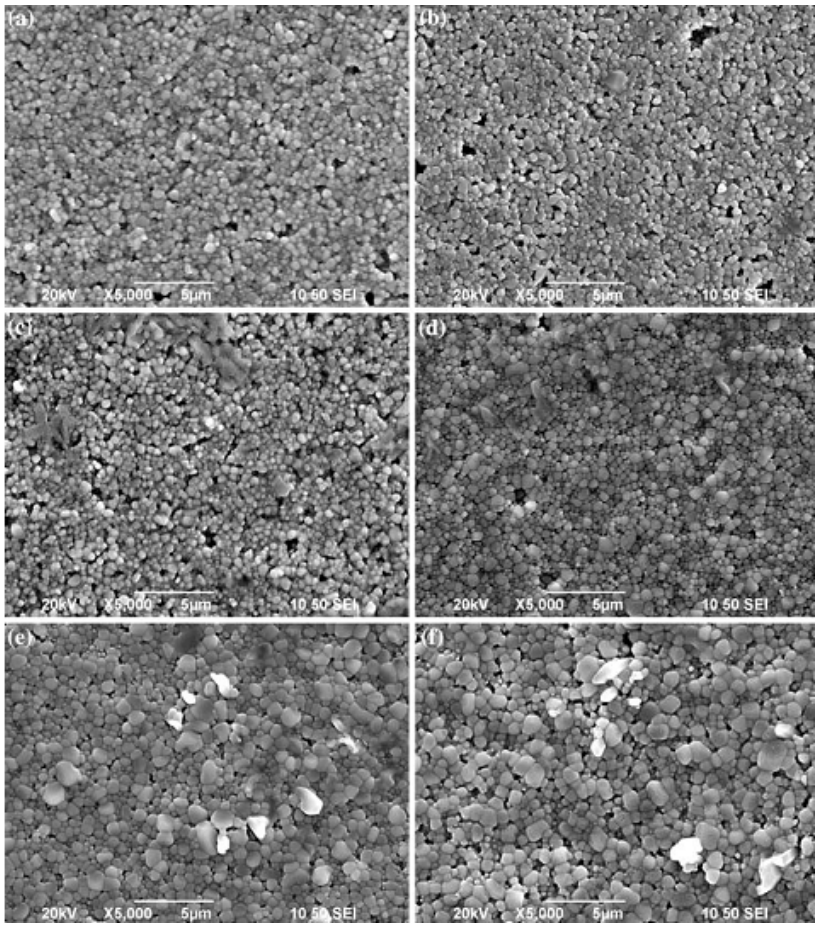

Fig. 1.13: SEM micrographs of Nb_2O_5-doped $BaTiO_3$ ceramics sintered at 1280°C. Nb_2O_5 contents of these samples were a) 0.3, b) 0.6, c) 1.2, d) 2.4, e) 3.6, and f) 4.8 mole%. [12]

With 2.4 mole% Nb_2O_5addition, two types of grains were observed, that is, the matrix composed of fine grains and large secondary phase grains (Figure.1.14).

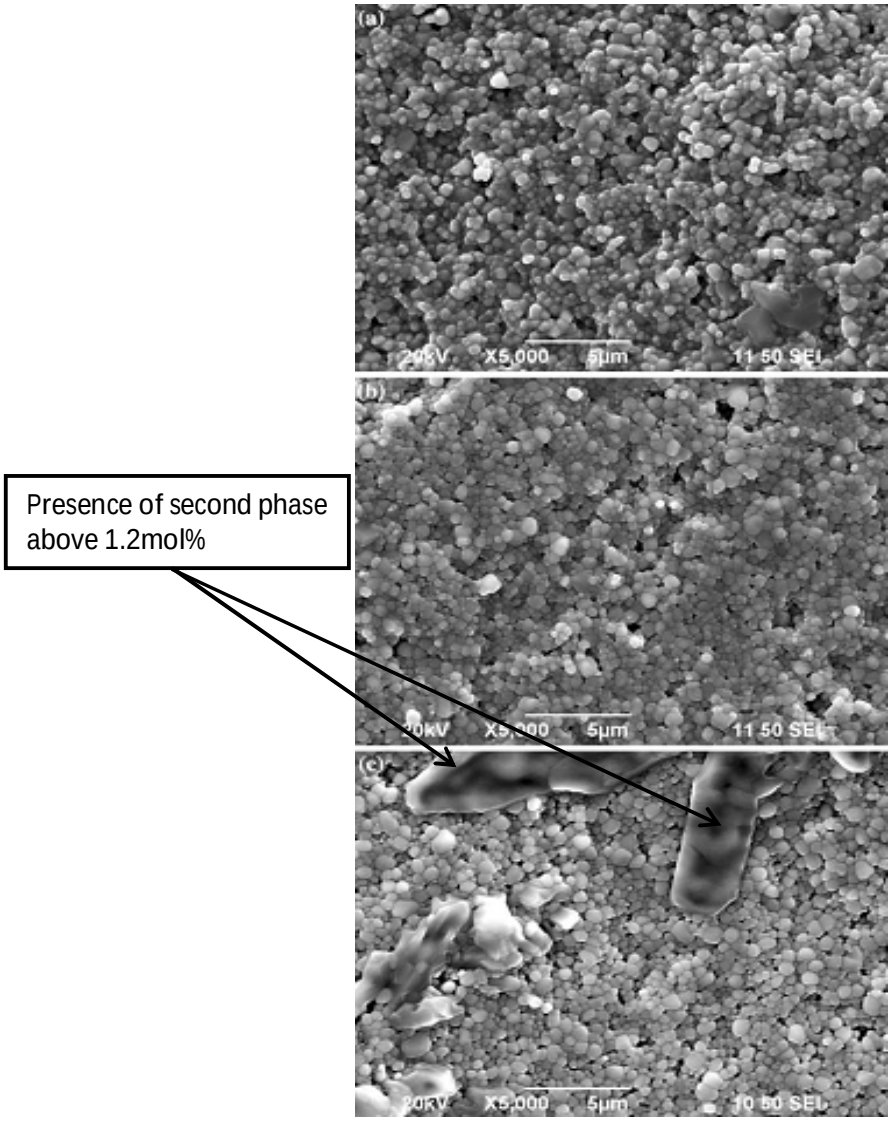

Fig. 1.14:SEM micrographs of Nb_2O_5-doped $BaTiO_3$ ceramics sintered at 1320°C. Nb_2O_5 contents of these samples were a) 0.3, b) 1.2, and c) 2.4 mole%. [12]

Yuan and his colleagues have also shown the effect of Nb_2O_5doping on the dielectric properties of $BaTiO_3$. Theimpact of sintering temperature on the temperature dependence of dielectric constant is slight for the sample doped with 0.3 mole% Nb_2O_5, which suggested that the grain shell is thin when a low concentration $Nb_2O_5$was added. However, as Nb_2O_5 concentration exceeded 1.2 mole%, the dielectric constant peak at TC was greatly depressed, whereas the dielectric constant peak at lower temperature was enhanced with increasing sintering temperature. Especially, for the samples doped with more than 3.6 mole% Nb_2O_5, the Curie peak disappeared by sintering at temperature above 1280^0C, indicating the collapse of core–shell structure and homogeneous distribution of Nb in $BaTiO_3$(Figure.1.15).

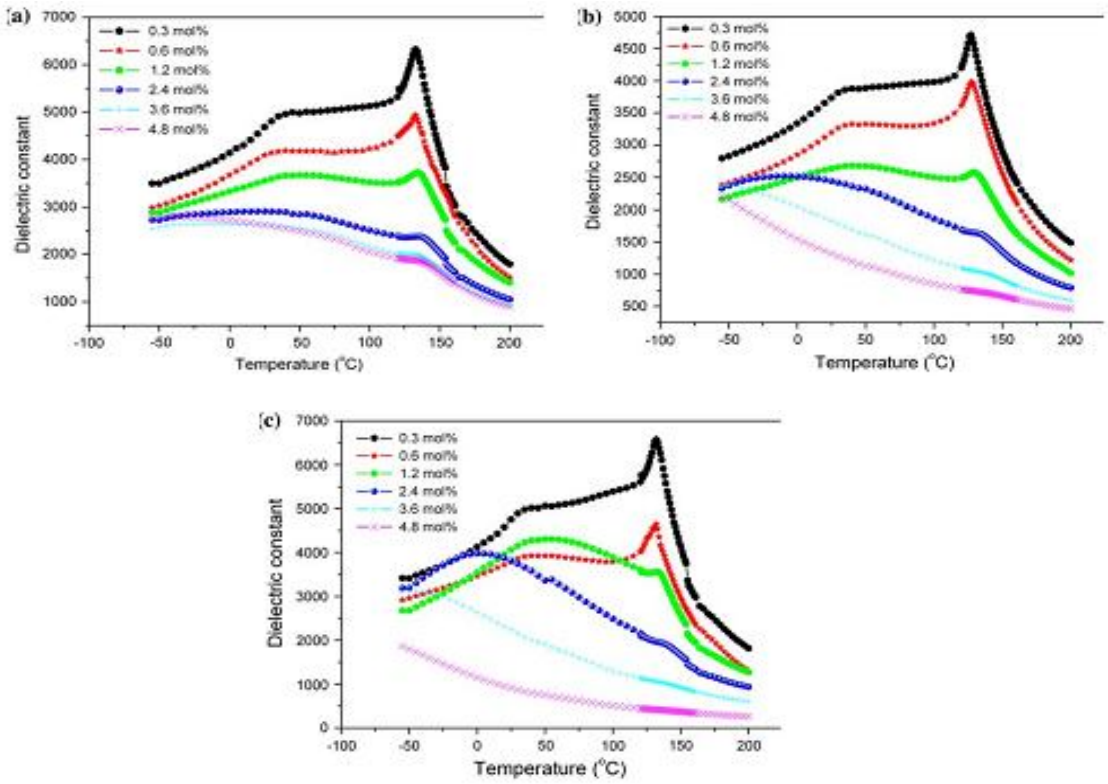

Fig. 1.15: Temperature dependence of dielectric constant for BaTiO3 ceramics with various Nb_2O_5 contents: a) 1240°C, b) 1280°C, and c) 1320°C. [12]

They have also suggested that Nb_2O_5shifts the Curie temperature to high temperature. For a fixed sintering temperature, Curie temperature increases with increasing doping level (Fig.1.16).

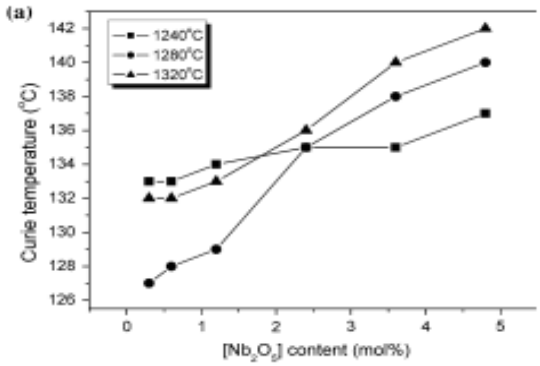

Fig. 1.16: Curie temperature TC as functions of Nb_2O_5 contents for BaTiO3 ceramics sintered at 1240, 1280, and 1320°C, respectively. [12]

1.3.4 Effect of doping with Ta_2O_5

Similar to Niobium, Tantalum is a donor dopant. As Tantalum ion has different valence than that of the barium or titanium ions, substitution by Tantalum also produces a charge imbalance and charge compensation requires that electron, electron holes, or vacancies be produced.

Like Niobium, Tantalum is also known to play strong role as grain growth inhibitor in barium titanate [14-15]. Ta^{5+} at lower concentrations enhances grain growth thereby improving the dielectric properties. On the other hand, they inhibit grain growth and alter the electrical properties at levels close to or above the dopant solubility in $BaTiO_3$. M. N. Rahman et al. reported that for pentavalentdonarcations, the boundary mobility initially increases with cation concentration but then decreases markedly above a doping threshold of 0·3-0·5 at%[16].

Many researchers have reported that Ta-doping has an effect on the Curie temperature of $BaTiO_3$. It tends to shift the Curie peak to lower temperature.

According to Kim and his colleagues, Ta^{5+}doped $BaTiO_3$solid solution show increasing grain size with increasing sintering temperature. The sample sintered at 1250°C showed smaller grain size (< 1.0 μm) where as large grain sizes (1.5~3 μm) were observed for the samples sintered at 1300°Cas shown in Figure.1.17.

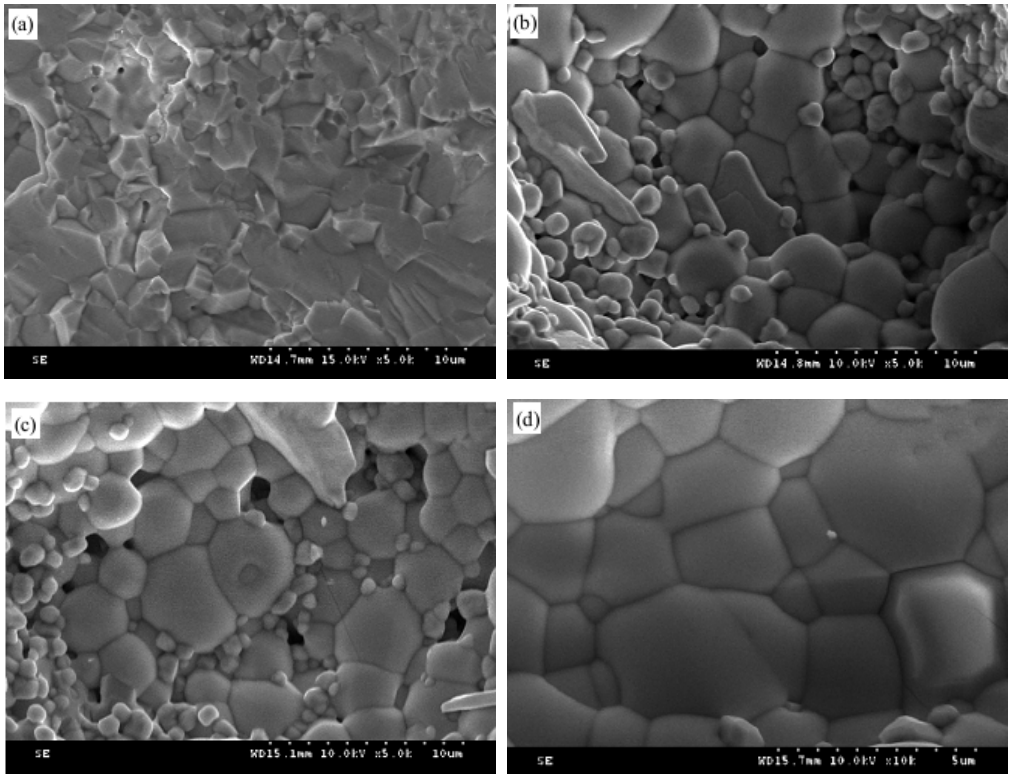

Fig.1.17. SEM micrographs of fracture surfaces at sintered (a) 1250°C, (b) 1270°C, (c) 1285°C,(d) 1300°C of 1.0 mole% Ta^{5+}doped $BaTiO_3$ ceramics.[14]

They have also shown the effect of Ta_2O_5 doping on the dielectric properties of doped $BaTiO_3$solid solution. Since Ta_2O_5 has high charge density, it improves the dielectric properties of doped $BaTiO_3$. For 1.0 mole % doping, dielectric constant as high as 9000 was reached at 10kHz frequency (Figure.1.18).

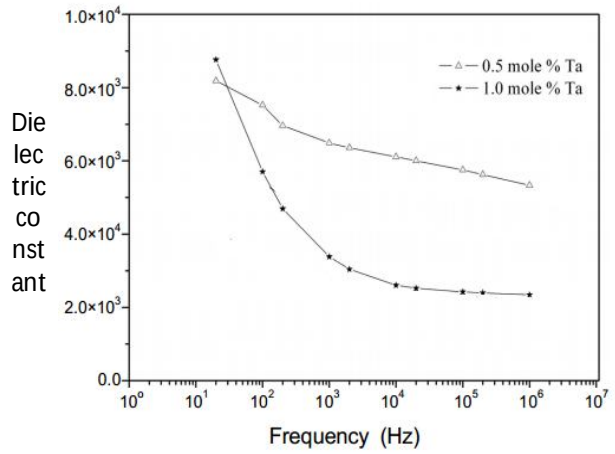

Fig. 1.18: Frequency dependence of dielectric constant. [14]

1.4 Justification for selecting Ta_2O_5 for the current research

Although Tantalum and Niobium both have 5+ charge, but Ta^{5+}ion has some advantages over Nb^{5+}ion. Ta^{5+}ion has higher charge density in comparison to Nb^{5+}ion because the radius of Ta^{5+}ion is smaller (.068nm) than that of Nb^{5+}ion (.069nm). It has been reported that for a particular mole%, Ta-doped samples show better dielectric properties in comparison to Nb-doped samples (Figure.1.19).

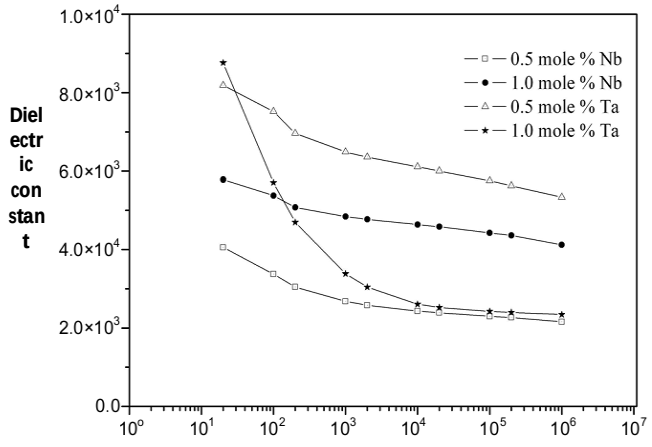

Fig. 1.19: Frequency dependence of dielectric constant. [14]

It has also been reported that Nb5+ ion results in a decreases of dielectric constant due to its non-uniform distribution and segregation in the local parts of the samples[12, 13].

Considering the above two factors, Ta_2O_5 was used as dopant for the current research.

1.5Challenges and targets of this thesis

First of all, the experimental procedure does not follow the conventional calcination-sintering route which has never been done in the department. On this point of view the work imposes entirely a new challenge. In addition the limitation of technical facilities further confines the scope of working. However the work, if done correctly has the potential to yield material with superior dielectric properties than that achieved from a conventional calcination and sintering route. From these respects the research is definitely exciting and worthy of being followed.

As the preparation of the compacts is simple, the biggest challenge is to achieve very fine grain structure with minimum porosity. On this occasion the toughest task is to find the optimum sintering temperature which will bring the desired microstructure. Control of the geometry of samples is another challenge to take over. Since this is attributed entirely on the rate of heating and cooling during sintering, the heating/cooling rate needs to be optimized as well.

Finally the structure property relationships need to be realized. Here a particular composition is related to the microstructure that results upon firing and the associated dielectric properties are correlated with all these variables.

One important thing here is the use of powder which has a size in nanometer range. Such powders possess very high surface energy and consequentially,are more reactive than coarser powders. Hence the sintering temperature needs to be modified accordingly.

CHAPTER 2
LITERATURE REVIEW

2.1 Introduction

There are number of materials that possess electrical conductivity, which means various charge carriers like electrons, ions can pass through it. These are conductors. On the other hand, there are also materials through which these conductors of electricity cannot pass through. These are insulators. There are certain other groups of materials, which in general acts as insulators. However, they can be made to have dipole structures by forming a combination of a couple of conductor plates and the insulator material (nonmetallic) sandwiched in-between. This certain arrangement is capable of storing charges without passing any of carriers through the insulator.

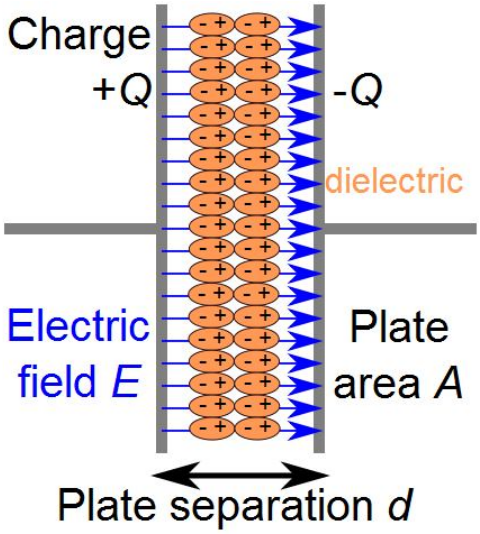

Fig. 2.1: Capacitor Schematic with dielectric[17]

This charge storing capability of the class of insulator materials is known as dielectric properties. The insulator material is called dielectric [17].

Dielectrics in capacitors serve three purposes:

1. to keep the conducting plates from coming in contact, allowing for smaller plate separations and therefore higher capacitances;
2. to increase the effective capacitance by reducing the electric field strength, which means you get the same charge at a lower voltage;
3. and to reduce the possibility of shorting out by sparking (more formally known as dielectric breakdown) during operation at high voltage.

2.2 Dielectrics– A Holistic Approach

Dielectric materials are most widely in relation to the capacitors in an electric circuit [17]. Hence, concept of various dielectric properties, like dielectric constants, dielectric loss factors, dielectric strength etc requires the knowledge of capacitance (the ability of charge storage) of material.

Considering the case of a simple parallel plate capacitors with metal plates of area A and separated by a distance d, and the medium inside being simply vacuum, when a voltage V is applied across the plates, one of them plates will acquire a net charge of +q and other will get a net –q. The charge is directly proportional to the applied voltage V as in-

$q=CV$ *or* $C=\frac{q}{V}$---------- *(1)*

Where Cis the proportionality constant called the capacitance of the capacitor. The SI unit of capacitance is coulombs per volt (C/V) or Farad (F).

The capacitance of a capacitor is a measure of its ability to store electric charge. The more charge stored at the upper and lower plates of the capacitor, the higher is its capacitance.

For parallel plate capacitor, with a vacuum in the space between the plates, the capacitance of the capacitor is –

$C_0 = \frac{A}{d} \epsilon_o$---------- *(2)*

Where, A = area of the plates

D = distance between the plates

ϵ_0 =permittivity of vacuum, constant having value of 8.85×10^{-12} F/m

Now, if a dielectric material fills the space between the plates, the capacitance of the capacitor is increased by a factor *k*, which is called the dielectric constant of the dielectric material. For a parallel plate capacitor with a dielectric between the capacitor plates, capacitance-

$C = \frac{A}{d} \epsilon_0 k$or $C = \frac{A}{d} \epsilon$---------- *(3)*

Where, ϵ= permittivity of the dielectric medium which is greater in magnitude than ϵ_0. The factor *k* is known as relative permittivity or the dielectric constants, which is equal to the ratio of the permittivity of the dielectric medium to that of vacuum. As in-

$k = \epsilon/\epsilon_0$ ---------- *(4)*

Dielectric constant is greater than unity and represents the increase in charge storing capacity by insertion of the dielectric medium between the plates.

It is important to note that the electric field between the capacitor plates is reduced by the presence of the dielectric. Because, the induced surface charges on the dielectric (Figure.2.1) cause an electric field in the opposite direction of the original field in the charged capacitor. These fields tend to cancel each other resulting in a reduction of the original field.

2.3 Polarization

When the atoms or molecules of a dielectric are placed in an external electric field, the nuclei are pushed with the field resulting in an increased positive charge on one side while the electron clouds are pulled against it resulting in an increased negative charge on the other side. This process is known as polarization and a dielectric material in such a state is said to be polarized [17]. There are two principal methods by which a dielectric can be polarized: stretching and rotation.

The interaction of dielectric with the field varies from free space since it contains charge carriers that can be displaced, and charge displacements within the dielectrics can neutralize a part of the applied field.

From equation 1 and 2 the surface charge in vacuum, $\sigma_{vac}$is given as in-

$$\sigma_{vac} = \left[\frac{Q}{A}\right]_{vac} = \epsilon_0 \frac{V}{d} = \epsilon_0 E \quad \text{----------(5)}$$

Where, E = Applied electric field across the plates of the capacitor, V/m.

Similarly, equation 1 and 3 directs to the surface charge on the metal plates in the presence of dielectrics, which is-

$$\left[\frac{Q}{A}\right]_{Die} = \in_0 k \frac{V}{d} = \sigma_{vac} + \sigma_{pol} \text{----------} \quad (6)$$

Where, σ_{pol}= Excess charge per unit surface area present on the dielectric surface. This numerically has the same dimension as the polarization, P of the dielectric material.

$$\Sigma_{pol} = P \text{ ----------(7)}$$

The total charge can be divided to *free charge* Q/k that sets up the electric field and voltage toward the outside; the other portion being the *bound charge*, is neutralized by polarization of the dielectric.

Schematically it can be represented that the total electric flux density D is the sum of the electric field E and the dipole charge P:

$D=\in_0 E + P = \in' E$---------- *(8)*

Polarization P is the surface charge density of the bound charge, equal to dipole moment per unit volume of material.

$P = N \bar{\mu}$---------- *(9)*

In other words, the total change on the capacitor D is the sum of the charge that is present in vacuum and an extra charge that results from the polarization of the dielectric material P. Thus polarization can equivalently designate either the bound charge density or the dipole moment per unit volume. From 8-

$P =\in' E - \in_0 E = \in_0 (k-1) E = \chi_{die} \in_0 E$ ---------- *(10)*

Where, χ_{die}= dielectric susceptibility of the material.

$X_{die} = k-1 = P/ \in_0 E$ ---------- *(11)*

The susceptibility is the ratio of the bound charge density to the free charge density.

Considering from microscopic point of view –

The charge carriers in dielectric materials cause to react with and affect the electromagnetic radiation. The relationship between applied field and the medium can be considered as resulting from the presence of elementary electric dipoles having an average dipole moment, $\bar{\mu}$. If the dipole moment is represented by two charges of the opposite polarity, + and –Q, separated by a distanceδ, and then $\bar{\mu}$ equals Qδ.

$\bar{\mu} = Q\delta$ ---------- *(12)*

With the above considerations if the center of electron charge moves by an amountδ, then the total volume occupied by these electrons would be Aδ. If the number of molecules per unit volume by N then the total charge appearing in that volume Aδ is AδNQ.

Over the range of optical frequencies the source of this dielectric polarization is the shift of the electron cloud around the atomic nucleus. The average dipole moment is proportional to the local electric field strength (E') that acts on the particle; the proportionality constant (α) being called the polarizability.

$\bar{\mu} = \alpha E$ ---------- *(13)*

Regarding to the statement and equation 9 we can end up with –

$P = N \alpha E$ ---------- *(14)*

2.4 Mechanism of polarization

The formation of an electric dipole or polarization can happen in a number of mechanisms [17].Like –

1) Electronic polarization
2) Ionic or atomic polarization
3) Orientation polarization
4) Space charge polarization

2.4.1 Electronic polarization:

Electronic polarization occurs in all dielectric materials. Upon an external electric field being applied a slight relative shift of positive and negative electric charge in opposite directions occurs within an insulator, or dielectric. Polarization occurs when the induced electric field distorts the negative cloud of electrons around positive atomic nuclei in a direction opposite the field. This slight separation of charge makes one side of the atom somewhat positive and the opposite side somewhat negative. As soon as the electric field is removed the electrons and nuclei return to their original position and the polarization disappears. The displacement of charge is very small for this mode of polarization. Hence total amount of polarization is small compared to other modes of polarization.

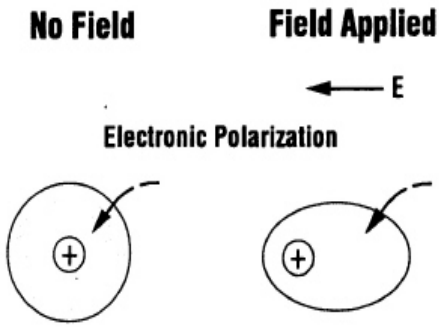

Fig. 2.2: Electronic polarization

2.4.2 Atomic polarization:

It is also known as ionic polarization. It involves the displacement of positive and negative ions in relation to one another within crystal structure when an electric field is applied. The magnitude of the dipole moment for each ion pair p_i is equal to the product of the relative displacement d_i and the charge on each ion as in-

$$p_i = q\, d_i$$

Various popular effects like piezoelectricity, pyroelectricity, ferroelectricityetc occurs by ionic polarization phenomena. Wide range of polarization effects are possible through this mechanism depending upon the crystal structure, solid solution and various other factors.

Ionic polarization is inversely proportional to the mass of the ions and square of the natural frequency of vibration of the ions. Covalently bonded ceramics do not show ionic polarization due to lack of charged atoms, but ionic bonded structures show ionic polarization.

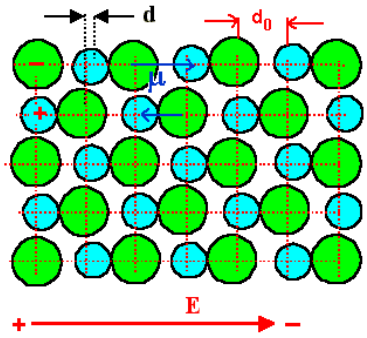

Fig. 2.3: Atomicpolarization

2.4.3 Dipolar polarization:

This mode of polarization mainly attributed to the unequal charge distribution between partners in a molecule or complex ion. When a field is applied, these tend to line up with the electric dipoles in the direction of the field, giving rise to an orientation polarization. That is why this polarization is found only where substance possesses permanent dipole moments.

Upon electric field these permanent moments rotate into the direction of the applied field, therefore contribute to the dipolar polarization. The tendency to alignment is counterbalanced by thermal vibrations of the atoms such that the polarization decreases with the increasing temperature.

Dipolar polarization occurs at lower frequencies of the field and thus can greatly affect the capacitive and insulating properties of glasses and ceramics in low frequency applications.

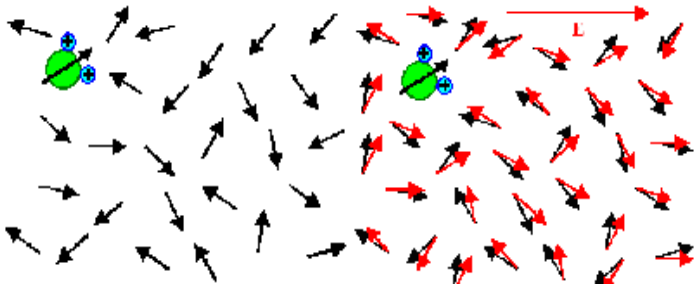

Fig. 2.4: Dipolar polarization

2.4.4 Space charge polarization:

The final source of polarization is mobile charges which are present because they are impeded by interfaces, because they are mot supplied at an electrode or discharged at an electrode. Or they are trapped in the material during fabrication process. Space charges resulting from these phenomena appear as an increase in capacitance as far as the exterior circuit is concerned.

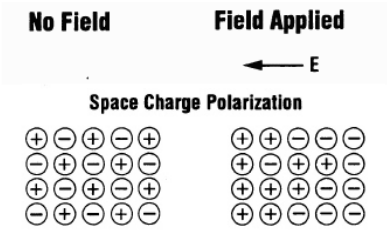

Fig. 2.5: Space Charge polarization

2.5 Frequency response of polarizability

The dielectric response of solids is a complex function of frequency, temperature, and type of solid. Under dc conditions all mechanism operates and the maximum polarization results which eventuates to the maximum of dielectric constants. An ideal dielectric is supposed to adjust itself instantaneously to any change in voltage. However in practice there is inertia to charge movement that shows up as a relaxation time for charge transport. When the frequency of the applied field increasesthe mechanisms start to fade out and the value of polarizability starts falling [17].

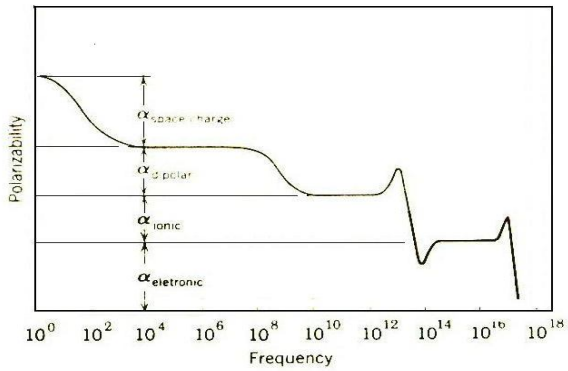

Fig. 2.6: Variation of polarization with frequency[17]

It is already been noticed that the electronic polarization is the only process that can follow the rapid change in the alternate field so to cause a variation in the polarizability. That is why this is still operative in the visible range of the spectrum and the cause factors like index of refraction which only due on to this process.

Ionic polarization processes are able to follow an applied high frequency field and contribute to the dielectric constant at frequencies up to infrared region of the spectrum. Dipolar and space charge polarization have relaxation time corresponding to the particular system and process but in general participate and contribute only at lower frequencies. As far as this thesis is concerned, this factor is very important in getting the dielectric behavior of the ceramics.

2.6 Dielectric loss

An ideal dielectric would allow no flow of electric charge but only a displacement of charge via polarization. If a thin plate of such an ideal material were placed between parallel plate electrodes to form a capacitor and if an alternating electric field was applied, the current would lead the voltage by a phase angle of$\frac{\pi}{2}$. Under these circumstances, no power will be absorbed by the dielectric and the capacitor would have zero loss.

We know voltage- $V = V_0 \sin \omega t$ hence, $Q = C\,V = CV_0 \sin \omega t$

So the current would be - $I_{chg} = \frac{dQ}{dt} = C\frac{dV}{dt} = \omega CV_0 \cos\omega t = \omega CV_0 \sin\left(\omega t + \frac{\pi}{2}\right)$

Hence we see that the applied current is leading the voltage by 90^0 or$\frac{\pi}{2}$ radian. At this provision, no power would be absorbed by the dielectric.

When alternating current passes through the capacitor with a dielectric in between the capacitor plates, the molecules of the dielectric fail to align instantaneously with the alternating electric field. These molecules do not keep in phase with changing field. The time required for polarization shows up as phase retardation of the charging current. As a result, instead of being 90° advanced, the angle of leading current is slightly reduced.

In this case the current, I have two components. An imaginary, charging component which is I_{chg} = iωCV; and a real loss component I_{loss}. The charge component is a capacitive current that is proportional to the charge stored in the capacitor. The loss current is an ac conduction current that is in phase with the voltage V and represents the energy loss or power dissipated in the dielectric material.

New lead angle is *Ø*. Value *90-Ø* is known as loss angle and is given by symbol δ. The power factor is defined as *cos Ø* and the dissipation factor or the amount of lag as tan δ. tan δ is also called loss tangent. For small values of δ, *sin δ* (Power Factor) and tan δ (dissipation factor) are almost equivalent.

We can define the loss factor, which is numerically the product of dissipation factor and the dielectric constant. So loss tangent –

$$\tan \delta = \frac{k''}{k'}$$

where k" is *relative loss factor* and k' is the *relative dielectric constant*.

Dielectric loss could result from several mechanisms: (1) Ion migration; (2) Ion vibration and deformation; (3) Electronic polarization. The most important mechanism to most ceramics is ion migration, which is strongly affected by temperature and frequency. The loss due to ion migration increases at low frequencies and as the temperature rises.

2.7 Dielectric strength & breakdown

An important property of dielectric materials is the ability to withstand large field strengths without electrical breakdown. Dielectric strength is a measure of the ability of the material to hold energy at high voltages. It is defined as the voltage per unit length at which failure occurs. Thus it is the maximum electric field that the dielectric can maintain without electrical breakdown [18].

At low field strengths there is a certain dc conductivity corresponding to the mobility of a limited number of charge carrier related to electronic or ionic imperfections. As the field strength is increased

this dc conduction increases, but also when some sufficient large value of potential is reached, a field emission from the electrodes makes available sufficient electrons for a burst of currents which produces breakdown channels, jagged holes, or metal dendrites bridging the dielectric and render it unusable.

Various processes may contribute to these dielectric breakdown phenomena. However, different measurement techniques give considerable scatter in the outcomes and detail interpretations are still in some doubt.

Dielectric breakdown of insulating material under an applied field takes place two different ways. The first is electronic in origin and is referred to as intrinsic dielectric strength. The second process is caused by local overheating, arising from electrical conduction. The local conductivity increases to a point at which instability occurs and permits a rush of currents and melting and puncture is likely to occur. The tendency toward thermal breakdown increases at higher temperatures and voltages are applied for a long time.

In electronic breakdown, failure occurs when a localized voltage gradient reaches some value corresponding to intrinsic electrical breakdown. Electrons within the structure are accelerated by the field to a velocity that allows them to liberate additional electrons by collision. This process continues at an accelerating rate and finally results in an electron avalanche which correspond to breakdown and sample rupture. At low temperatures (below room temperature) the intrinsic breakdown strength of crystalline materials increases with rising temperature, corresponding to increased lattice vibrations and a resulting increase in electron scattering by the lattice; a greater field strength is required to accelerate electrons to a point at which electron avalanche is initiated. On the other hand glassy material's intrinsic dielectric strength is independent of temperature at low temperatures.

Thermal breakdown behavior is associated with electrical stress of appreciable time duration for local heating to occur and it requires high enough temperatures for the electrical conductivity to increase. The loss in electrical energy causes the temperature to rise further and increase the local conductivity. This causes channeling of currents; thus local instability and breakdown occur which results in the passage of high currents along with fusion and vaporization that constitute the puncture of the insulator.

2.8 Piezoelectric ceramics

The Piezoelectric Effect is the name given to the electromechanical interaction of certain materials. Discovered in 1880 by Pierre and Jacques Curie, it is the relationship between electric polarization and mechanical stress or distortion. The word originates from the Greek word “piezein”, which means, “to press”. Anything, that is said to give off an electric field under mechanical stress and vice versa, is said to be piezoelectric [19].

The effect is explained by the displacement of ions in crystals that have a nonsymmetrical unit cell. When the crystal is compressed, the ions in each unit cell displace, causing the electric polarization of the unit cell. Because of the regularity of crystalline structure, these effects accumulate, causing the appearance of an electric potential difference between certain faces of the crystal.When an external electric field is applied to the crystal, the ions in each unit cell are displaced by electrostatic forces, resulting in the mechanical deformation of the whole crystal.

The Piezoelectric Effect has two pathways dependent on cause and effect. Two factors are involved: *Mechanical stress* and *electric polarization*. When a piezoelectric object is subjected to a physical distortion or compression, the object acquires an electric charge. This pathway, where mechanical stress leads to polarization is known as the *Direct Piezoelectric Effect*.

Object (strain) ⟶ Object (Electric Polarization)

When a piezoelectric object undergoes an electrical charge, observed mechanical distortions take place in what is known as the *Converse Piezoelectric Effect*.

Object (electrical field) ⟶ Object (stress)

An object with piezoelectric property has many applications. Quartz, a crystal with piezoelectric property, is utilized by applying an electrical field, thus leading to a deformation of the quartz. The sense of the strain depends on the direction of the field. A majority of computers contains at least one clock frequency which is generated by a quartz crystal. Aside from quartz, Rochelle salts, $BaTiO_3$,$(NH_4)H_2PO_4$, $LiTaO_3$, and $LiNbO_3$ are other noted salts and crystalline objects that display piezoelectric properties.

This electromechanical property, however, is not rare. Twenty of the thirty-two crystal classes are piezoelectric. Of the thirty-two crystal classes, twenty-one are non-centrosymmetric (not having a centre of symmetry), and of these, twenty exhibit direct piezoelectricity. Ten of these are polar (i.e.

spontaneously polarize), having a dipole in their unit cell, and exhibit pyroelectricity. If this dipole can be reversed by the application of an electric field, the material is said to be ferroelectric. Unlike the ferroelectric class of materials, piezoelectric material does not store charge after the force is removed.

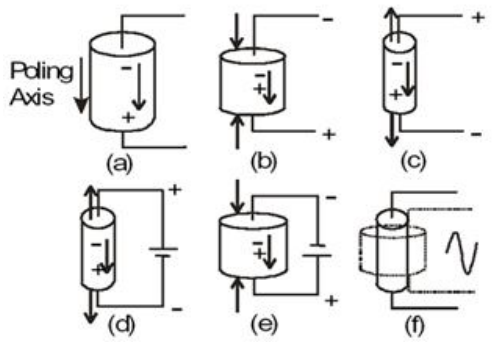

Fig. 2.7: Piezoelectric effect

Figure.2.7 illustrates the piezoelectric effect. Figure (a) show the piezoelectric material without a stress or charge. If the material is compressed, then a voltage of the same polarity as the poling voltage will appear between the electrodes (b). If stretched, a voltage of opposite polarity will appear (c). Conversely, if a voltage is applied the material will deform. A voltage with the opposite polarity as the poling voltage will cause the material to expand, (d), and a voltage with the same polarity will cause the material to compress (e). If an AC signal is applied then the material will vibrate at the same frequency as the signal (f).

2.9 Pyroelectric ceramics

Pyroelectricity is the ability of certain materials to generate an electrical potential when they are heated or cooled [19]. Because of this change in temperature, positive and negative charges move to opposite ends through migration (i.e. the material becomes polarized) and hence, an electrical potential is established.

Certain dielectric (electrically nonconducting) crystals develop an electric polarization (dipole moment per unit volume) when they are subjected to a uniform temperature change. This effect occurs only in crystals which lack a center of symmetry and also have polar directions (that is, a polar axis). These conditions are fulfilled for ten of the thirty two crystal classes. Typical examples of pyroelectric crystals are tourmaline, lithium sulfate monohydrate, cane sugar, and ferroelectric barium titanate.

Pyroelectric crystals can be regarded as having a built-in or permanent electric polarization. When the crystal is held at constant temperature, this polarization does not manifest itself because it is

compensated by free charge carriers that have reached the surface of the crystal by conduction through the crystal and from the surroundings. However, when the temperature of the crystal is raised or lowered, the permanent polarization changes, and this change manifests itself as Pyroelectricity.

Crystal structures can be divided into thirty two classes, according to the number of rotational axes and reflection planes, they exhibit that leave the crystal structure unchanged. Twenty one of them classes lack a center of symmetry, and Twenty of them are piezoelectric.Of these Twenty crystal classes ten of them are pyroelectric (polar). Any material develops a dielectric polarization when an electric field is applied, but a substance which has such a natural charge separation even in the absence of a field is called a polar material. Whether or not a material is polar, is determined solely by its crystal structure. Only ten of thirty two classes are polar.

The property of Pyroelectricity is the measured change in net polarization (a vector) proportional to a change in temperature. The *total pyroelectric coefficient* measured at constant stress is the sum of the pyroelectric coefficients at constant strain (primarypyroelectric effect) and the piezoelectric contribution from thermal expansion (secondary pyroelectric effect).

The pyroelectric coefficient may be described as the change in the spontaneous polarization vector with temperature.

$$p_i = \frac{\partial Ps,i}{\partial T}$$

Where, p_i ($Cm^{-2}K^{-1}$) is the vector for the pyroelectric coefficient.

2.10 Ferroelectric ceramic

Ferroelectricity is a physical property of a material whereby it exhibits a spontaneous electric polarization, the direction of which can be switched between equivalent states by the application of an external electric field with a hysteresis loop being followed [19]. If the material shows a perfect cubic lattice, no Ferroelectricity can be observed.

Ferroelectric materials are also nonlinear and demonstrate a spontaneous polarization. Typically, materials demonstrate Ferroelectricity only below a certain phase transition temperature, called the Curie temperature T_c, and are paraelectric above this temperature.

Ferroelectric behavior is dependent on the crystal structure. The crystal must be noncentric and must contain alternate atom positions to permit the reversal of the dipole and the retention of polarization after the voltage is removed. An example can be made of barium titanate, a typical ferroelectric

material. Within the range of 120 to 1460 ^{0}C temperatures, the structure is cubic and therefore does not show any Ferroelectricity. Since in this temperature range, the Ti^{4+} ion lies in the centre of an octahedron of oxygen ions. The Ti^{4+} ion does shift positions and result in polarization when an electric field is applied, but it returns to its central stable position as soon as the field is removed. Hence no ferroelectric behavior is observed.

As the temperature reduces to below 120 ^{0}C, a displacive transformation occurs in which the structure shifts from cubic to tetragonal. the transition can be understood in terms of a *polarization catastrophe*, in which, if an ion is displaced from equilibrium slightly, the force from the local electric fields due to the ions in the crystal, increases faster than the elastic-restoring forces. This leads to an asymmetrical shift in the equilibrium ion positions; the ion moves to an off center position towards one of the two oxygen ions of the long axis, resulting in a spontaneous increase in positive charge in this direction and permanent dipole moment, thus exhibit Ferroelectricity.

All ferroelectrics are piezoelectric and pyroelectric; but not vice versa. For instance, tourmaline shows Pyroelectricity but is not ferroelectric. The alignment of electric dipoles is opposed by thermal vibrations and thus the property deteriorates as the temperature increases. The alignment disappears at the curie temperatures. For $T>T_c$,Curie Weiss law holds:

$$\chi = \frac{P}{\varepsilon E} = \varepsilon/\varepsilon_0 - 1 = k' - 1 = \frac{3Tc}{T-Tc}$$

χ represents the electrical susceptibility, P represents polarization, E electric field, ε and $\varepsilon_0$representspermittivity of material and vacuum respectively, and k' represents dielectric constants.

2.10.1Ferroelectric domains

As the material develops its charge, a 'domain' structure is developed in order to attain the minimum free energy state for the crystal.Ferroelectric domains, sometimes known as Weiss domains, are areas of local dipole alignment - with an associated net dipole moment and net polarization. 'Domain walls' separate domains from each another. These domain boundaries are usually described according to the angle between the domains that they separate. The most common found are 90° and 180° boundaries.

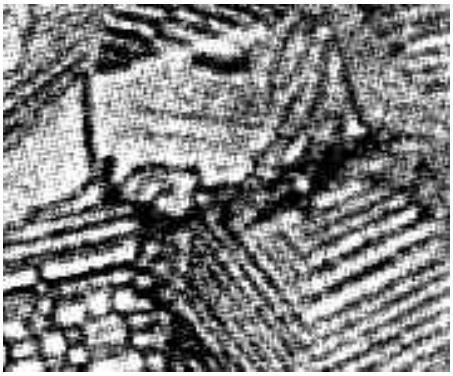

Fig. 2.8: Ferroelectric Domain [19]

The picture above shows an area of a ferroelectric material clearly displaying a domain structure. The dark lines are 90° domain walls. The domain structure and behavior of a material will critically affect its operational performance.

In the presence of an applied electric field, domains that are aligned with the direction of the field will grow at the expense of the less well-aligned domains. This may be visualized in terms of the boundary between the domains moving. The domain structure can also change over time by a process known as ageing. This causes degradation to the dielectric properties and often causes device failure due to loss of insulation resistance.

In barium titanate each titanium ion has equal probability of shifting in six directions towards one of the corners of the octahedron. As a result the tetragonal crystal contains some dipoles in one portion of the crystal in one direction, whereas others in another portion may point in a direction 90° or 180° away from the first. The regions of the crystal in which the dipoles are aligned in a common direction are the domain.

Presence of an electric field is vital for getting the maximum of domains to be aligned in one direction. The temperature also plays a vital role on that occasion. For example, maximum alignment of domains in barium titanate can be achieved by cooling the crystal through the 120° C cubic to tetragonal transition while an electric field is being applied. This is referred to as *poling*. This results in maximum polarization. It's been found upon research to characterize the domains and their activities that 180° domains are easy to remove than 90°. That is because the surface strain generated during cooling and the crystal fabrications restrict the motion of the domain. There may be many domains in a crystal separated by interfaces called domains.

2.10.2 Ferroelectric Hysteresis loop

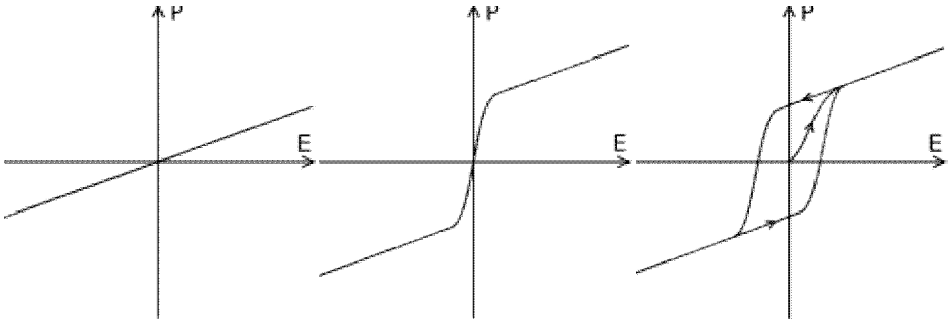

Dielectric polarization paraelectric polarization ferroelectric polarization

Fig. 2.9: Response of different type of materials to electric fields[20]

One of the prime characteristics of the ferroelectric materials is the retention of dipole without the presence of the any field and the reversibility of the direction of polarization by application of an electric field. Such reversal upon the application of the electric field results in a hysteresis loop. Figure shows such a hysteresis loop. Where E is the applied field and P is the polarization.

Ferroelectric domains are randomly oriented prior to application of the electric field. Net polarization at zero fields is zero. At low field strengths in unpolarized material, the polarization is also reversible and nearly linear with the applied field. Here the slope of the curve gives the initial dielectric constant. At higher fields strengths the polarization increase more rapidly because of switching of ferroelectric domains that is the changing polarization direction in domains by 90 or 180; this occurs by domain boundaries moving through the crystal. At the highest field strengths the increase of polarization for a given increase in field strengths is again less, corresponding to polarization saturation, having all the domains of like orientation aligned in the direction of the applied field. This is called saturation polarization or spontaneous polarization.

When the electric field is cut off the polarization does not go to zero but remains at a finite value, called the remanent polarization, P_r. This results from the oriented domains being unable to return to their original random state without an additional energy input by an oppositely directed field. That is energy is required for change in domain orientation. The magnitude of the electric field required to return the polarization to zero is known as the coercive field E_c.

At higher temperatures, the hysteresis loop becomes fatter, and the coercive field becomes greater, corresponding to a larger energy required to reorient the domain walls. At higher temperatures, the coercive force decrease until at the Curie temperature, where no hysteresis remains, and there is only a single value for the dielectric constant.

The hysteresis here has been originated from the existence of irreversible polarization through partial polarization reversals of a single ferroelectric lattice cell. The separation of the total polarization into reversible and irreversible contributions might facilitate the ferroelectric polarization. Irreversible polarization would be important say for ferroelectric memory device, since the reversible process can't be used to store information. Similarly, a reversible ferroelectric may be a requisite of dielectric materials for application such as capacitors.

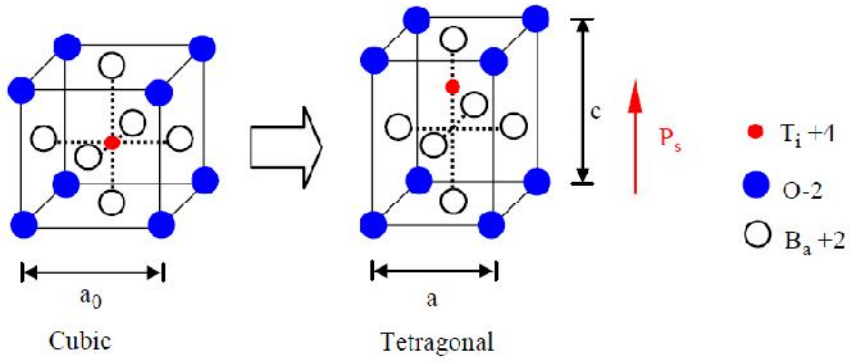

Fig. 2.10: The perovskite structure ($BaTiO_3$) Showing structures below and above curie point[20]

2.11 Science of Barium Titanate

With a general formula ABO_3, the A cation and the anions effectively form an FCC array with a large octahedron in the center of the cell but no available tetrahedra (because of the charge). The ideal perovskite structure is simple cubic, and this is what we generally imply when we refer to the perovskite structure. The mineral perovskite is $CaTiO_3$ and is actually orthorhombic at room temperature, becoming cubic only at temperatures above 900°C. Other ceramics with the perovskite structure include $BaTiO_3$, $SrTiO_3$, and $KNbO_3$, each being written in the general form ABO_3. The structure is not similar to that of ilmenite ($FeTiO_3$)though, which is related to the alumina structure.

Looking at the ionic radii, a trend can be seen. The O^{2-} anion and the larger cation (A^{2+}) have similar radii, so that the structure is not just determined by O^{2-}. The larger cation and the anion combine to form a "close-packed" arrangement with the smaller cation, B^{4+}, sitting in the oxygen octahedral

interstices. The octahedra then link together by sharing corners as shown in Figure.2.10.The bond strength is given as

$$Ti-O=+\frac{4}{6}=\frac{2}{3};\qquad Ca-O=+\frac{2}{12}=\frac{1}{6}$$

Each O^{2-} anion coordinates with two $Ti^{4+}$and four Ca^{2+}cations so that the total bond strength is -

$$2\times\frac{2}{3}+4\times\frac{1}{6}=+2$$

Barium titanate ($BaTiO_3$) is the prototype ferroelectric material. It has the ideal perovskite structure above 120°C. At temperatures below 120°C the small cation (Ti^{4+}) shiftsoff its ideal symmetric position at the center of each octahedral interstice. This shift creates an electric dipole; it polarizes the structure electrically, which in turn causes the material to become noncubic; this changes the cell dimensions. Spontaneous electrical polarization in the absence of an applied electric field is termed ferroelectricity. The link between electric field and mechanical deformation of the unit cell is known as the piezoelectric effect:it allows us to convert an electrical signal to a mechanical one and vice versa. This shift actually has the same origin as the flexibility of this structure: many ions can fit in the central ocahedron.The perovskite structure is particularly important for several reasons:

- Many perovskites are ferroelectric
- Many perovskites are piezoelectric
- Many perovskites have a high dielectric constant

The perovskite structure is also of interest to mineralogists. A mineral with the perovskite structure of composition close to MgSiO3 is believed to be the predominant mineral in the lower mantle (depths of about 600 km) of the earth. The perovskite structure of $MgSiO_3$ is stable only at very high pressures.

Barium titanate ($BaTiO_3$) was the first ceramic in which ferroelectric behavior was observed and is probably the most extensively investigated of all ferroelectrics. Its discovery made available κs up to two orders of magnitude greater than had been known before. This property was very soon utilized in capacitors and $BaTiO_3$ remains the basic capacitor dielectric in use today (although not in its pure form). There are several reasons why $BaTiO_3$ has been so widely studied:

Relatively simple crystal structure, durability, Ferroelectric at room temperature (θc = 120°C), easily prepared as a polycrystalline ceramic, single crystal, or thin films.

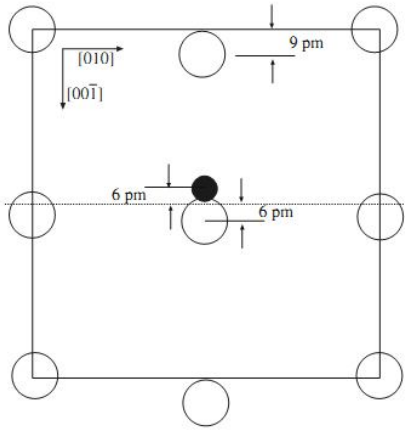

Fig. 2.11: [100] projection of barium titanate showing the ion displacement below θ_c[17]

Aboveθc the unit cell of $BaTiO_3$ is cubic (point group m3m) with the ions arranged as shown in Figure. 2.11: Each Ba^{2+} is surrounded by 12 nearestneighbor oxygen ions; each $Ti4^{+}$ has six oxygen-ion neighbors. Together the $Ba^{2+}$and O^{2-} ions form a face-centered cubic (FCC) arrangement with Ti^{4+} fitting into the octahedral interstices. The octahedral site is actually expanded because of the large Ba^{2+}ions (r_{Ba2+} = 0.136 nm). The Ti4+ion is quite small (r_{Ti4+} = 0.064 nm) giving a radius ratio with oxygen of r_{Ti4+} /r_{O2-} = 0.44. This value is close to the limiting value ($\geq$0.414) for a coordination number of 6. The result is that the Ti4+often finds itself off-centered within its coordination octahedron. This is why it is sometimes referred to as the "rattling" titanium ion (think back to Pauling's rules). The direction of off-centering may be along one of the 6 <001> directions, one of the 8 <111> directions, or one of the 12 <110>directions.

2.11.1 The effect of temperature - The phase transformations

Barium Titanate assumes two basic structures;a*perovskite* form, which is ferroelectric at certain temperatures and a *non-ferroelectric hexagonal* form. The hexagonal form is stable above 1460℃ temperatures and can stay up to room temperature metastably. At 1460℃, the hexagonal form transforms to a cubic perovskite form and it is the basic ceramic product.

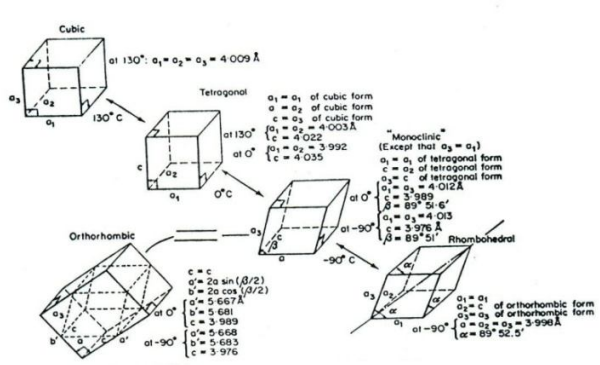

Fig. 2.12: Polymorphic transitions in $BaTiO_3$[19]

On cooling $BaTiO_3$ below θ_c (120°C) the structure spontaneously changes to the tetragonal form (point group 4 mm) with a dipole moment along the c axis. The c/a ratio becomes more than one.Such change marks the onset of extreme dielectric anomalies and the emergence of ferroelectricity. A *tetragonal* polar one replaces the centrocemetric cubic structure. The magnitude and direction of the ion displacements accompanying this transformation are given in Figure.2.12.

Upon further cooling, another polymorphic transformation occurs at 0°C, the cube here elongates along a face diagonal. The structure on this stage is pseudo monoclinic but actually is *orthorhombic*. At even lower temperatures like at -90°C, a third displacive transformation takes place and the previously turned *rhombohedral* cell elongates along a body diagonal. In each temperature range, the direction of the ferroelectric dipole parallels the elongation of the unit cell.

2.11.2 Curie point

Like any magnetic materials, all ferroelectric materials experience a temperature transition regarding its ferroelectric behavior. This temperature is called the *Curiepoint* (T_c). At temperatures higher than T_c, the material does not exhibit any ferroelectricity, whereas below this temperature, the material does show the property. It's possible that there might be more than one ferroelectric phases. In that case, the temperature at which one ferroelectric phase transforms from one phase to another is called the *transition temperature.*

The basic change through the Curie point is marked by the change in crystal structure. In the case of barium titanate for instance, a cubic lattice structure prevails above 120°C. The thermal vibration causes the titanium ions to be oriented randomly in the octahedral holes. At Curie point 120°C, the structure changes to tetragonal form on decreasing temperature. This brings a distortion in the size of the octahedral site with the titanium ion being at an off center position. This produces a permanent dipole. Hence, the phase transformation from cubic to tetragonal turns spontaneous random

polarization to permanent dipole domains. This point (temperature) marks the curie point of the barium titanate crystal.

It is important to realize that the Ba-O framework suggests an interstitial site, which is much larger than the size of titanium ion. The series of reaction thus helps reducing the size of the octahedral site and allows titanium ion to be positioned more compactly. It is found that the size of the ions that make up the framework has important role in deciding the ferroelectric property. Thus, both $BaTiO_3$ and $PbTiO_3$ have ferroelectric phases since the size of both Ba^{2+} and Pb^{2+} allows Ti^{4+} ion to customize its position with the changing phase. On the other hand, $CaTiO_3$ and $SrTiO_3$ do not have any ferroelectric phase since the Ca^{2+} and Sr^{2+} ions are not large enough to offer Ti^{4+} ion enough space to move upon Curie point.

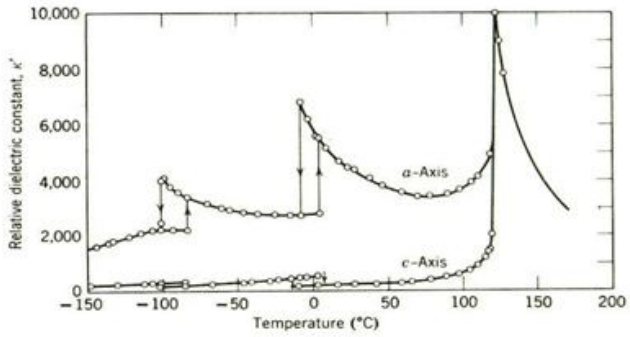

Figure 2.13 (a): Change of phases with temperature in $BaTiO_3$[18]

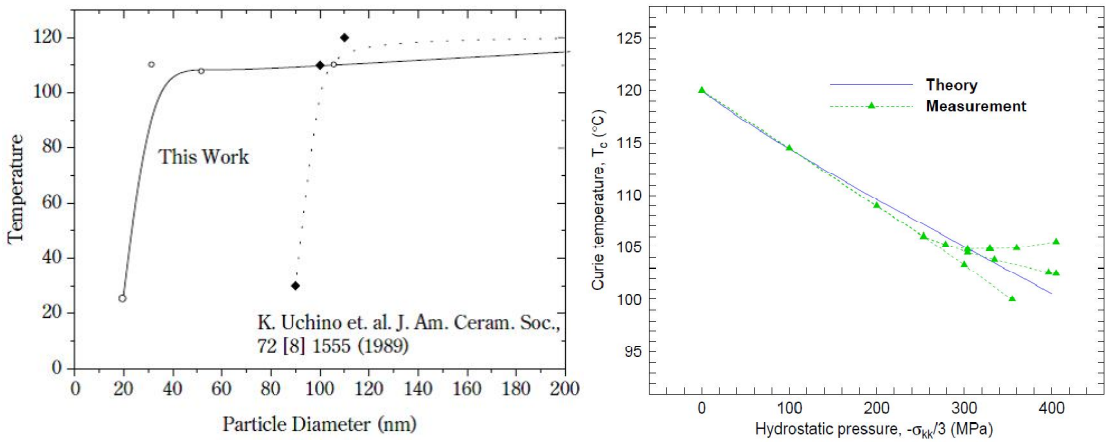

(b) Change in the curie temperature as a function of particle diameter, [21] *(c)Effect of hydrostatic pressure on Curie temperature of $BaTiO_3$,respectively*[28]

Figure.2.13 (a) shows the variations of relative permittivity, polarization, lattice constant with temperature for $BaTiO_3$, as the crystal is cooled from its paraelelctric cubic phase to ferroelectric

tetragonal, orthorhombic, and rhombohedral phases. Near the Curie point or the transition points, various thermodynamic properties like dielectric, elastic, optical, and thermal constants show an anomalous behavior, which is attributed in the change in the crystal structure as the phase change, occurs.

2.11.3 Curie point shift in $BaTiO_3$

According to Ohna and Suzuki [21] the size effect for ferroelectric materials results in the Curie temperature shift to the lower temperature. Therefore, the Curie temperature shift for $BaTiO_3$nano-particles has been investigated. Figure.2.13 (b)shows the Curie temperature shift as a function of the particle diameter. According to them, some lattice vibration remained above the Curie temperature by the secondary scattering and so on, in the case of $BaTiO_3$. They found that the Curie temperature for $BaTiO_3$nano-particles was shifted to the lower temperature at around 20-30 nm of particle diameter. This tendency was almost same as that of the result of Uchino et. al. [22-23] measured by the change in the lattice constants as a function of the particle diameter using XRD. However, their result showed that the Curie temperature shift to the lower temperature began at around 100 nm of particle diameter. This difference in the critical size for $BaTiO_3$ was ascribed to the measurement techniques of the particle diameter and the crystal symmetry.

Merz [24-27] has measured the pressure dependence of the transition temperature of $BaTiO_3$ over the range of pressure from0 to 400MPa. His data were reproduced by Weng [28] in Figure.2.13 (c). As the pressure increases, both the test data and the theory show a steady decrease of the transition temperature, with a slope of about -6.0×10^{-2}°C/MPa during the first 200 MPa.

2.12Effect of grain size on dielectric property

Grain sizes of barium titanate is very important for dielectric properties. It is now well established that reduction in grain size causes higher dielectric constants [29-30] and lower dielectric losses. Reduction of grain size depends on sintering parameters like sintering temperatures, soaking time and the design of sintering cycle. For example, sintering with double stage heating can keep the grains from exaggerated growth [31]. Various processing techniques have been shown to be yielding fine grain structure with a very short sintering time. Fine grain size achievement in conventional pressing-sintering method depends on judicious design of sintering cycles.

If the situation of grain development is analysed then it would seem that different particles with different crystal space orientation would meet up at the line of contact and then by means of grain boundary motion those regions would end up as one single grain. During the transformation from cubic phase to tetragonal phase, the crystal changes its c/a ratio to become tetragonal which is

accompanied by a certain amount of volume change. The change in volume is associated with the the crystal orientation and the degree of change depends upon the surroundings of the crystal. Since it was already discussed that a single grain can hold multiple domains and since all these domains have different crystal orientation in space, there is a certain amount of resistance from surroundings to changing the volume or c/a ratio of the crystal for that matter. Its like one crystal is on the way of its surrounding crystal while the latter tries to change its dimension along one direction (c) as the first crystal is not trying to change its dimension along the same direction. This mutual resistance works accross the whole number of crystals (or domains) in a grain and therefore successful domain formation gets severely disrupted. As the grain size increases, the number of individual crystals it hold increases and therefore lesser the formation of domains in it. For a ceramic like barium titanate where its dielectric properties are heavily dependent upon these domain formation which eventually gets the material to be highly polarized, large grain sizes may have serious harmful effect on the final dielectric properties of the material.

On the other hand for fine grain sizes, the number of distinctive crystals it holds in the grain is not as much as large grains do. Therefore, as the grain size decreases, the resistance on the individual grains to changing its *c/a* ratio becomes much less across the grain. When it reaches the transition point of cubic to tetragonal phase change, it can change its dimension with much ease and thus domains can form successfully. It has been shown that the fine grain sized materials possess lower residual stress than large grain sized materials which is a representation of the same theory discussed above. Suitable design of sintering process is essential to bring such stress free microstructure. For barium titanate based materials [29, 31] double stage sintering has been proven to yield stress free grains. This thesis has been able to produce grains as small as 500 nm size by means of sintering for very short time.

In bulk $BaTiO_3$, the grain size has a string effect on the low frequency permittivity for grain sizes below approx. 10 micron. The permittivity is rising at decreasing grain sizes up to a maximum grain size of 0.5 to 0.7 micron since the internal stress caused which clamped by its surrounding neighbors or by the increase of the number of domain walls contributing to the dielectric constants. Below this grain size the permittivity decreases sharply again due to reduction of tetragonality and of the remanent polarization.

It is suggested that the lowering of permittivity is caused by the low permittivity of interfacial layer of 0.5 to 2 nm thickness at the grain boundaries. This layer shows no difference of the composition and crystal structure in comparison to the bulk and is believed to be of photonic nature. In $BaTiO_3$ thin films significant increase in the room temperature permittivity from 500 to 900 is observed, induced by the change in morphology from granular to columnar structure.

The variation of dielectric constant with temperature for $BaTiO_3$ ceramics may vary from a fine (<1 micron) to a coarse (>50 micron) grain size. Large grained sample showed extremely high dielectric constant at the Curie point. This is due to formation of multiple domains in a single grain, the motion of whose increase the dielectric constant at the Curie point. In case of the fine grained samples a single domain forms at the grain and the movement of domain walls are restricted by the movement of grain boundaries. This leads to a low dielectric constant at the Curie point compared to the coarse-grained sample.

The room temperature dielectric constant of fine-grained samples is found to be about 3500 to 6000, which is 1500 to 2000 for the coarse-grained sample. Scientists suggested that in fine-grained sample $BaTiO_3$ must be of higher internal stress than the coarse-grained sample. This leads to a higher permittivity at room temperature. Moreover, the room temperature permittivity reaches its peak value at a grain size of about 0.7 micron.

As the $BaTiO_3$ ceramics have very high room temperature dielectric properties, they can be used in multilayer ceramic capacitor application. The control of grain size is very important on this occasion.

2.13Motion of Domain walls with Electric field

The motion of domain walls in ferroelectrics is not simple. In an electric field a 180° wall in $BaTiO_3$ appears to move by the repeated nucleation of steps by thermal fluctuations along the parent wall. Domains misoriented by 180° tend to switch more easily than 90° domain walls since no net physical deformation is required; domains misoriented by 90° are inhibited from changing orientation by the strain that accommodates switching of c and a axes.

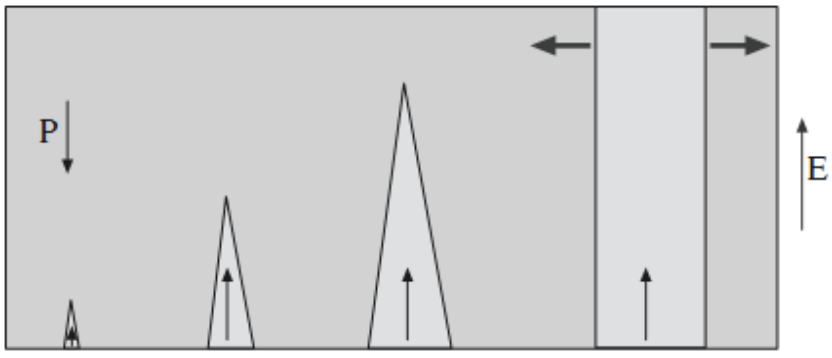

Fig.2.14: Growth of ferroelectric domain under applied field[17]

The almost horizontal portions of the hysteresis loop represent saturated states in which the crystal is a single domain during a cycle. Defects and internal strains within the crystallites impede the movement

of domain walls. Domain wall mobility has been found to decrease with time (even without an applied mechanical or electrical stress or thermal changes). This is due to internal fields

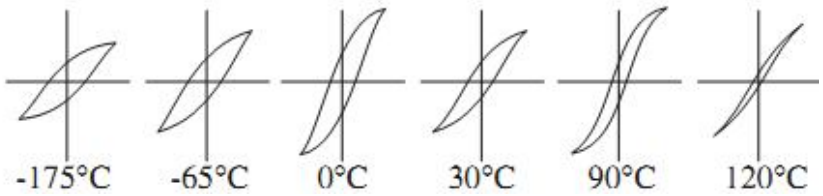

Fig.2.15: Hysteresis loop for Barium titanate as a function of temperature[17]

associated with charged defects, redistribution of lattice strains, and accumulation of defects at domain walls.The size of the hysteresis loop also depends on temperature as shown in Figure.2.15. At low temperatures the loops are fatter and Ec is greater, corresponding tothe larger energy requiredfor domain reorientation. At higher temperatures Ec decreases until at $\theta_c$where no hysteresis remains and the material becomes paraelectric.

2.14Core shell structure

Core shell structure is found in many sintered materials Such as doped barium titanate, silicon carbide, silicon nitride etc.In all these materials grain coarsening occur during sintering in the presence of a liquid phase. It was suggested that during the dissolution of small grains and growth on larger grains, a solid solution in equilibrium with liquid phase was observed to precipitate on the growing grains. Hence a core will have the original composition while the shell will have the composition of the newly formed solid solution.

Near-theoretical densities (~96%) were achieved when the ZrO_2-modified $BaTiO_3$ samples were sintered in the range of 1300 to 1320°C for 2 h. Microstructural observation of the as sintered surfaces revealed a near-uniform grain size as indicated for the modified $BaTiO_3$ sintered at 1320°C (Figurre.2.16 a). The average grain size of the specimen shown in Figure.2.16a is 0.43 µm. The grain size decreased to 0.36 µm at 1310°C and further to 0.28 µm when the specimens were sintered at 1300°C. TEM evaluation of the microstructure showed the distribution of ZrO_2 to be non-uniform, residing primarily at the grain boundaries.

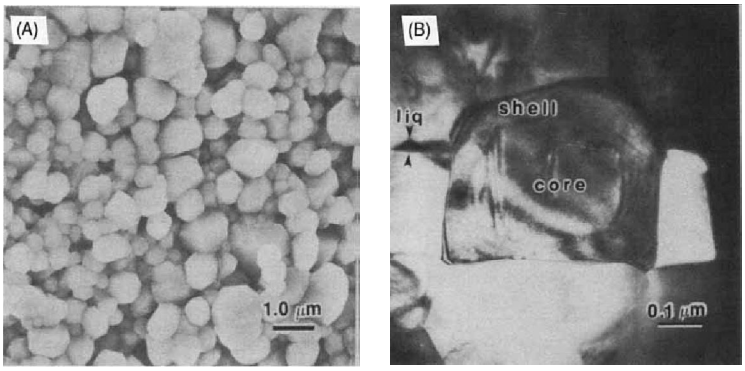

Fig.2.16:(a) Microstructural images of $BaTiO_3$ modified with 2.0 wt% ZrO_2 SEM image of typical as-sintered surface and (b) TEM image of core-shell grain.[32]

Some ZrO_2 diffusion into the $BaTiO_3$ lattice could, however, be inferred from the slight downshift in the Curie peak. Asshown in Figure.2.16 (b), incorporation of the ZrO_2into the $BaTi0_3$ at 1320°C coincided with the formation of core-shell grains in the microstructure and with liquid formation in the $BaTiO_3$ during sintering [32], as indicated by the arrows in Figure.2.16(b). Samples sintered at 1320°C were comprised of approximately 50 vol% core-shell grains while the ZrO_2modified $BaTiO_3$ sintered at 1310°C had only *5* vol% of such grains and samples sintered at 1300°C had none. The X-ray intensity distribution, derived from EDS data, of Zr from a typical core-shell grain is shown in Fig.2.17. It can be seen that the relative concentration of Zr decreases as the core is approached and that no Zr is present in the core. The core-shell grains contain, therefore, a core of pure $BaTiO_3$ surrounded by a shell of Zrmodified $BaTiO_3$ [32].

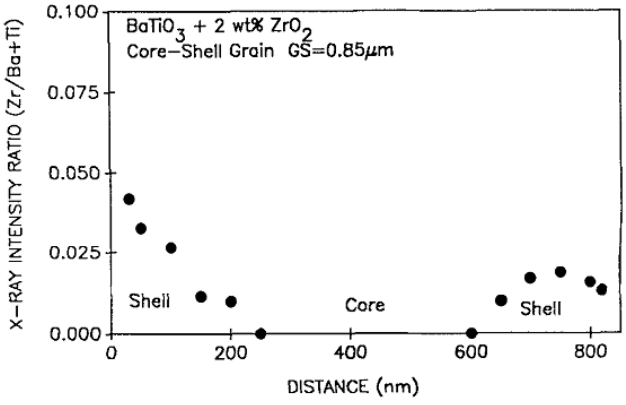

Fig.2.17: X-ray intensity ratio showing Zrdistribution across typical core-shell grain[32]

CHAPTER 3
EXPERIMENTAL

3.1 Introduction:

For quality research, it is very important to use high purity raw materials. Another vital thing during sample preparation is to remain careful so that no impurity gets incorporated into the samples. Finally, during all experimentsstarting from sample preparation to property measurement, all parametersshould be maintained for getting good consistent results.

3.2 Raw materials and their characterization

$BaTiO_3$with an average particle size of 100nm and purity of 99.99% (manufactured by Inframat-USA) and$Ta_2O_5$with an average particle size of 200nmand purity of 99.95% (manufactured by Inframat-USA) were used as the starting powders for the research.

Table 3.1: Element information

Components	Atomic number	Atomic weight	Molecular weight	Density (gm/cc)
Barium (Ba)	56	137.33	-	3.51
Titanium (Ti)	22	47.67	-	4.506
Tantalum (Ta)	73	180.94	-	16.69
Oxygen (O)				
Barium Titanate($BaTiO_3$)	-	-	233.00	6.02
Tantalum Oxide (Ta_2O_5)	-	-	441.89	8.20

3.3 sample preparation

3.3.1 Weight measurement

Depending on the various compositions, 30gram batches of powders were weighed according to the following table.

Table 3.2: Raw powder requirements for formulation of samples

Doping level	Powder	Wight of powder in 30 gmbatch
0.5%	$BaTiO_3$	29.71
	Ta_2O_5	0.29
1.0%	$BaTiO_3$	29.44
	Ta_2O_5	0.56
1.5%	$BaTiO_3$	29.16
	Ta_2O_5	0.84

3.3.2 Ball milling

The purpose of milling was to homogenize the starting powders. For the milling purpose, a milling pot made of high density Polyethyline (HDPE) and Y_2O_3-stabilized zirconia balls(dia=5mm and 3mm)were used. Acetone (purity>99%) was used as milling media during the milling operation. The milling operation was carried out using a locally made motor driven ball mill and the milling was carried out for 18-20hours.After the milling operation the powders were kept at 100^0C for 30 to 60 minutes to make sure that all the acetone and moisture are completely removed. Afterwards, the powders were taken for pressing.

3.3.3 Preparation of binder

PVA or polyvinyl alcohol was used as binder. To make binder solution, at first 3-3.5gram PVA was added to 50 milliliter of water. Then it was placed on a hot plate and stirred continuously until the PVA pellets dissolved in water completely. During stirring, temperature is kept below 80°C to avoid agglomeration.

3.3.4 Pressing

Milled powder was mixed with PVA and then dried in oven at 100°C before pressing into pellets. Samples were pressed into disks using pressure of ~ 150MPa for all the samples using hydraulic press. At highest pressure level, holding time was 2 minutes. Green samples were not made thick to avoid density variation.

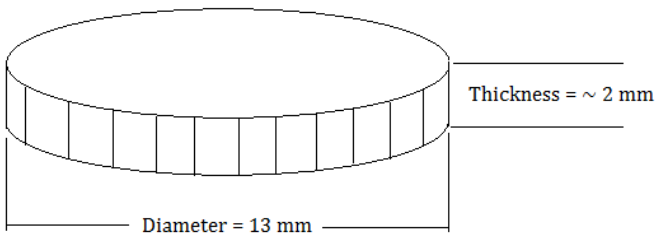

Fig. 3.1: The powder compacts after pressing

3.3.5 Drying and binder removal

After pressing the discs were kept at 110°C for about 3 hours to remove any moisture present within the discs.

After drying the sample discs were put into sintering furnace with a suitable sintering cycle. It should be kept in mind that the binder is removed at this stage. At about 450 to 500°C the binder is removed upon soaking for 1 hour.

Control of heating rate is crucial at this stage to avoid warping of sample at high temperatures. Sintering is marked with temperature and soaking time. Proper combination of these two is required to achieve optimum densification and close to percent theoretical density.

3.4 Sintering

A number of cycles were applied to compacts of various compositions which varied principally on the sintering temperature and soaking time. The temperature and the soaking time were modified progressively as the experiment proceeded on trial and error basis.The dwell time at the primary stages are for the removal of binder. Usually binders' boiling point is 300^0C. Hence holding at 450°C is well enough to get the binder off of the disc. Up to this point it is important to keep the heating rate low otherwise during binder burning sample will crack down. Depending upon the composition and the samples' tendency to warp during sinter the heating rate may be changed at each stage.

.

(a) (b)

Fig. 3.2: Experimental setup for sample preparation (a) Hydraulic press for pelletizing, (b) High temperature furnace for sintering

3.5 Property measurement

3.5.1 Percent theoretical density

After sinteringoperation, sample's dimensions were measured e.g. thickness and diameter using a micrometer. Then the sample was weighed using electrostatic balance. From these data densities were calculated. These resultant densities were then compared to the theoretical densities and expressed in terms of percent theoretical density. Theoretical densities are listed below for the tested compositions.

Table 3.3: Theoretical densities of different composition

Material	Theoretical density (gm/cc)
$BaTiO_3$ doped with 0.5% Ta_2O_5	6.0309
$BaTiO_3$ doped with 1.0% Ta_2O_5	6.0418
$BaTiO_3$ doped with 1.5% Ta_2O_5	6.0527

3.5.2 Microstructure analysis using FE-SEM

The SEM analysis was conducted using the FE-SEM (JEOL JSM-7600F) facility available at GCE, BUET. Since the sintered samples were meant to be observed under FE-SEM which is a very powerful tool, no further samplepreparation was needed for the analysis. The FE-SEM is such a strong tool that it is capable of revealing the grains and the boundaries among them without the help of any etching given that a proper sintering cycle is operated.

3.5.3 Dielectric property measurement

Dielectric properties of samples were measured using an in impedance analyzer [WAYNE KERR 6500B series] at GCE, BUET. All the measurements were subject to AC current only. Both room temperature and high temperature frequency dependency were measured. Dielectric constant was measured from the capacitance value obtained from the analyzer according to equation as below –

$$K' = C_p d / \varepsilon_o A$$

Where k' is the dielectric constant, $C_p$is the capacitance value measured by the impedance analyzer, d is the thickness of the sample, $\varepsilon_o$is the permittivity of vacuum, A is the area of the sample in contact with the conducting layer.

Fig. 3.3:Experimental setup for characterization and dielectric property measurement (a) FE-SEM for microstructural analysis, (b) Impedance analyzer for dielectric property measurement

3.5.4X ray Diffraction (XRD) analysis

X-ray diffractionanalysis was conducted using the XRD (Bruker D8 Advance) facility available at BCSIR, Dhaka in order to determine the phases present in the samples.

Fig. 3.4: XRD Machine

CHAPTER 4
RESULTS AND DISCUSSION

4.1 Overview of experiments

Initially, the experiments were conducted using single stage sintering in the temperature range of 1250-1300^{0}C for 2hours. The aim of the experiments was to determine a suitable temperature range over which double stage sintering could be conducted.

From the experiments it was revealed that, sintering at 1250^{0}C for 2hours proved to be insufficient for 0.5-1.5 mole% Ta_2O_5 doped $BaTiO_3$ samples. All samples had moderate %theoretical density and fine grain size. As a result, the dielectric properties of those samples were very poor. The situation remained same for 0.5-1.5 mole% Ta_2O_5 doped $BaTiO_3$samples sintered at 1275^{0}C for 2hours. However, sintering at 1300^{0}C for 2 hours revealed some aspiring results. For, 0.5 mole% Ta_2O_5 doped $BaTiO_3$ sample, this sintering condition proved to be ideal because the sample showed good %theoretical density and optimum grain size. As a consequence, it exhibited decent dielectric properties. Butaxx, the sintering condition still was not sufficient for 1.0-1.5mole% Ta_2O_5 doped $BaTiO_3$samples as they exhibited moderate %theoretical density and fine grain size.

Generally, dopants need very low to almost no energy to concentrate at the grain boundaries. However, energy is required to incorporate a dopant ion into an individual lattice site in complex oxides. The amount of energy required is related to distortions, i.e. difference in ionic radii, and the formation of compensating defects during the incorporation of aliovalent ions that have different valence states [14]. Thus, more energy was required in our research for diffusion of the dopants to move inwards from the grain boundary into the lattice and to reduce pinning effect. The required energy could have been supplied by increasing the dwelltime of single stage sintering. But, this path would lead to exaggerated grain growth of the sintered samples and deterioration of dielectric properties. As a result, further research was focused on double stage sintering.

From these experiments with single stage sintering, it was clear that double stage sintering near 1300^{0}C can improve the microstructure and dielectric properties of Ta_2O_5 doped $BaTiO_3$samples.

So, at the first phase of experiments using double stage sintering, 1320^{0}C was set as the first stage sintering temperature and 1280^{0}C was set as the second stage sintering temperature. The dwell time at first stagesintering was 0hrs, but for second stage sintering the dwell time was varied between 4-6hours. The reason for increasing the dwell time at second stage sintering was to develop optimum microstructure without allowing grains to grow excessively.

The experiments conducted with double stage sintering gave positive results. From those experiments, best combination of microstructure and dielectric properties was obtained for 1.5 mole% Ta_2O_5 doped $BaTiO_3$ sintered at 1320^{0}C for 0hours and 1280^{0}C for 6hours. But, there were

scopes of further improvement.

So, at the final phase of experiments using double stage sintering, first sintering temperature of double stage sintering was varied between 1300-1310^{0}C and thesecond stage sintering temperature was kept constant at 1280^{0}C. Like before, dwell time at first stage of sintering was 0hrs and dwell time at second stage sintering was varied between 4-6 hours. From all the experiments, best combination of microstructure and dielectric properties was obtained for 1.5 mole% Ta_2O_5 doped $BaTiO_3$ sintered at 1310^{0}C for 0hours and 1280^{0}C for 6hours.

4.2 Experiments conducted with single stage sintering

4.2.1Summary of the key experiments

Numerical data of the effect of single stage sintering on %theoretical density (%TD) andaverage grain size of Ta_2O_5 doped $BaTiO_3$ samples are tabulated in Table 4.1.

Table 4.1: Parameters of single stage sintering and their effect on %theoretical density and average grain size

SI No:	Sintering rate (^{0}C/min)	Sintering temperature (^{0}C)	Dwell time (Hours)	Cooling rate (^{0}C/min)	Doping mole %	%TD	Avg. grain size (µm)
1	15	1250	2	3	0.5	91.0	0.43
2	15	1250	2	3	1.0	90.5	0.33
3	15	1250	2	3	1.5	88.0	0.24
4	15	1275	2	3	0.5	91.7	0.58
5	15	1275	2	3	1.0	91.6	0.41
6	15	1275	2	3	1.5	90.0	0.29
7	15	1300	2	3	0.5	93.8	1.10
8	15	1300	2	3	1.0	92.0	0.50
9	15	1300	2	3	1.5	91.5	0.34

From Table-4.1 it can be seen that, for a particular mole% of Ta_2O_5 doping, %theoretical density and grain size of the Ta_2O_5 doped $BaTiO_3$ samples increased with increasing temperature. However, at a particular temperature, increase of Ta_2O_5 mole% resulted in lowering of both %theoretical density and grain size.

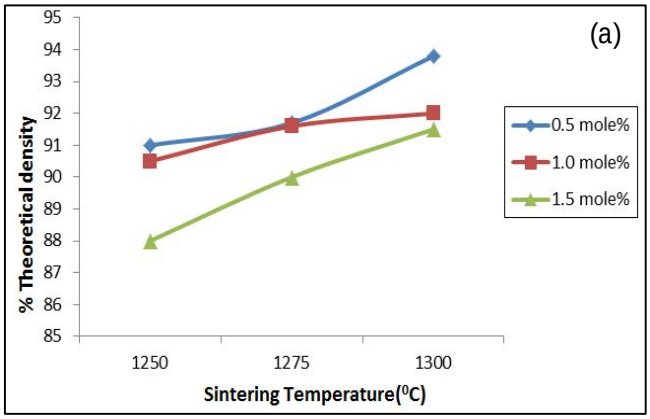

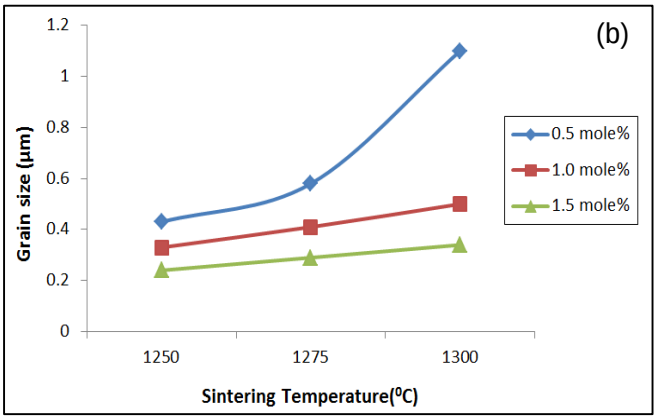

Fig. 4.1:(a) Variation of %theoretical density with sintering temperatureof single stage sintering, (b) Variation of average grain size with sintering temperature of single stage sintering

From Figure 4.1(a-b) it can be seen that, for 1.0 and 1.5 mole% Ta_2O_5 doped $BaTiO_3$ samples, % theoretical density and average grain size gradually increased with increase of sintering temperature of single stage sintering.

However, for 0.5 mole% Ta_2O_5 doped $BaTiO_3$ sample the trend was different. %Theoretical density and average grain size gradually increased up to 1275^0C. But, at 1300^0C, there was a sharp increase of both %theoretical density and average grain size. The results are consistent with the findings ofDrofenik and his colleagues according to whom anomalous grain growth is frequently encountered during the sintering of $BaTiO_3$ doped below the critical dopant concentration [33].

4.2. 2 Development of microstructure

Figure4.2 shows SEM micrograph of 0.5-1.5 mole% Ta_2O_5 doped $BaTiO_3$ samples sintered at 1250^0C for2hours. Due to unviability of SEM facility at MME (BUET), the samples were sent to JEOL, Singapore for SEM analysis. Unfortunately, the received images were of very high magnification(X50,000) and could not be used forproper establishment of structure property relationship. In the above circumstances, all the experiments wereagain repeated and this time around, the SEM analysis was conducted at lower magnification (X20,000)using the newly installed FE-SEM facility at GCE, BUET.

It is clearly evident from Figure 4.2(a-c) and 4.3(a-c) that all Ta_2O_5 doped $BaTiO_3$ samples sintered at 1250^0C for2hours showed fine grain size. For 0.5 mole% Ta_2O_5 doped $BaTiO_3$ sample, there were no sign of bimodal grain size distribution and the average grain size was around 0.43 micron. The

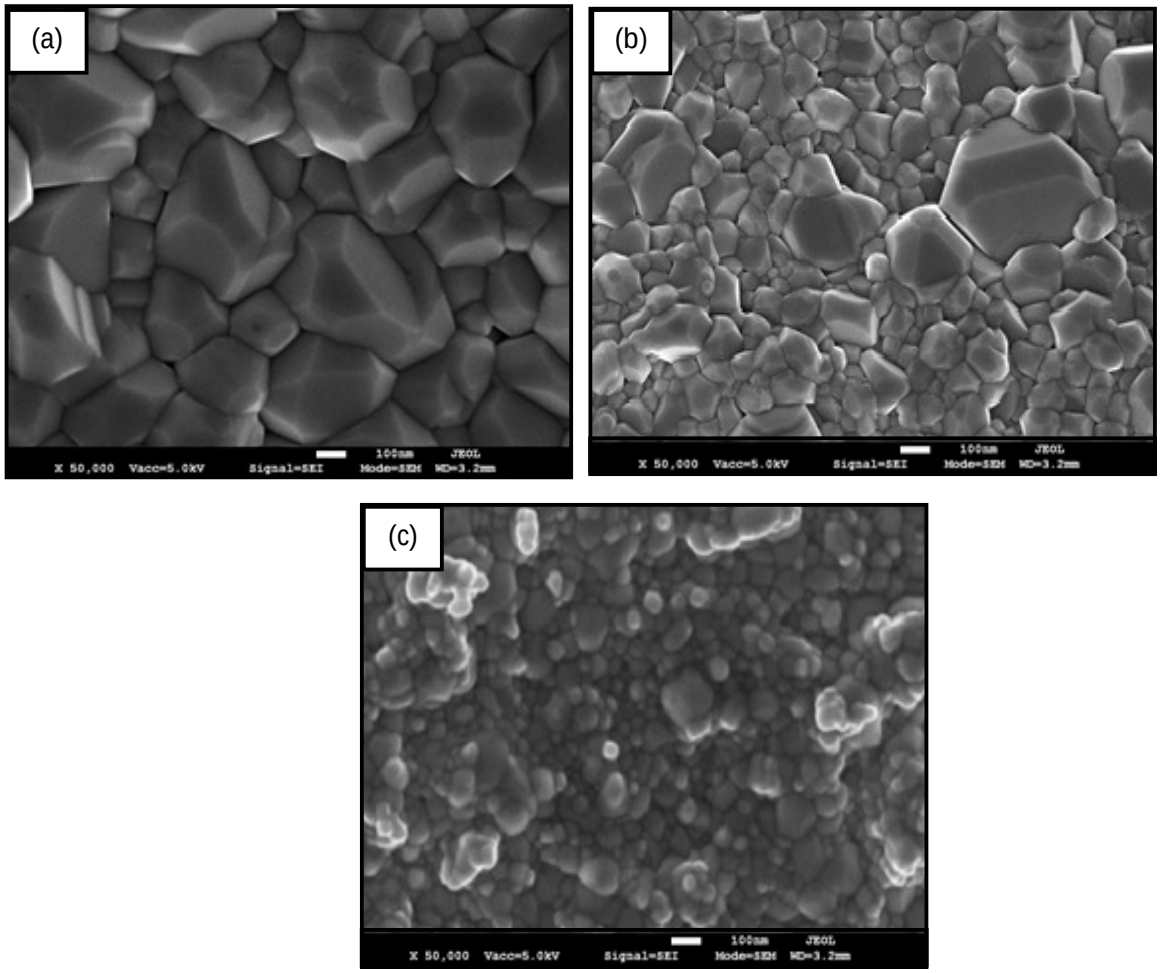

Fig. 4.2: SEM micrographs (X 50,000) of Ta_2O_5doped $BaTiO_3$ samplessintered at 1250^0C for 2hrs:(a) 0.5 mole%, (b) 1.0 mole% and (c) 1.5 mole%.

Sample also showed decent %theoretical density. But, with increase of doping level, average grain size of the samplesstarted to decrease due to the pinning effect of Ta_2O_5. For 1.0 mole% Ta_2O_5 doped $BaTiO_3$ sample, the average grain size dropped to 0.33 micron and there were clear evidence of bimodal grain size distribution. The sample also showed low %theoretical density.For 1.5 mole% Ta_2O_5 doped $BaTiO_3$ sample, the pinning effectwas so severe that it resulted in further reduction of both average grain size and %theoretical density. All these results are in coherence with the findings of M. N. Rahman and R. Manalert who concluded that the amount of pentavalent oxide dopants controls the microstructure of Ta_2O_5 doped $BaTiO_3$ samples.For the penta-valance donor cations, grain boundary mobility initially increases with cation concentration but then decreases significantly above a doping threshold of 0·3-0·5 mole % [16].

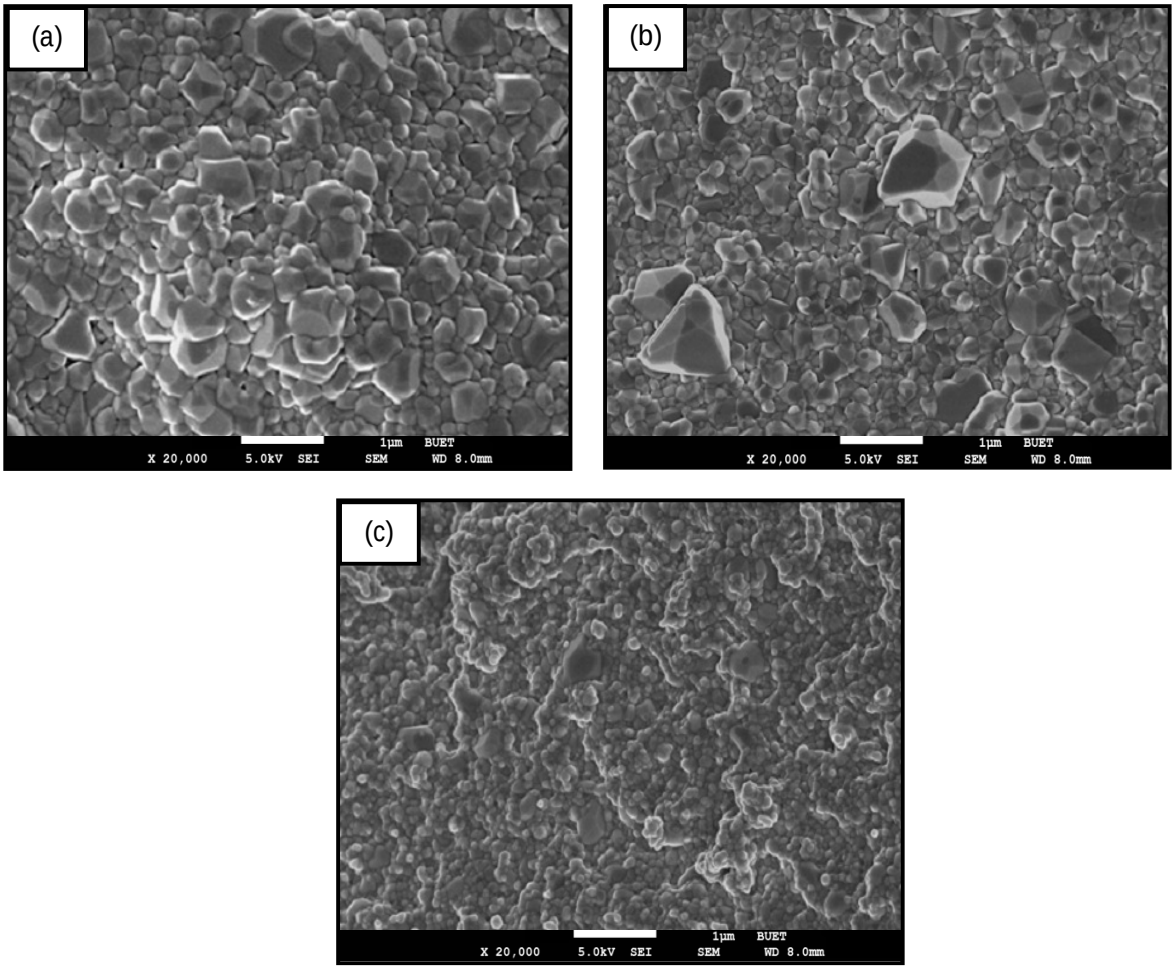

Fig.4.3: SEM micrographs (X 20,000) of Ta_2O_5doped $BaTiO_3$ samplessintered at 1250^0C for 2hrs: (a) 0.5 mole%, (b) 1.0 mole% and (c) 1.5 mole%.

Figure 4.4 shows the higher magnification SEM micrographs of 0.5-1.5mole% Ta_2O_5 doped $BaTiO_3$ samples sintered at 1275^0C for 2hours (Figure 4.4).Due to the increase of sintering temperature, the average grain size of all the samples was larger than samples sintered at 1250^0C for 2hours and showed better %theoretical density.

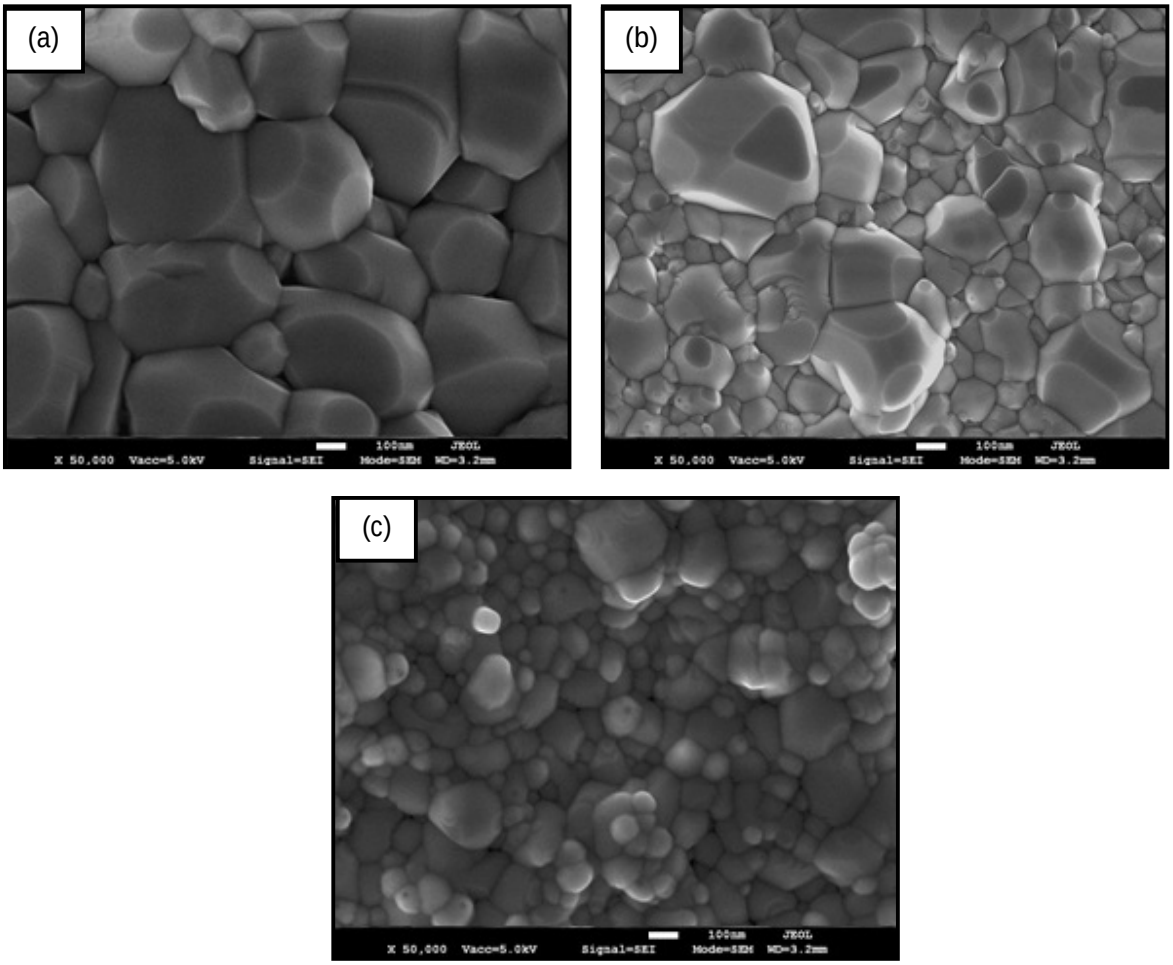

Fig.4.4: SEM micrographs (X 50,000) of Ta_2O_5 doped $BaTiO_3$ samplessintered at 1275^0C for 2hrs: (a) 0.5 mole%, (b) 1.0 mole% and (c) 1.5 mole%

However, the trend of microstructure development remained same which is clear from the SEM micrographs of lower magnification at the same sintering condition [Figure 4.5(a-c)]. It can be seen that, with increase of doping level there was a reduction of average grain size of the samples.

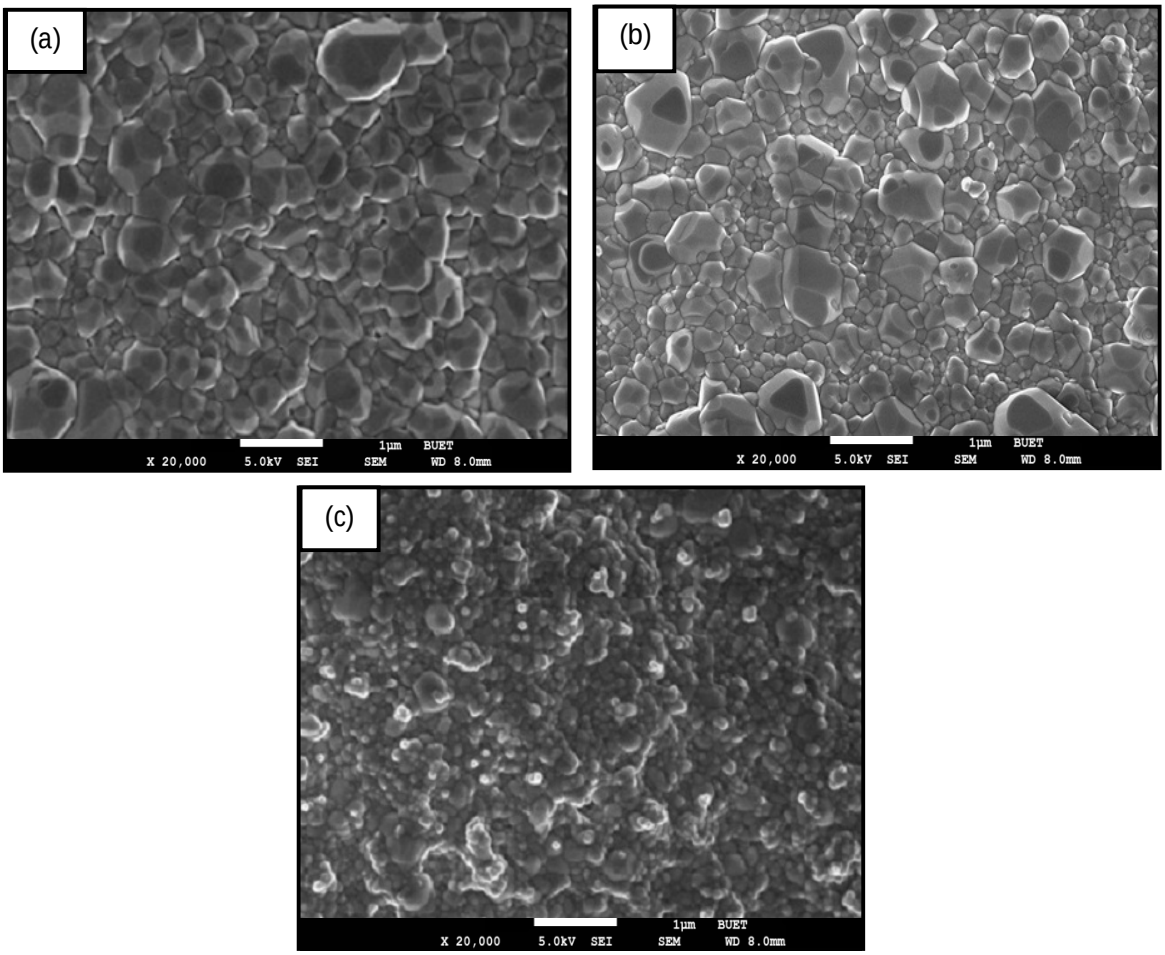

Fig.4.5: SEM micrographs (X 20,000) of Ta_2O_5 doped $BaTiO_3$ samplessintered at 1275^0C for 2hrs: (a) 0.5 mole%, (b) 1.0 mole% and (c) 1.5 mole%

Figure 4.6 shows the SEM micrographs of higher magnification for all Ta_2O_5 doped $BaTiO_3$ samples sintered at 1300^0C for 2hours. Due to the increase of sintering temperature, the average grain size of all the samples was larger than samples sintered at 1275^0C for 2hours and showed better %theoretical density.

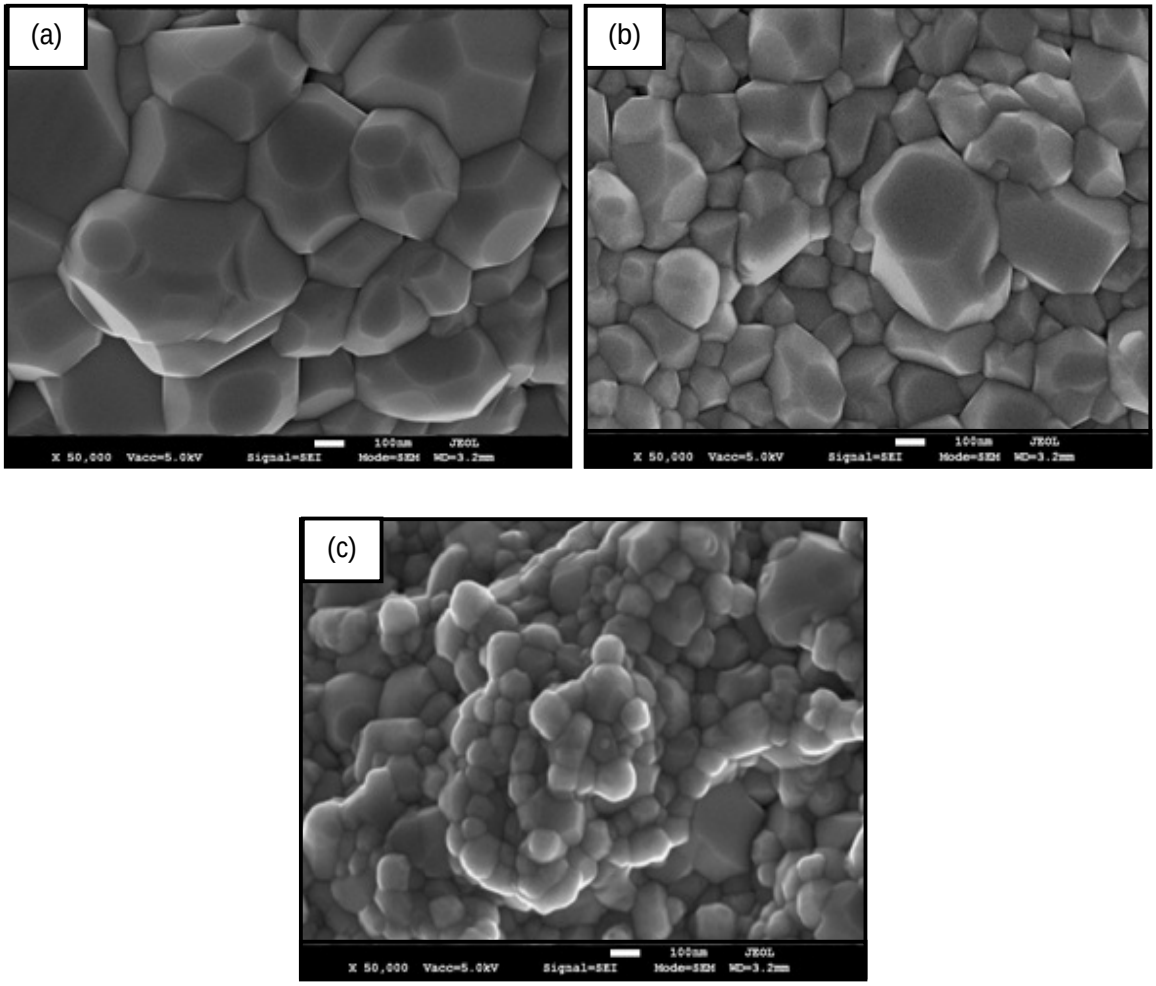

Fig.4.6: SEM micrographs (X 50,000) ofTa_2O_5 doped $BaTiO_3$ samplessintered at 1300^0C for 2hrs: (a) 0.5 mole%, (b) 1.0 mole% and (c) 1.5 mole%.

However, the trend of microstructure development remained same which is clear from the SEM micrographs of lower magnification at the same sintering condition [Figure 4.7(a-c)]. At 1300^0C, 2hours of the dwell time proved to be sufficient for 0.5 mole% Ta_2O_5 doped $BaTiO_3$ sample. Optimum average grain size of around 1 micron resulted in good % theoretical density of the sample (Figure 4.7a) [3-4]. But, for 1.0-1.5 mole% Ta_2O_5 doped $BaTiO_3$ samples, the sintering condition again proved to be inadequate and resulted in samples with fine grain size and poor %theoretical density [Figure 4.7(b-c)].

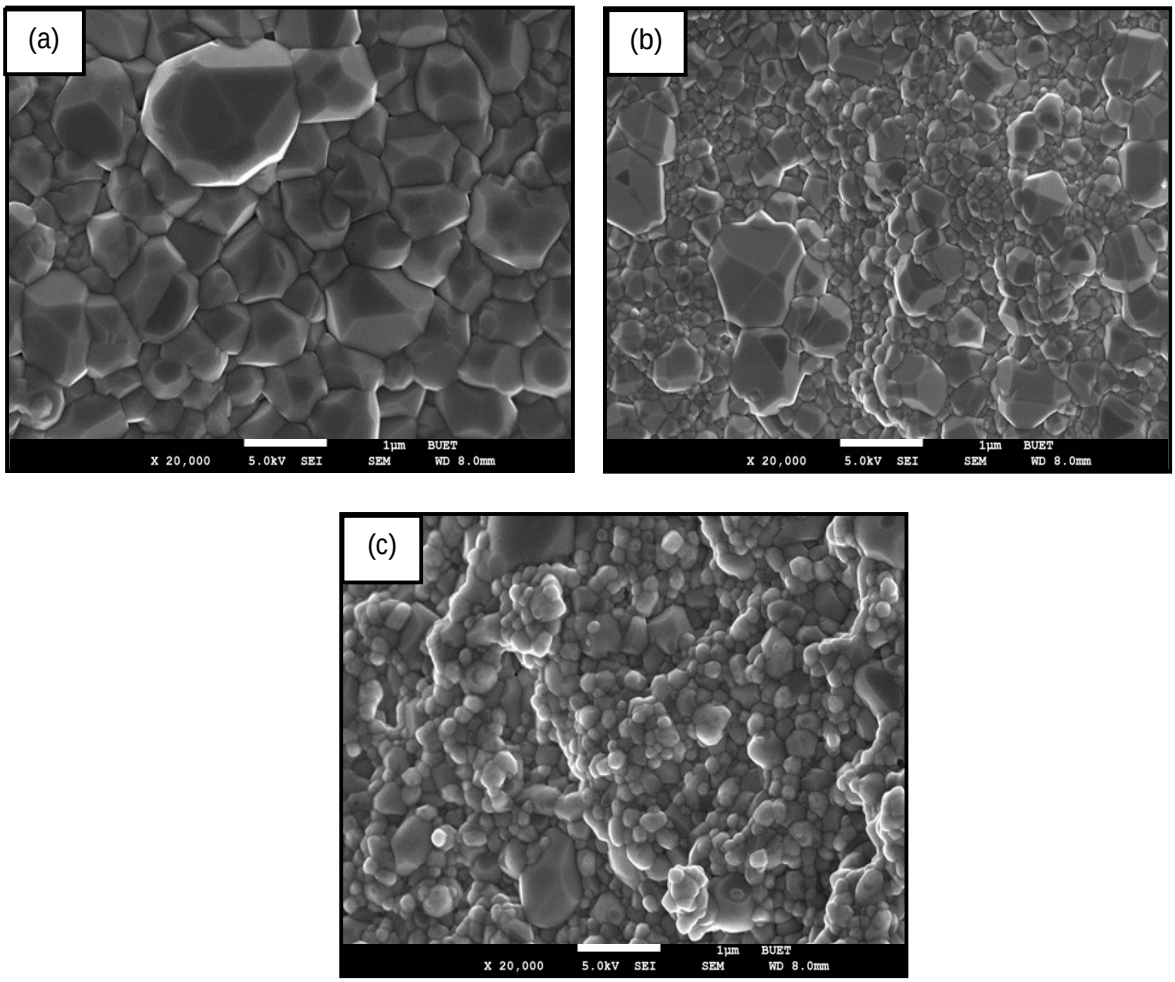

Fig.4.7: SEM micrographs (X 20,000) of Ta_2O_5 doped $BaTiO_3$ samplessintered at 1300^0C for 2hrs:(a) 0.5 mole%, (b) 1.0 mole% and (c) 1.5 mole%.

4.2.3 Dielectric Property Measurement

Figure4.8 shows variation of room temperature dielectric constant of Ta_2O_5 doped $BaTiO_3$ samples with sintering temperature measured at 10kHz frequency.It can be seen that, for 1.0 and 1.5 mole% Ta_2O_5 doped $BaTiO_3$ samples values of room temperature dielectric constant gradually increased with increasing sintering temperature. But, unfortunately dielectric constant values of all these samples were not that satisfactory because the combination of average grain size and % theoretical density of these samples were not up to the mark.

On the other hand, for 0.5 mole% Ta_2O_5 doped $BaTiO_3$ samples value of room temperature dielectric constant gradually increased with increasing sintering temperature upto1275^{0}C. However, at 1300^{0}C, value of dielectric constant drastically increased to around 11,000.

Dielectric constant of pore space is very low [17]. As %theoretical density increases, it results in lowering of porosity content. So, sample with high %theoretical density shows better dielectric response. On the other hand, fine grained pure $BaTiO_3$samples exhibitpoor dielectric constant at room temperature. With increase of average grain size up to 1 micron, value of dielectric constant increases.But,when average grain size increases above 1 micron, dielectric constant again starts to decrease[3-4,17].

Since, 0.5 mole% Ta_2O_5 doped $BaTiO_3$ exhibited good %theoretical density and optimum average grain size near 1 micron, it exhibited dielectric constant of around 11,000.

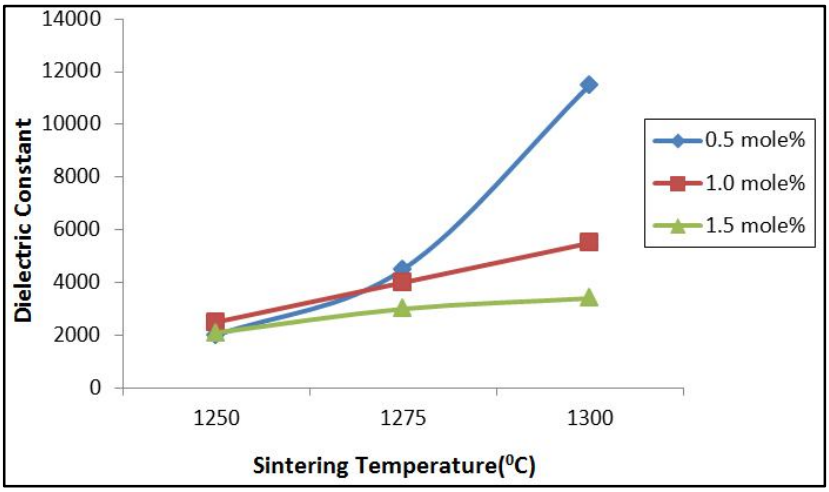

Fig. 4.8: Variation of dielectric constant with sintering temperature of single stage sintering

4.3 Experiments conducted with double stage sintering (Part- 1)

4.3.1Summary of the key experiments

Numerical data of the effect of double stage sintering on %theoretical density (*%TD*) andaverage grain size of Ta_2O_5 doped $BaTiO_3$ samples are tabulated in Table 4. 2.

Table 4.2: Parameters of double stage sintering and their effect on %theoretical density andAverage grain size

SI No:	Sintering rate (^{0}C/min)	Sintering temperature and dwell time (1st stage)	Sintering temperature and dwell time (2nd stage)	Cooling rate (^{0}C/min)	Doping mole %	%TD	Avg. grain size (μm)
1	15	1320^{0}C for 0 hrs	1280^{0}C for 4hrs	3	0.5	95.0	1.80
2	15	1320^{0}C for 0 hrs	1280^{0}C for 4hrs	3	1.0	93.0	1.30
3	15	1320^{0}C for 0 hrs	1280^{0}C for 4hrs	3	1.5	91.0	1.10
4	15	1320^{0}C for 0 hrs	1280^{0}C for 6hrs	3	0.5	93.5	1.90
5	15	1320^{0}C for 0 hrs	1280^{0}C for 6hrs	3	1.0	92.1	1.40
6	15	1320^{0}C for 0 hrs	1280^{0}C for 6hrs	3	1.5	92.9	1.20

From Table 4.2 it can be seen that, for 0.5 and 1.0 mole% Ta_2O_5 doped $BaTiO_3$ samples,%theoretical density decreased and average grain size increased with increase of dwell time of second stage sintering from 4hours to 6hours. However, for 1.5 mole% Ta_2O_5 doped $BaTiO_3$ samples, %theoretical density and average grain size both increased with increase of dwell time of second stage sintering from 4hours to 6hours.

From Figure 4.9, it is visible that, 1.5 mole% Ta_2O_5 doped $BaTiO_3$ sample sintered at 1320^0C for 0hours and 1280^0C for 6hours exhibited good dielectric propertiesdue to the combination of good%theoretical density and average grain sizenear optimum grain size [3-4, 17].Although 0.5mole% Ta_2O_5 doped $BaTiO_3$ sample sintered at 1300^0C for 2hours exhibited almost similar combination of %theoretical density and average grain size, but in this case room temperature dielectric constant was enhanced due the combination of grain size refinement and substitution of Ta^{5+}ion in $BaTiO_3$ lattice.

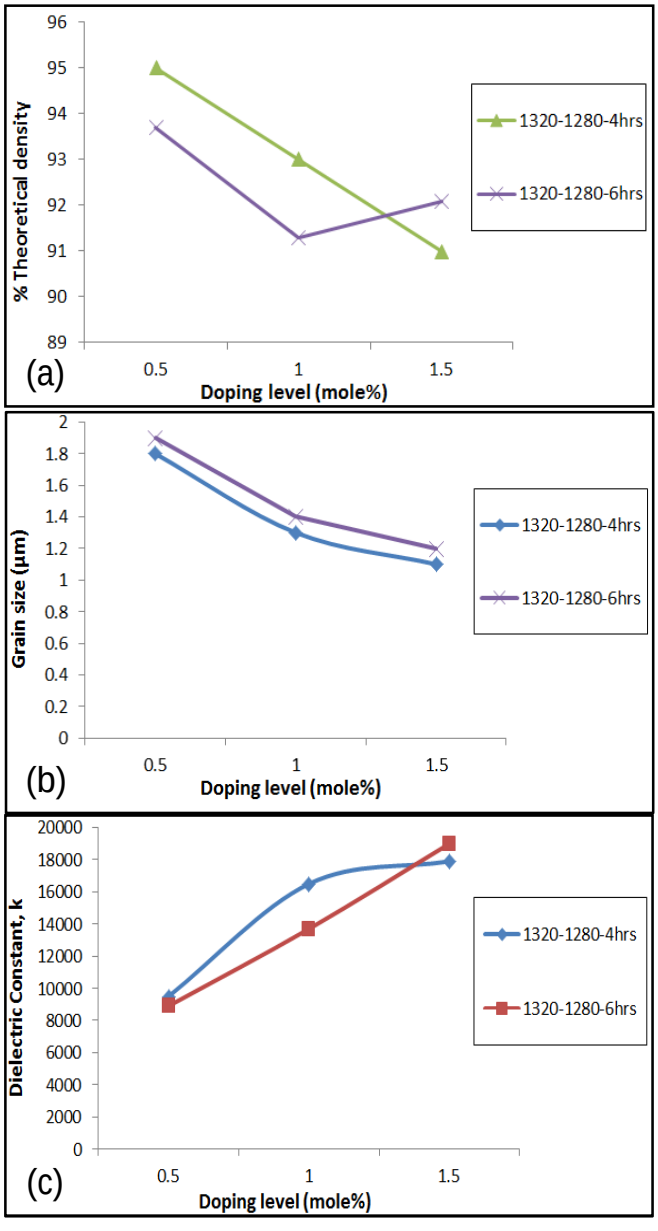

Fig. 4.9: (a) Variation of %theoretical density with doping level (mole%), (b) Variation of average grain size with doping level (mole%), (c) Variation of room temperature dielectric constant with doping level (mole%)

4.3.2Development of Microstructure

Figure 4.10shows the higher magnification SEM micrographs of 0.5-1.5 mole% Ta_2O_5 doped $BaTiO_3$ samples sintered at 1320^0C for 0hoursand 1280^0C for 4hours. It can be seen from Figure 4.10 that, average grain size of all the samples was larger than samples sintered with single stage sintering.

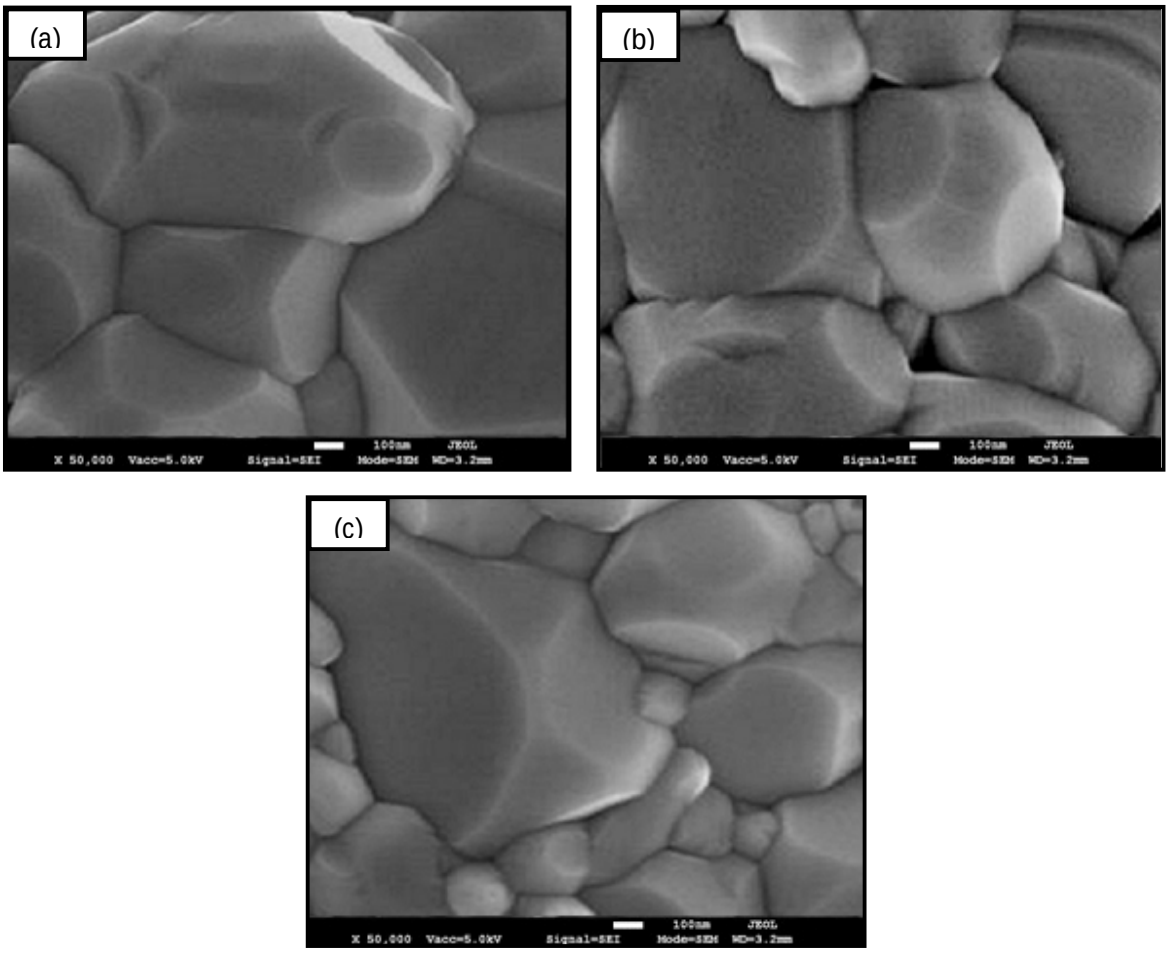

Fig.4.10: SEM micrographs (X 50,000) of Ta_2O_5 doped $BaTiO_3$ samplessintered at 1320^0C for 0hrs and 1280^0C for 4hrs:(a) 0.5 mole%, (b) 1.0 mole% and (c) 1.5 mole%

Figure 4.11shows the lower magnification SEM micrographs of 0.5-1.5 mole% Ta_2O_5 doped $BaTiO_3$ samples sintered at 1320^0C for 0hours and 1280^0C for 4hours.Figure 4.11a shows that for 0.5 mole% Ta_2O_5 doped $BaTiO_3$ sampleshowed exaggerated grain growth due to 4 hours of dwell time during second stage sintering. However the sample achieved high density.This phenomenon is clearly evident from the SEM micrograph of Figure 4.11a, which show no evidence of bimodal grain size distribution or pinning effect. However, for 1.0 mole% Ta_2O_5 doped $BaTiO_3$ sample, grain growth was not as severe as for 0.5mole% doped sample (Figure 4.11b). For 1.5 mole % Ta_2O_5 doped $BaTiO_3$ sample, 4 hours of dwell was not sufficient for complete diffusion of the dopants in the lattice and as a result, there was evidence of pinning effect (Figure 4.11c).

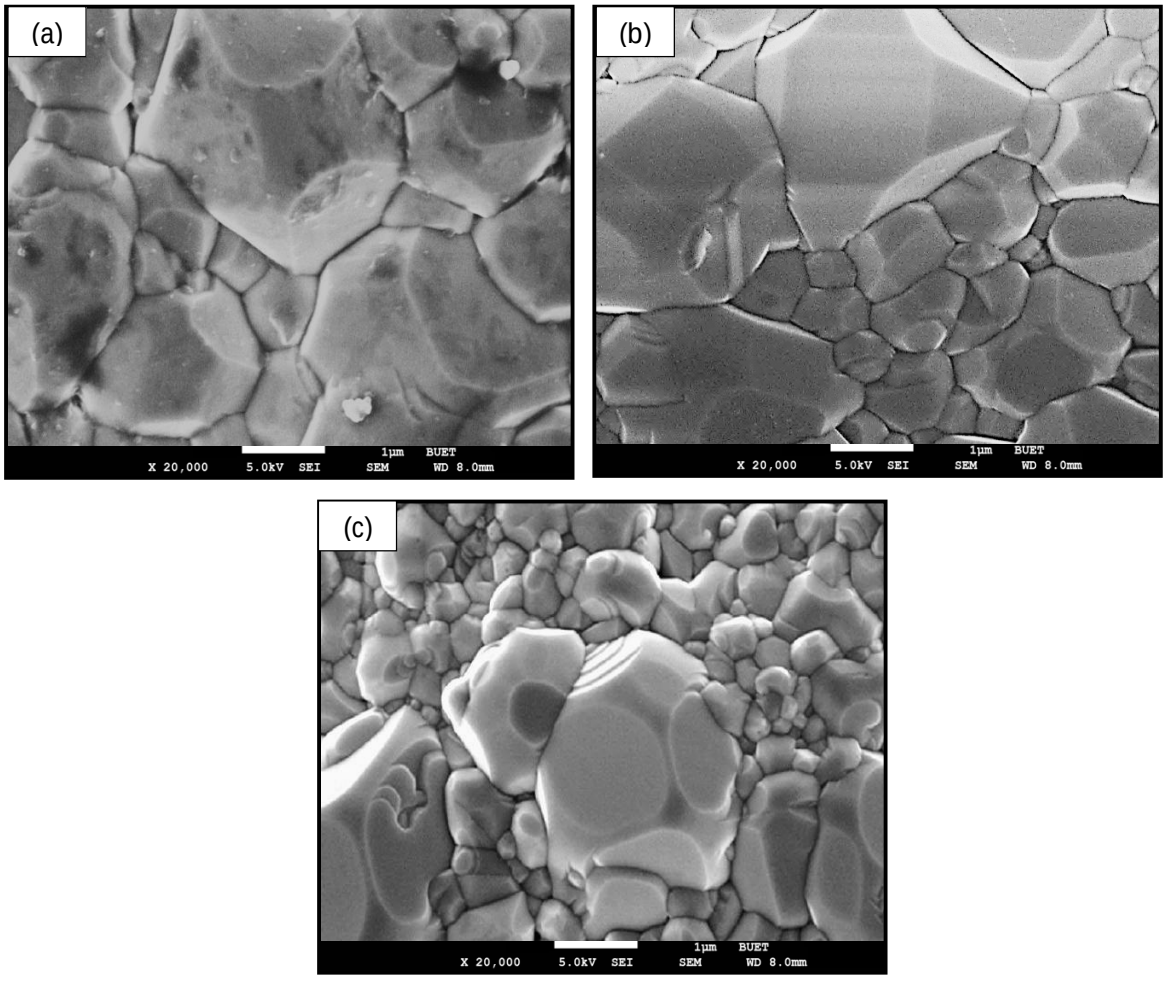

Fig.4.11: SEM micrographs (X 20,000) of Ta_2O_5 doped $BaTiO_3$ samplessintered at 1320^0C for 0hrs and 1280^0C for 4hrs: (a) 0.5 mole%, (b) 1.0 mole% and (c) 1.5 mole%

Figure 4.12shows the higher magnification SEM micrographs of 0.5-1.5 mole% Ta_2O_5 doped $BaTiO_3$ samples sintered at 1320^0C for 0hours and 1280^0C for 6hours. It can be seen from the figure that, average grain size of all the samples was larger than samples sintered with 4 hours of dwell time.

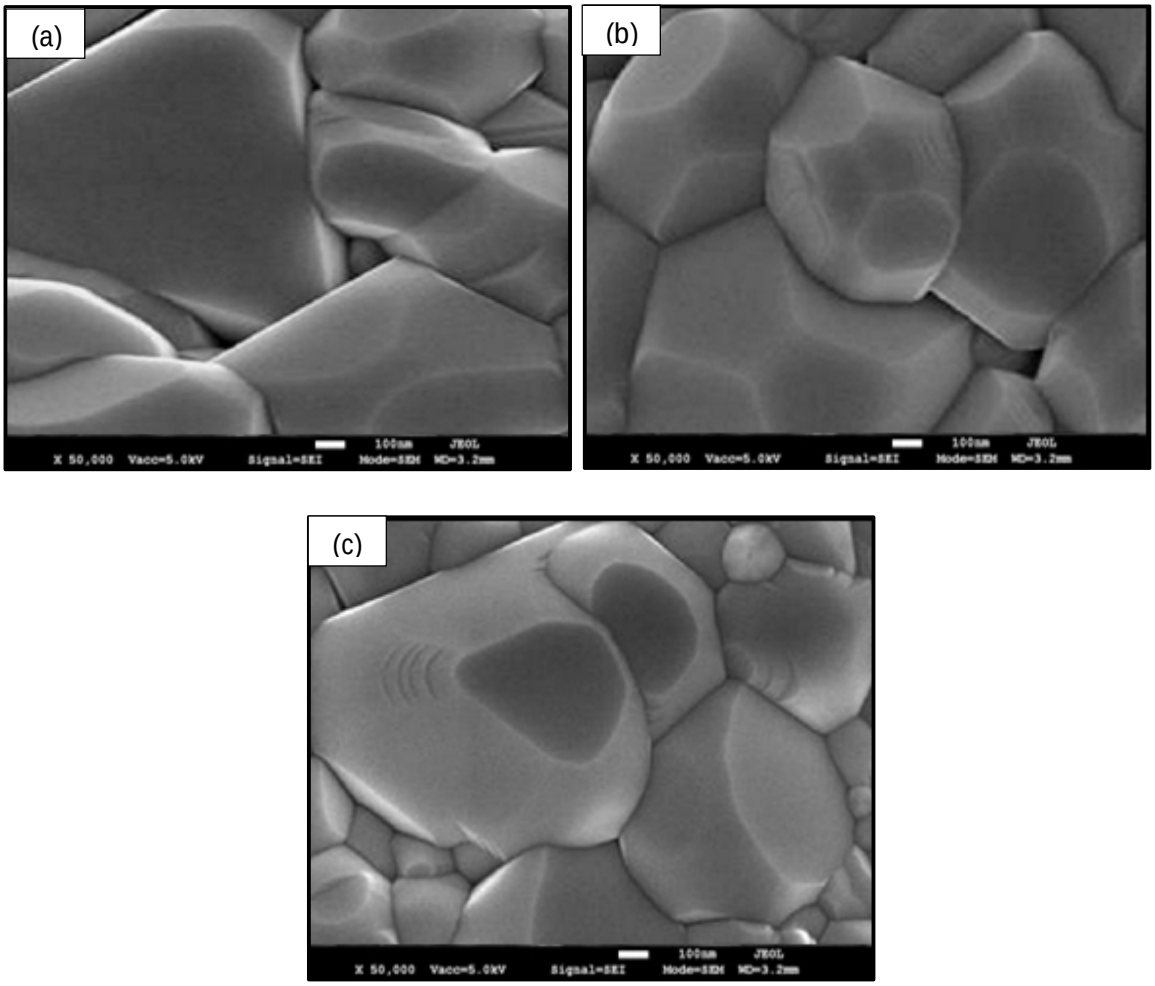

Fig.4.12: SEM micrographs (X 50,000) of doped $BaTiO_3$ samplessintered at 1320^0C for 0hrs and 1280^0C for 6hrs:(a) 0.5 mole%, (b) 1.0 mole% and (c) 1.5 mole%Ta_2O_5

Figure 4.13 shows the lower magnification SEM micrographs of 0.5-1.5 mole% Ta_2O_5 doped $BaTiO_3$ samples sintered at 1320^0C for 0hours and 1280^0C for 6hours. Figure 4.13a show that for 0.5 mole% Ta_2O_5 doped $BaTiO_3$ sample,6hoursdwell time excessivelyincreased the average grain size of the sample [17]. As a result, %theoretical density of the sample decreased due to dedensification [34-36]. However, under the same sintering condition, 1.0 mole % Ta_2O_5 doped $BaTiO_3$ sample showed controlled grain growth but larger than the sample sintered at previous sintering condition (Figure 4.13b). For 1.5 mole% Ta_2O_5 doped $BaTiO_3$ sample, even dwell time of 6hours showed signs of pinning effect. But, the grain size of the sample was slightly higher than the sample sintered at 4hrs of dwell time (Figure 4.13c).

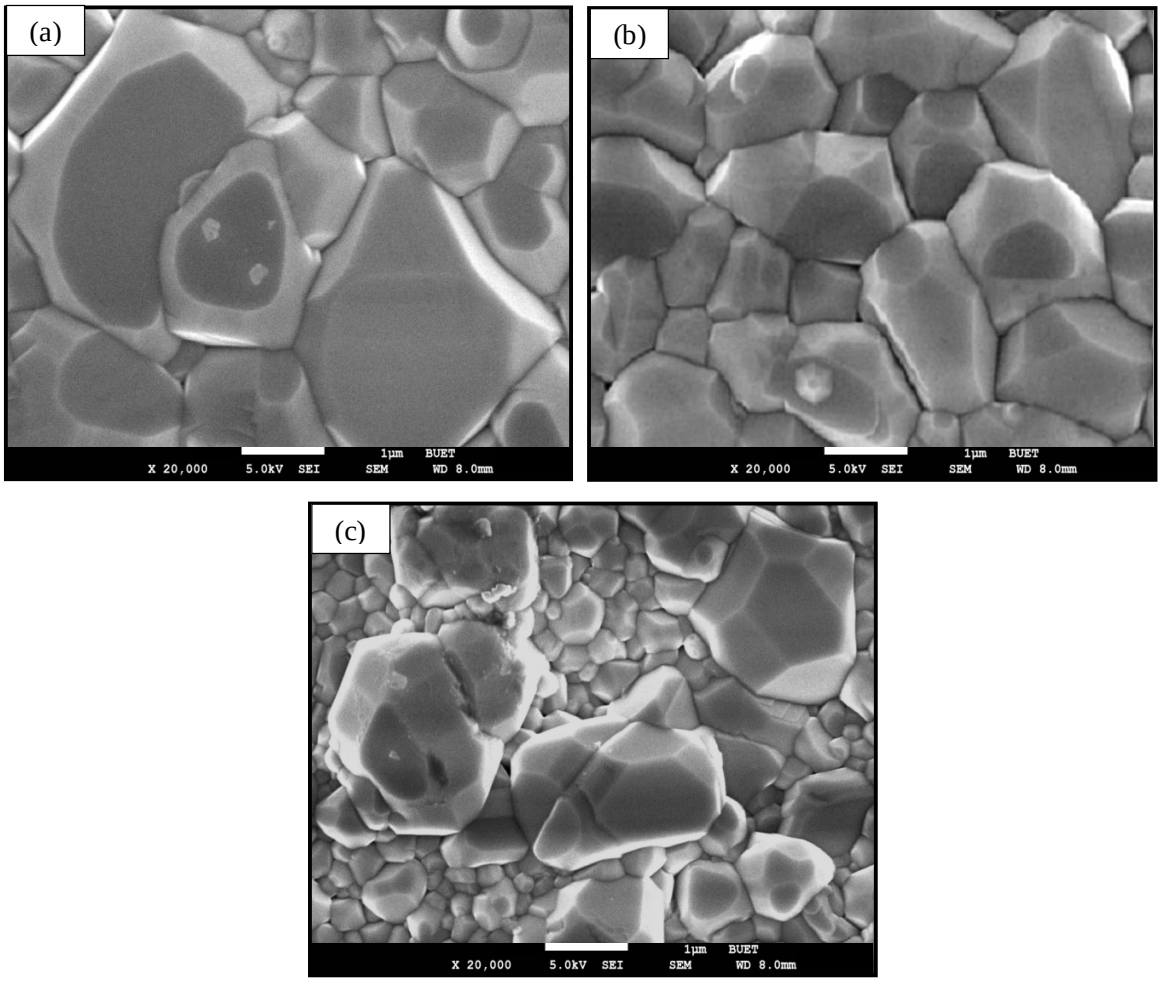

Fig.4.13: SEM micrographs (X 20,000) of doped $BaTiO_3$ samplessintered at 1320^0C for 0hrs and 1280^0C for 6hrs: (a) 0.5 mole%, (b) 1.0 mole% and (c) 1.5 mole%Ta_2O_5

4.3.3 Dielectric Property Measurement

Since 1.5mole% Ta_2O_5 doped $BaTiO_3$ sample sintered at 1320^0C for 0hours and 1280^0C for 6hours showed highest room temperature dielectric constant, its detailed dielectric properties were measured. From Figure4.14a it can be seen that, with increase of frequency, value of room temperature dielectric constant showed a decreasing trend which is in accordance with literature [17].Highest value of room temperature dielectric constant of 19000 was measured at 10kHz frequency. Figure 4.14b shows that for 1.5 mole% Ta_2O_5 doped $BaTiO_3$ sample, the Curie point was shifted to 84^0C whereas the Curie temperature (T_c) for pure $BaTiO_3$ is 120^0C. The best stable value of dielectric constant as a function of temperature was near 18000.

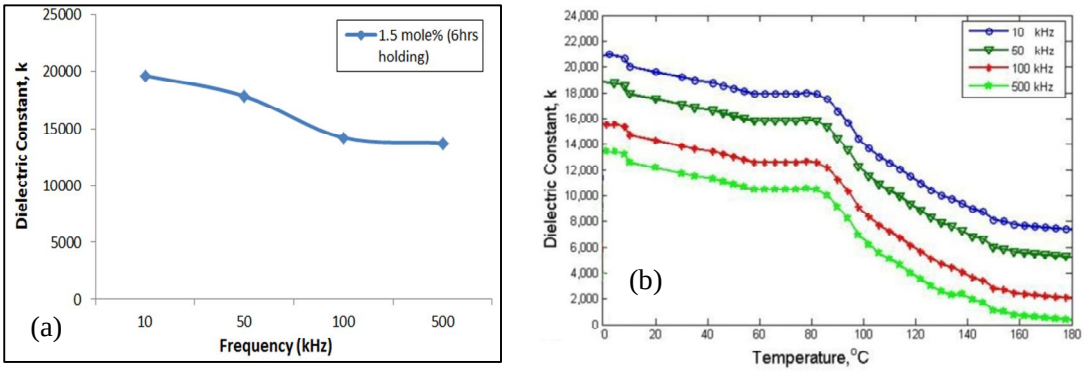

Fig. 4.14: (a) Variation of dielectric constant with frequency and (b) Variation of dielectric constant with temperature of 1.5 mole % Ta_2O_5 doped $BaTiO_3$ sintered at 1320^0C (0hrs) and 1280^0C (6hrs)

Figure 4.15 shows that, ignoring some fluctuation of values in between, in general at a particular frequency dielectric loss values at first decreased with increase of temperature. This trend continued up to 84^0C, above which values of dielectric loss increased with increase of temperature. However, all values of dielectric loss measured at the frequency range of 1-10kHz were below 0.2.

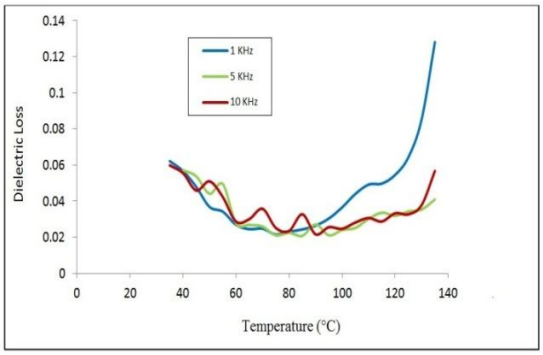

Fig. 4.15: Variation of dielectric loss with temperature of 1.5 mole % Ta_2O_5 doped $BaTiO_3$ sintered at 1320^0C (0hrs) and 1280^0C (6hrs)

4.4 Experiments conducted with double stage sintering (Part-2)

4.4.1Summary of the key experiments

Numerical data of the effect of double stage sintering on %theoretical density (*%TD*) andaverage grain size of Ta_2O_5 doped $BaTiO_3$ samples are tabulated in Table 4.3.

Table 4.3:Parameters of double stage sintering and their effect on %theoretical density and average grain size

SI No:	Sintering rate (^{0}C/min)	Sintering temperature and dwell time (1st stage)	Sintering temperature and dwell time (2nd stage)	Cooling rate (^{0}C/min)	Doping mole %	%TD	Avg. grain size (µm)
1	15	1310^{0}C for 0 hrs	1280^{0}C for 4hrs	3	0.5	94.6	1.68
2	15	1310^{0}C for 0 hrs	1280^{0}C for 4hrs	3	1.0	90.8	1.20
3	15	1310^{0}C for 0 hrs	1280^{0}C for 4hrs	3	1.5	90.2	0.9
4	15	1310^{0}C for 0 hrs	1280^{0}C for 6hrs	3	0.5	93.7	1.75
5	15	1310^{0}C for 0 hrs	1280^{0}C for 6hrs	3	1.0	91.3	1.25
6	15	1310^{0}C for 0 hrs	1280^{0}C for 6hrs	3	1.5	92.1	1.05
7	15	1300^{0}C for 0 hrs	1280^{0}C for 4hrs	3	0.5	92.6	1.51
8	15	1300^{0}C for 0 hrs	1280^{0}C for 4hrs	3	1.0	90.0	1.10
9	15	1300^{0}C for 0 hrs	1280^{0}C for 4hrs	3	1.5	88.7	0.60
10	15	1300^{0}C for 0 hrs	1280^{0}C for 6hrs	3	0.5	94.1	1.59
11	15	1300^{0}C for 0 hrs	1280^{0}C for 6hrs	3	1.0	90.6	1.17
12	15	1300^{0}C for 0 hrs	1280^{0}C for 6hrs	3	1.5	89.4	0.70

From Figure4.16 it can be seen that, optimum combination of %theoretical density and average grain size near 1 micron resulted in best room temperature dielectric constant for 1.5mole% Ta_2O_5 doped $BaTiO_3$ sample sintered at 1310^0C for 0hours and 1280^0C for 6hours.

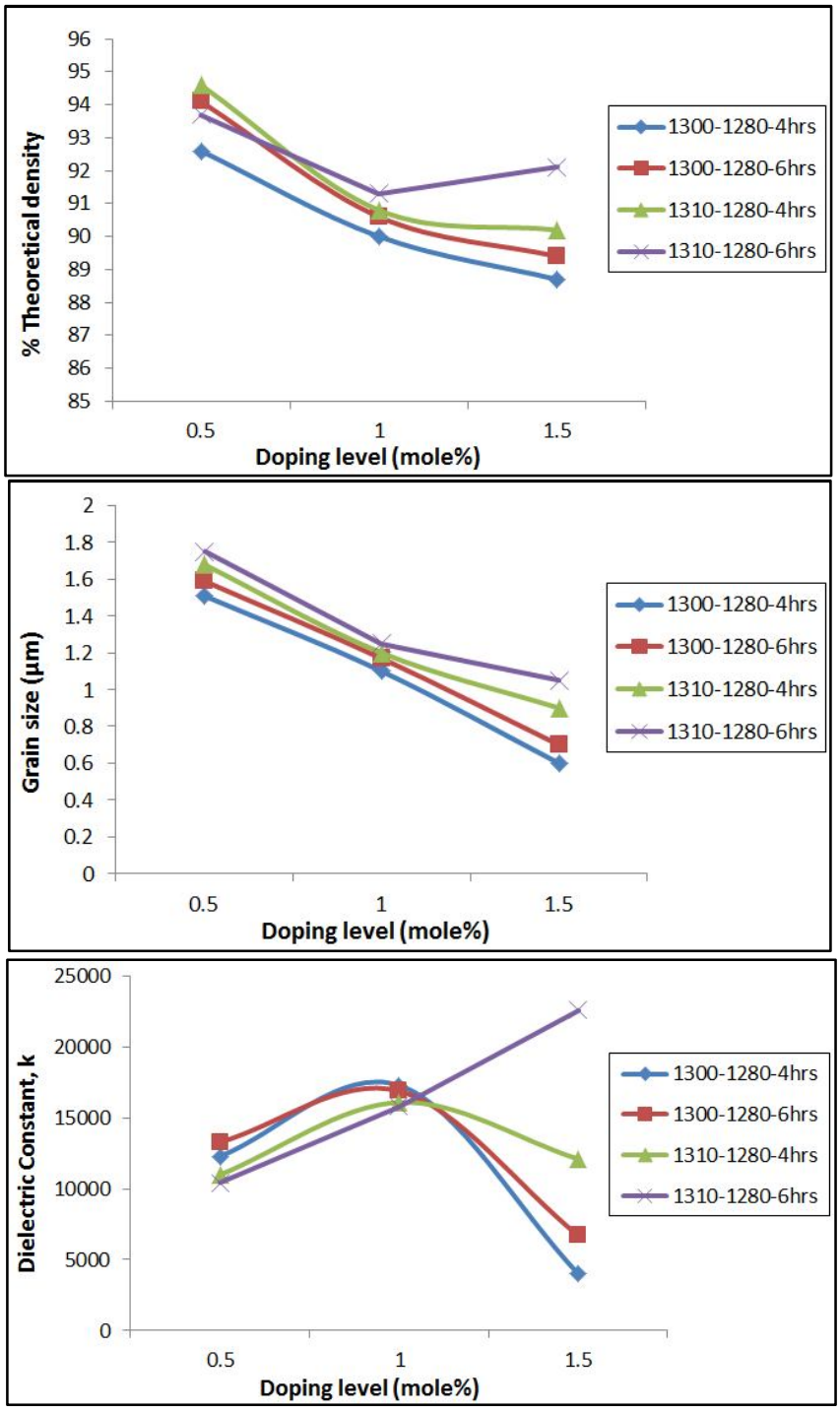

Fig. 4.16: (a)Variation of %theoretical density with doping level (mole%), (b) Variation of average grain size with doping level (mole%), (C) Variation of dielectric constant with doping level (mole%)

4.4.2 Development of microstructure

Figure 4.17 shows higher magnification SEM micrographs of 0.5-1.5 mole% Ta_2O_5 doped $BaTiO_3$ samples sintered at 1310^0C for 0hours and 1280^0C for 4hours.It can be seen from Figure 4.17 that, average grain size of all the samples was smaller than samples sintered at 1320^0C for 0hours and 1280^0C for 4hours.

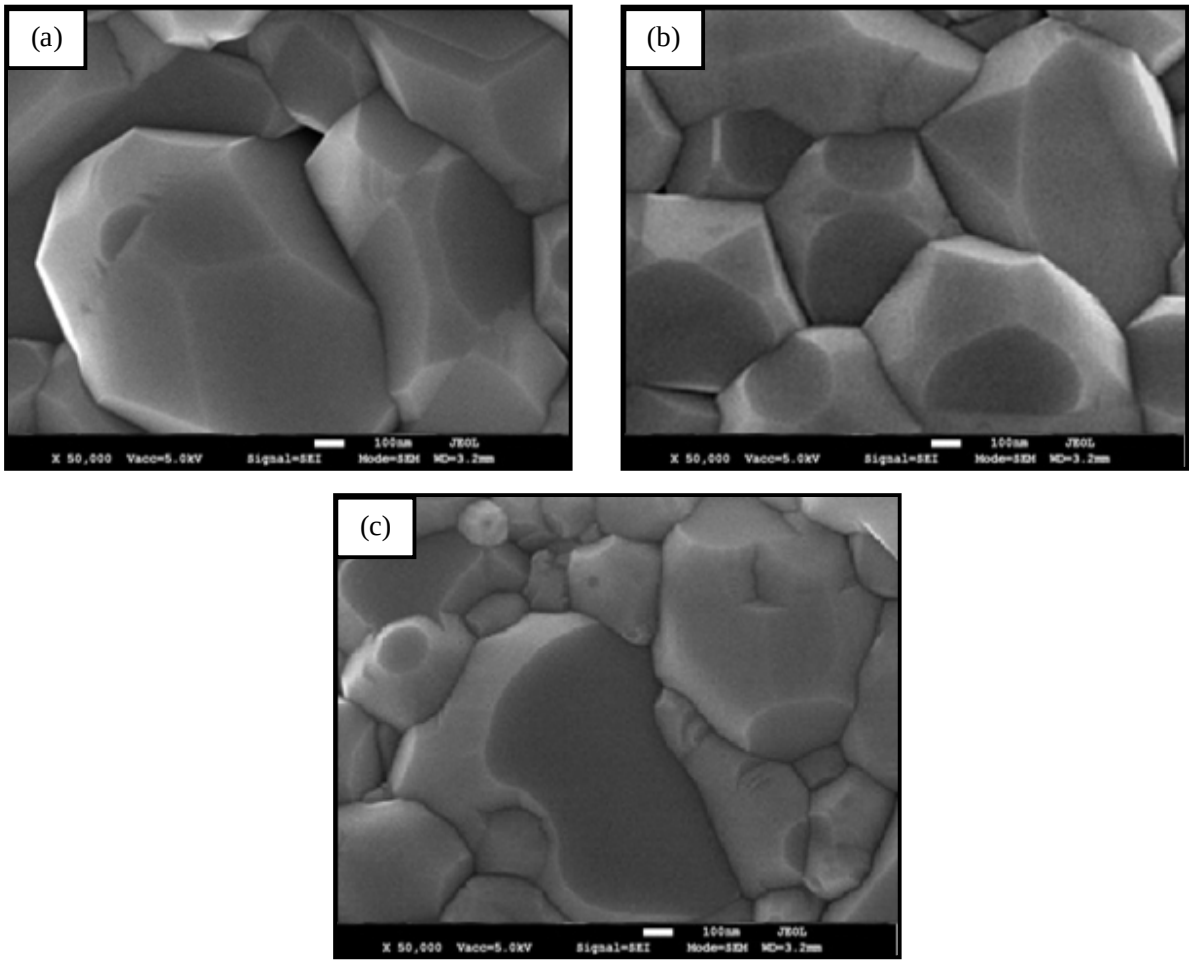

Fig. 4.17: SEM micrographs (X 50,000) of (a) 0.5 mole %, (b) 1.0 mole % and (c) 1.5 mole % Ta_2O_5 doped $BaTiO_3$ samplessintered at 1310^0C for 0hrs and 1280^0C for 4hrs

Figure 4.18 shows lower magnification SEM micrographs of 0.5-1.5 mole% Ta_2O_5 doped $BaTiO_3$ samples sintered at 1310^0C for 0hours and 1280^0C for 4hours. All these samples showed comparatively smaller average grain size because the first stage sintering temperature was lowered to 1310^0C [17].Among all 3 samples, 0.5 mole%Ta_2O_5 doped $BaTiO_3$ sample showed the largest average grain size and high %theoretical density. The microstructure fairly consisted of large grains (Figure 4.18a). With increased doping level, both average grain size and %theoretical density of the samples started to decrease. For 1.0 mole% Ta_2O_5 doped $BaTiO_3$ sample, the microstructure consisted of few large grains surrounded by small and medium sized grains (Figure 4.18b). But, 1.5mole% Ta_2O_5 doped $BaTiO_3$ sample showed bimodal grain size distribution where few large grains where surrounded by very fine grains (Figure 4.18c).

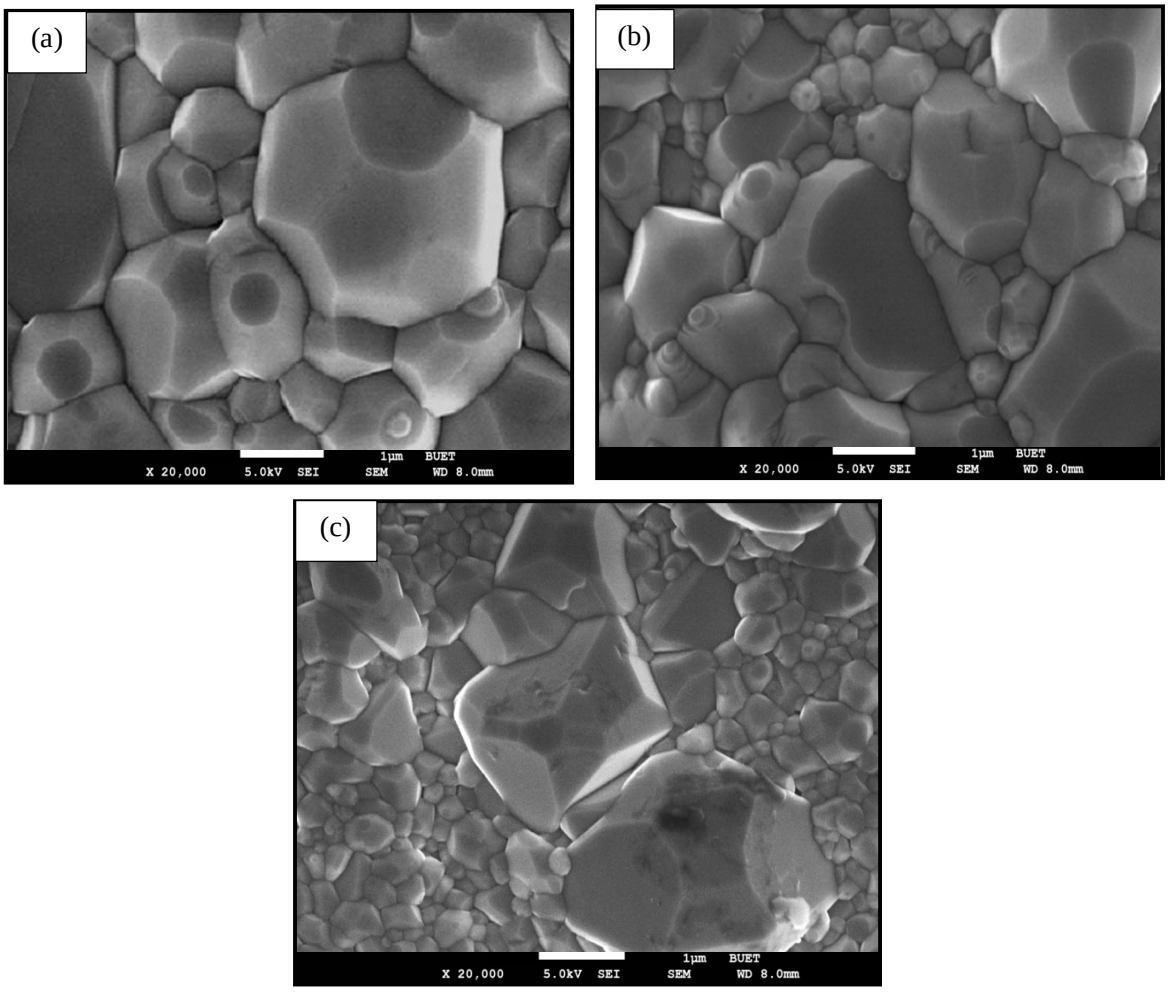

Fig. 4.18: SEM micrographs (X 20,000) of (a) 0.5 mole %, (b) 1.0 mole % and (c) 1.5 mole % Ta_2O_5 doped $BaTiO_3$ samplessintered at 1310^0C for 0hrs and 1280^0C for 4hrs

Figure 4.19 shows the higher magnification SEM micrographsof 0.5-1.5 mole% Ta_2O_5 doped $BaTiO_3$ samplessintered at 1310^0C for 0hours and 1280^0C for 6hours. It can be seen from Figure 4.19 that, average grain size of all the samples was larger than samples sintered at 1310^0C for 0hours and 1280^0C for 4hours.

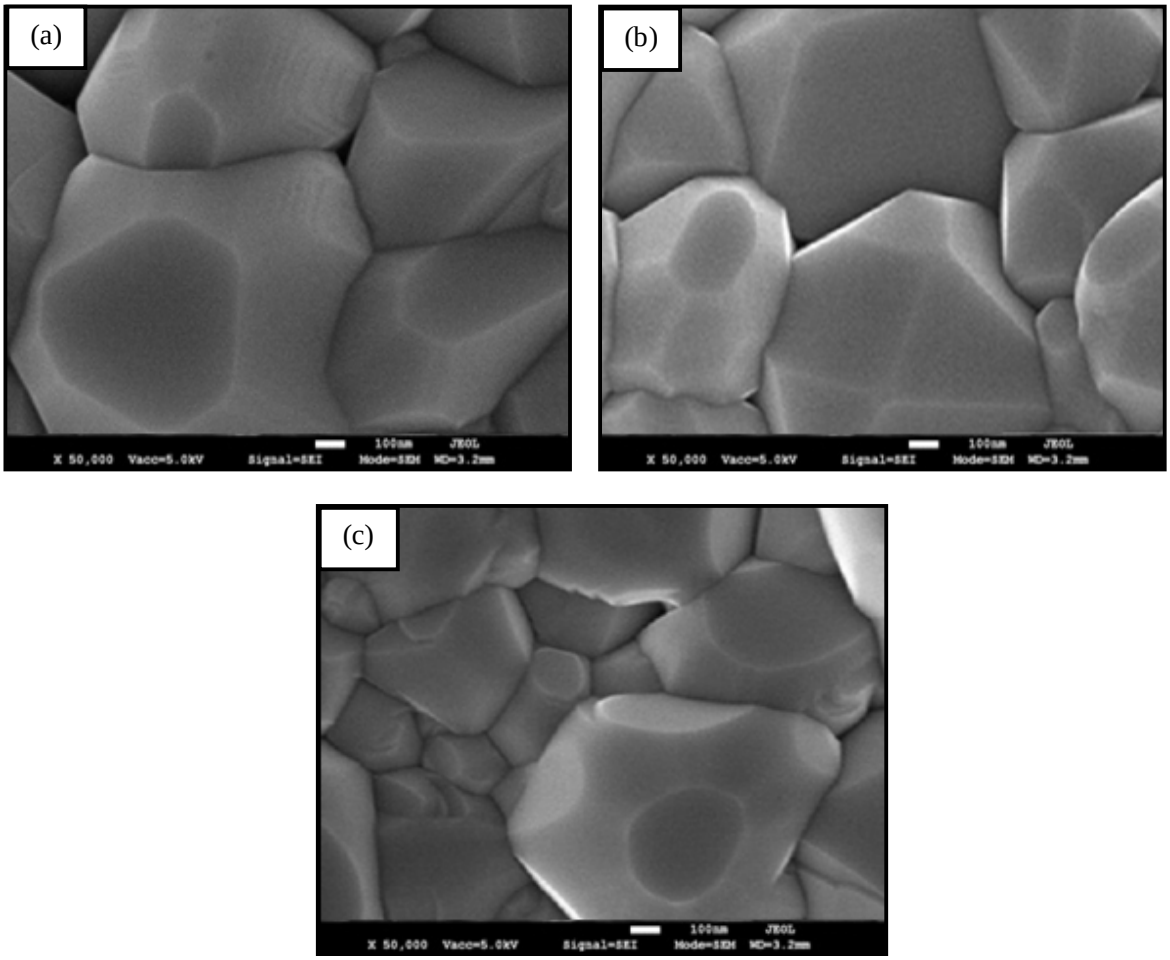

Fig. 4.19: SEM micrographs (X 50,000) of Ta_2O_5 doped $BaTiO_3$ samplessintered at 1310^0C for 0hrs and 1280^0C for 6hrs:(a) 0.5 mole %, (b) 1.0 mole % and (c) 1.5 mole %

Figure 4.20 shows the lower magnification SEM micrographsof 0.5-1.5 mole% Ta_2O_5 doped $BaTiO_3$ samplessintered at 1310^0C for 0hours and 1280^0C for 6hours. The trend of microstructure development due to doping with 0.5-1.5mole% Ta_2O_5remained similar. However, this time the microstructure of 1.5mole%Ta_2O_5 doped $BaTiO_3$ sample consisted of few large grains surrounded by medium and fine sized grains instead of showing bimodal grain size distribution.

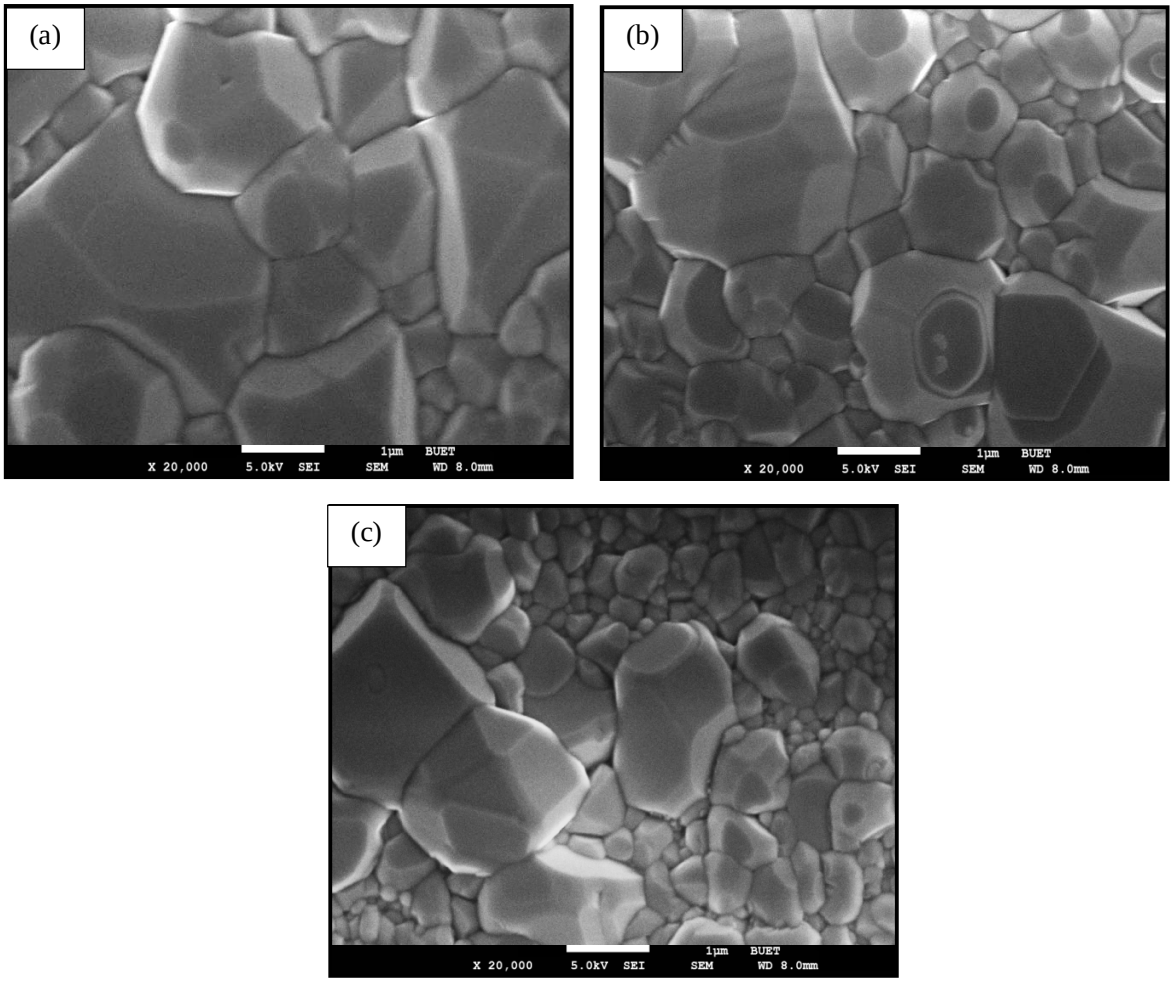

Fig. 4.20: SEM micrographs (X 20,000) of Ta_2O_5 doped $BaTiO_3$ samplessintered at 1310^0C for 0hrs and 1280^0C for 6hrs: (a) 0.5 mole %, (b) 1.0 mole % and (c) 1.5 mole %

Figure 4.21 shows the higher magnification SEM micrographsof 0.5-1.5 mole% Ta_2O_5 doped $BaTiO_3$ samplessintered at 1300^0C for 0hours and 1280^0C for 4hours. It can be seen from Figure 4.19 that, average grain size of all the samples was smaller than samples sintered at 1310^0C for 0hours and 1280^0C for 4hours.

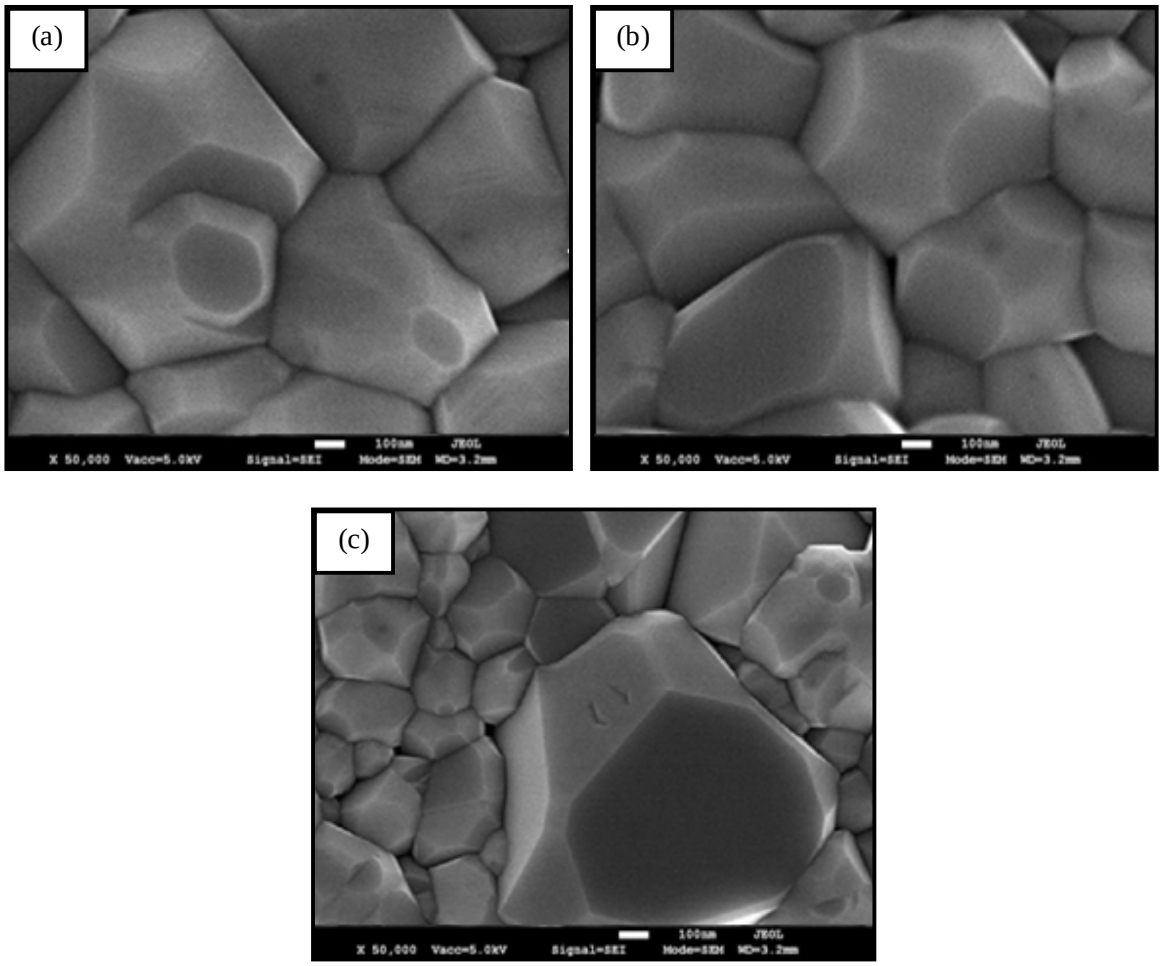

Fig. 4.21: SEM micrographs (X 50,000) of Ta_2O_5 doped $BaTiO_3$ samplessintered at 1300^0C for 0hrs and 1280^0C for 4hrs:(a) 0.5 mole %, (b) 1.0 mole % and (c) 1.5 mole %

Figure 4.22 shows the microstructure of 0.5-1.5 mole% Ta_2O_5 doped $BaTiO_3$ samplessintered at 1300^0C 0hours and 1280^0C 4hours. As the first stage sintering temperature was decreased to 1300^0C, there was a decrease of both %theoretical density and average grain size of all samples in comparison to the samples sintered at 1310^0C 0hours and 1280^0C 4hours. But, the trend of changes in microstructure development and %theoretical density due to doping with 0.5-1.5mole% Ta_2O_5remained same.

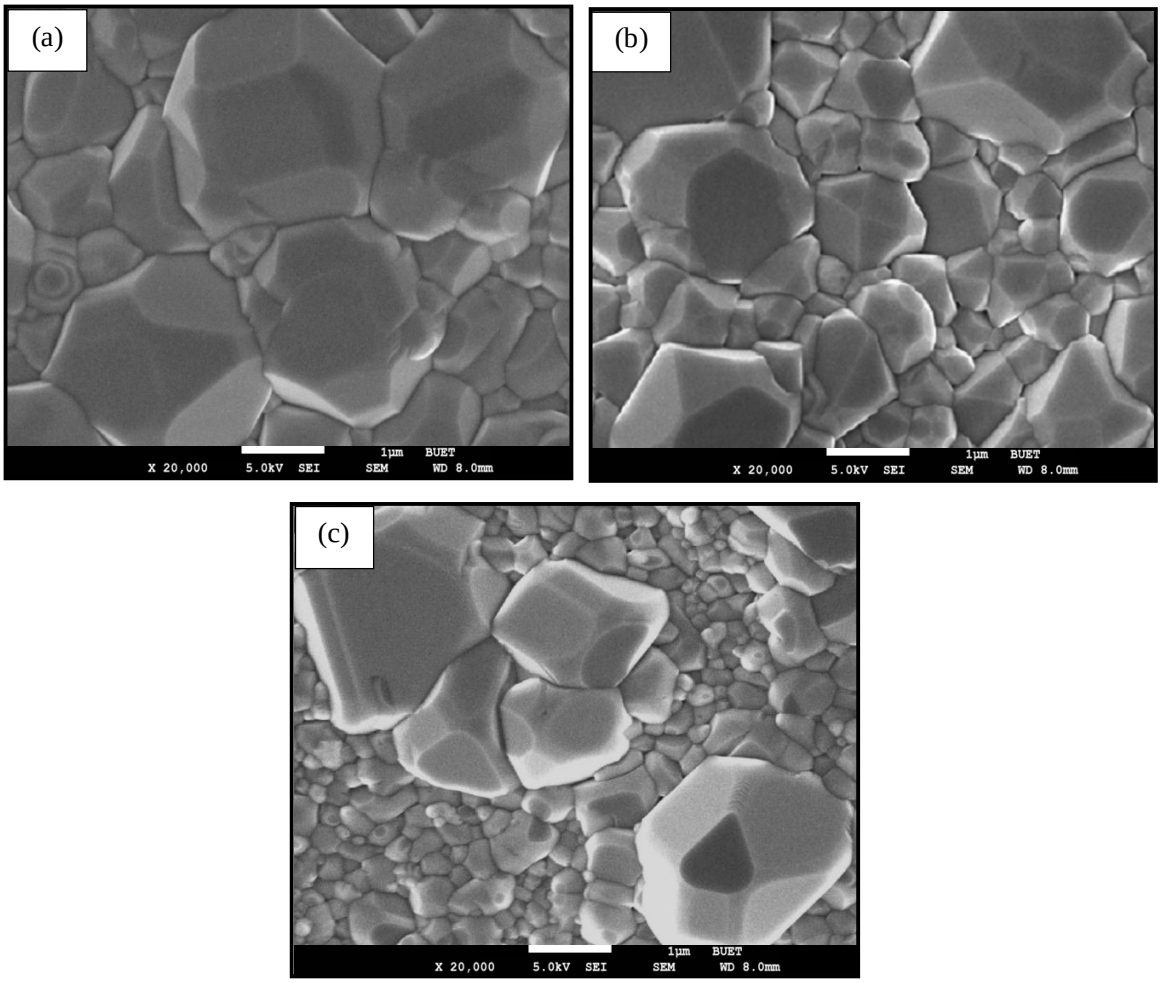

Fig. 4.22: SEM micrographs (X 20,000) of Ta_2O_5 doped $BaTiO_3$ samplessintered at 1300^0C for 0hrs and 1280^0C for 4hrs: (a) 0.5 mole %, (b) 1.0 mole % and (c) 1.5 mole %

Figure 4.23shows the higher magnification SEM micrographsof 0.5-1.5 mole% Ta_2O_5 doped $BaTiO_3$ samplessintered at 1300^0C for 0hours and 1280^0C for 6hours. It can be seen from Figure 4.19 that, average grain size of all the samples was larger than samples sintered at 1300^0C for 0hours and 1280^0C for 4hours.

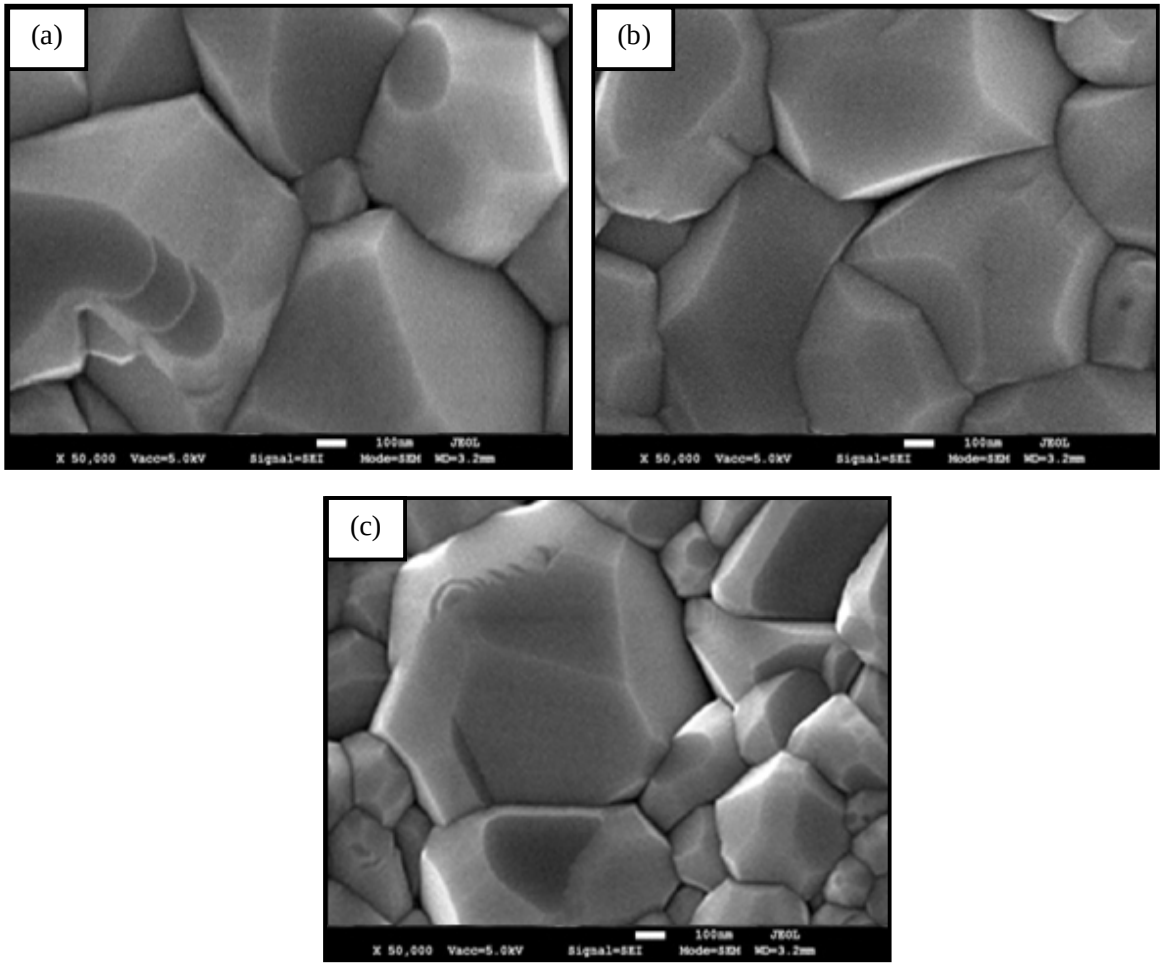

Fig. 4.23: *SEM micrographs (X 50,000) of Ta_2O_5 doped $BaTiO_3$ samplessintered at 1300^0C for 0hrs and 1280^0C for 6hrs: (a) 0.5 mole %, (b) 1.0 mole % and (c) 1.5 mole %*

Figure 4.24 show the microstructuresof 0.5-1.5 mole% Ta_2O_5 doped $BaTiO_3$ samplessintered at 1300^0C for 0hours and 1280^0C for 6hours. As the dwell time was increased to 6 hours, there was an increase of average grain size and %theoretical density of all samples in comparison to the samples sintered at 1310^0C for 0hours and 1280^0C for 4hours. But, the trend of changes in microstructure development and %theoretical density due to doping with 0.5-1.5mole% Ta_2O_5remained similar.

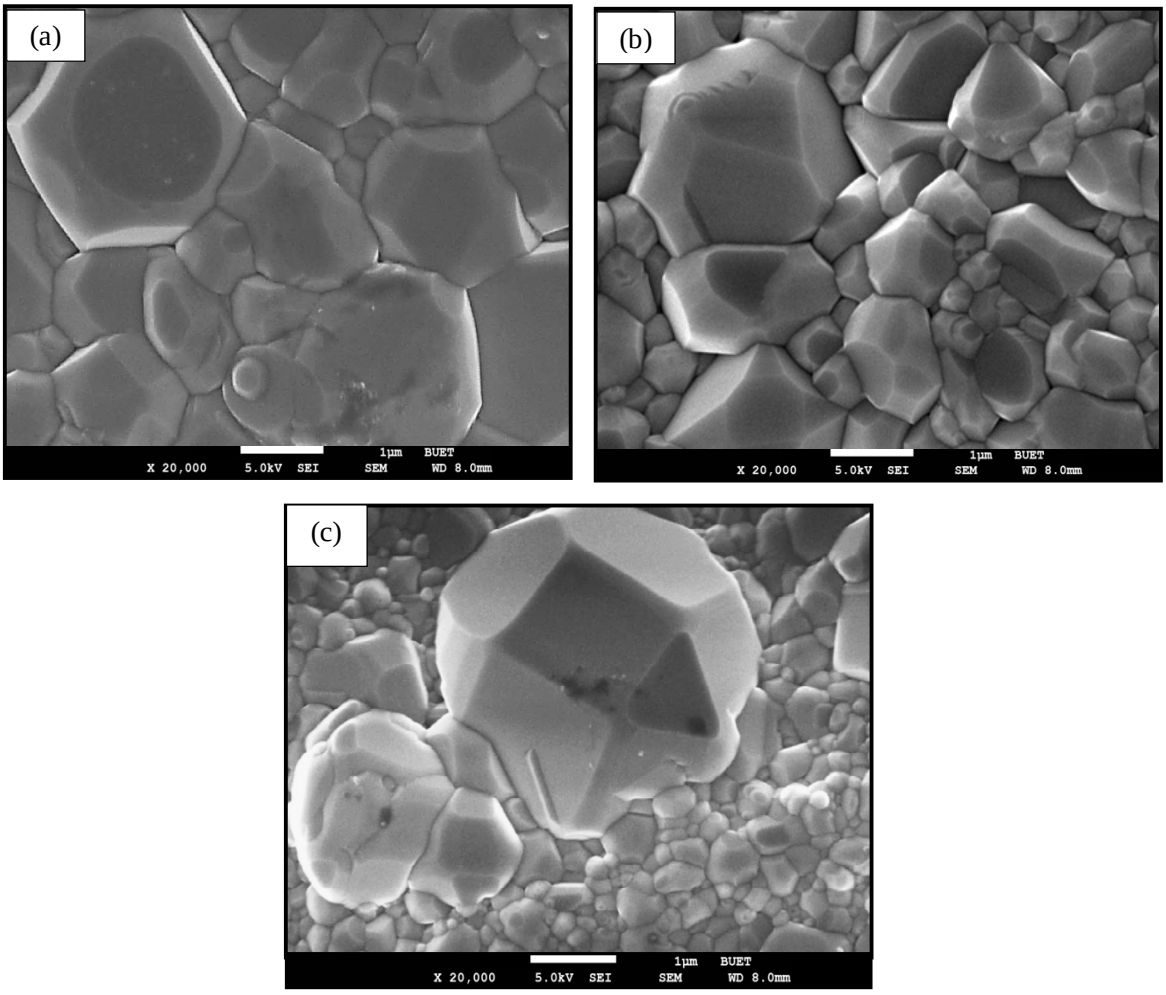

Fig. 4.24: *SEM micrographs (X 20,000) of Ta_2O_5 doped $BaTiO_3$ samplessintered at 1300^0C for 0hrs and 1280^0C for 6hrs:(a) 0.5 mole %, (b) 1.0 mole % and (c) 1.5 mole %*

4.4.3 Dielectric Property Measurement

Since 1.5 mole% Ta_2O_5 doped $BaTiO_3$ sample sintered at 1310^0C for 0hours and 1280^0C for 6hours showed highest room temperature dielectric constant, its detailed dielectric properties were measured. From Figure 4.25a it can be seen that, with increase of frequency, value of dielectric constant shows a decreasing trend which is in accordance with literature [17]. Highest value of room temperature dielectric constant of 22600 was measured at 10kHz frequency. Figure 4.25b shows that for 1.5 mole% Ta_2O_5 doped $BaTiO_3$ sample, the Curie point was shifted to 98^0C whereas the Curie temperature (T_c) for pure $BaTiO_3$ is 120^0C. The best stable value of dielectric constant as a function of temperature was obtained around 21000.

Similar to Figure 4.15, Figure 4.25c shows that at a particular frequency dielectric loss values at first decreased with increase of temperature. This trend continued up to 100^0C, above which values of dielectric loss increased with increase of temperature. Up to 100^0C, the values of dielectric loss measured at the frequency range of 1-10kHz were below 0.2.

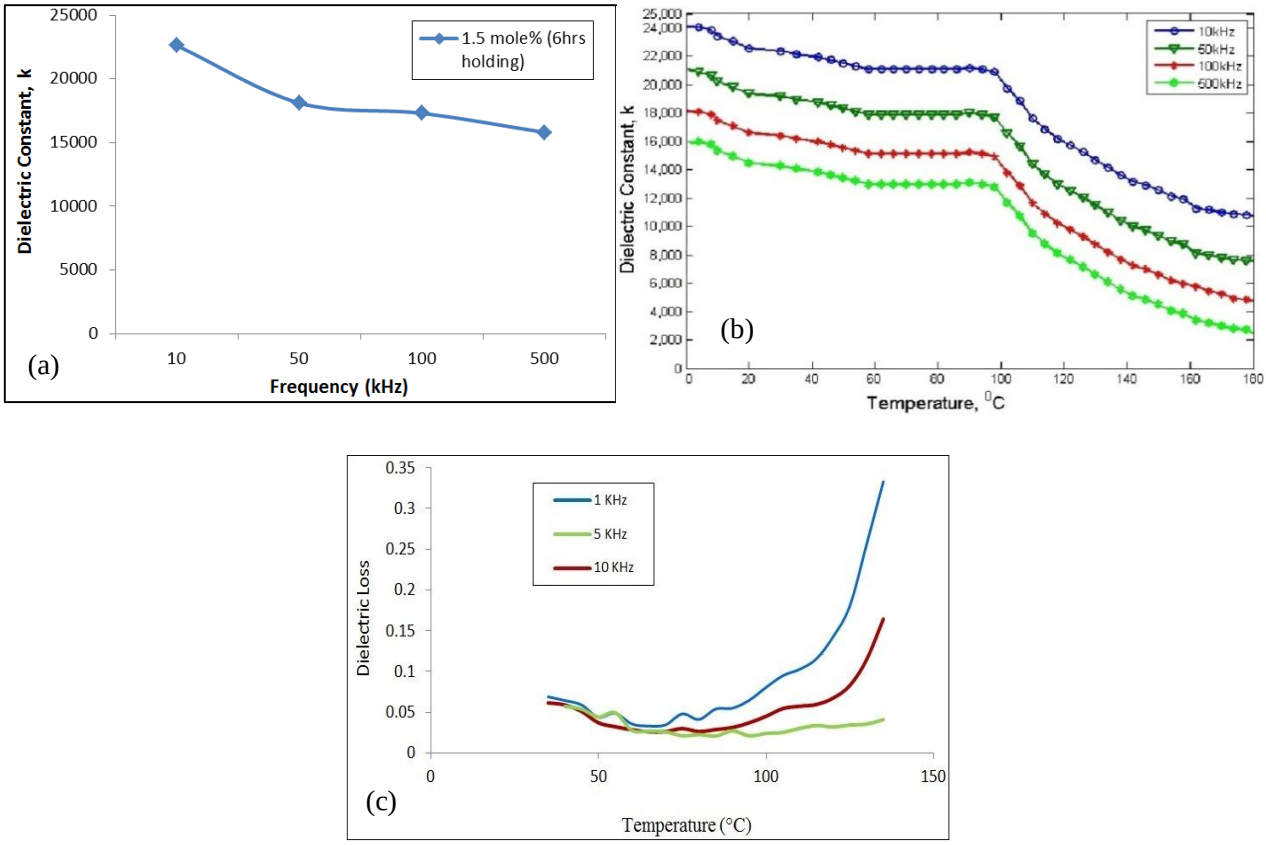

Fig. 4.25(a) Variation of dielectric constant with frequency, (b) Variation of dielectric constant with temperature, and (c)Variation of dielectric loss with temperatureof 1.5 mole % Ta_2O_5 doped $BaTiO_3$ sintered at 1310^0C for 0hrs and 1280^0C for 6hrs

4.5 XRD analysis

XRD patterns of Figure 4.26indicate the formation of both tetragonal and cubic phases of $BaTiO_3$. They also show that no second phase was formed during the sintering process.The XRD pattern for 0.5 mole% Ta_2O_5 doped $BaTiO_3$ sample sintered at 1320^0C for 0hours and 1280^0C for 6hours shows the presence of twin peaks similar to pure $BaTiO_3$ powder [Figure 4.26(a-b)]. So, it can be concluded that for 0.5 mole% Ta_2O_5 doping, $BaTiO_3$ retained the tetragonal perovskite structure. However, the XRD pattern for 1.0 and 1.5 mole% Ta_2O_5 doped $BaTiO_3$ samples sintered at 1320^0C for 0hours and 1280^0C for 6hours show no evidence of twin peaks, which indicates that doping with 1.0mole% Ta_2O_5 proved sufficient forreducing tetragonality and stabilizing the cubic phase of $BaTiO_3$ [Figure 4.26(c-d)].Tetragonality of $BaTiO_3$decreases with decreasing grain size [37-38]. So, the results are consistent.

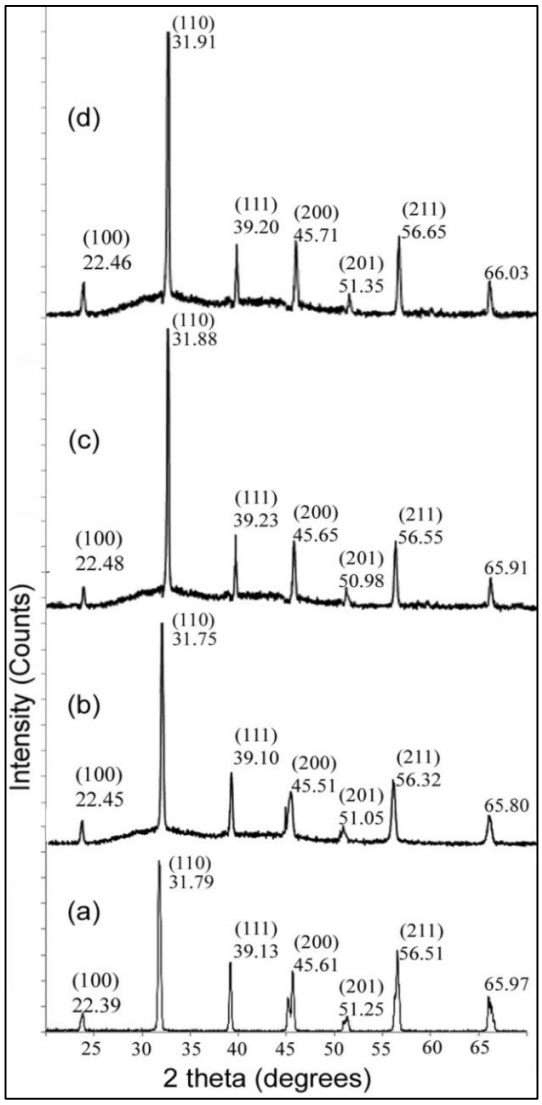

Fig. 4.26: XRD patterns for (a) Pure Barium Titanate powder, (b) 0.5 mole%, (c) 1.0 mole% and (d) 1.5 mole% Ta_2O_5 doped $BaTiO_3$ sintered at 1320^0C for 0hrs and 1280^0C for 6hrs

Similar to XRD patternsof Figure 4.26, XRD patterns of Figure 4.27(a-b) indicates that, the XRD pattern for 1.0 and 1.5 mole% Ta_2O_5 doped $BaTiO_3$ samples sintered at 1310^0C for 0hours and 1280^0C for 6hours show no evidence of twin peaks, which indicates that doping with 1.0-1.5 mole% Ta_2O_5 reduced tetragonality and stabilized the cubic phase of $BaTiO_3$ [Figure 4.27(c-d)].But, at this sintering condition even0.5 mole% Ta_2O_5stabilized the cubic phase of $BaTiO_3$ [37-38].

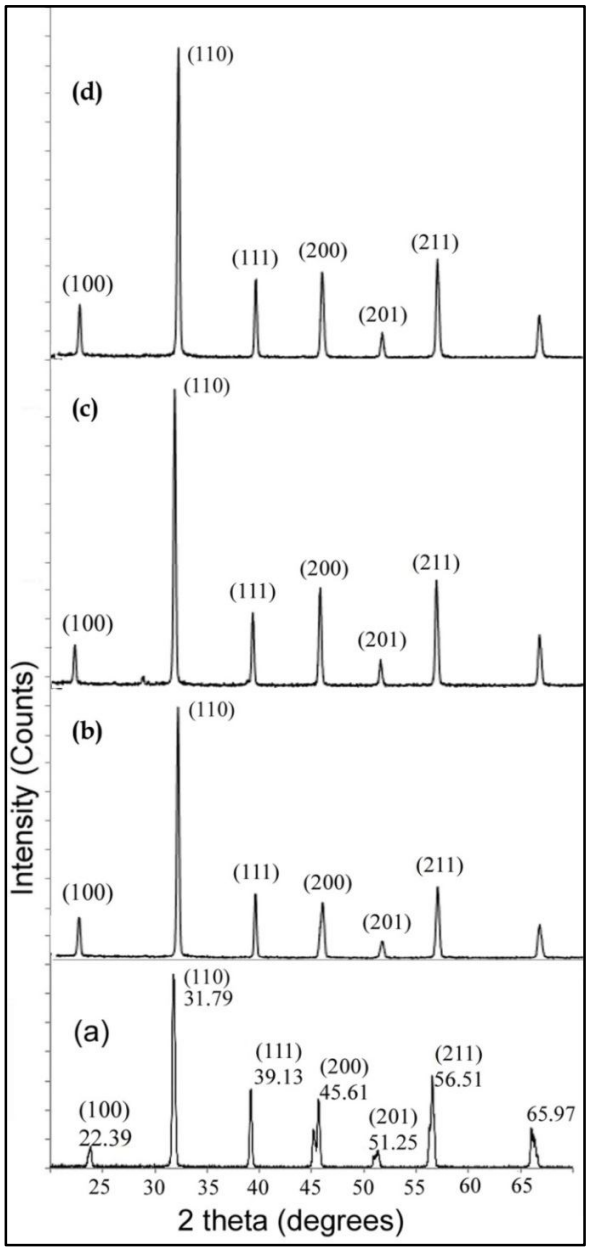

Fig. 4.27: XRD patterns for (a) Pure Barium Titanate powder, (b) 0.5 mole%, (c) 1.0 mole% and (d) 1.5 mole% Ta_2O_5 doped $BaTiO_3$ sintered at 1310^0C for 0hrs and 1280^0C for 6hrs

4.6EDX analysis

Figure4.28 shows the EDX analysis of0.5 mole% Ta_2O_5 doped $BaTiO_3$ samplessintered at 1310^0C for 0hours and 1280^0C for 6hours. The EDX pattern of Figure4.28b shows the elemental analysis of spot 003 (Figure4.28a). From the pattern, it can be seen that the pattern contains no trace of Ta. So, the large grains consisted of pure $BaTiO_3$. From this observation, it can be concluded that the chance of substituting Ti^{4+} ion with Ta^{5+} ion is quite minimum with 0.5 mole% Ta_2O_5 doping. However, 0.5mole% Ta_2O_5 might have enhanced the dielectric properties of doped $BaTiO_3$ by grain size refinement.

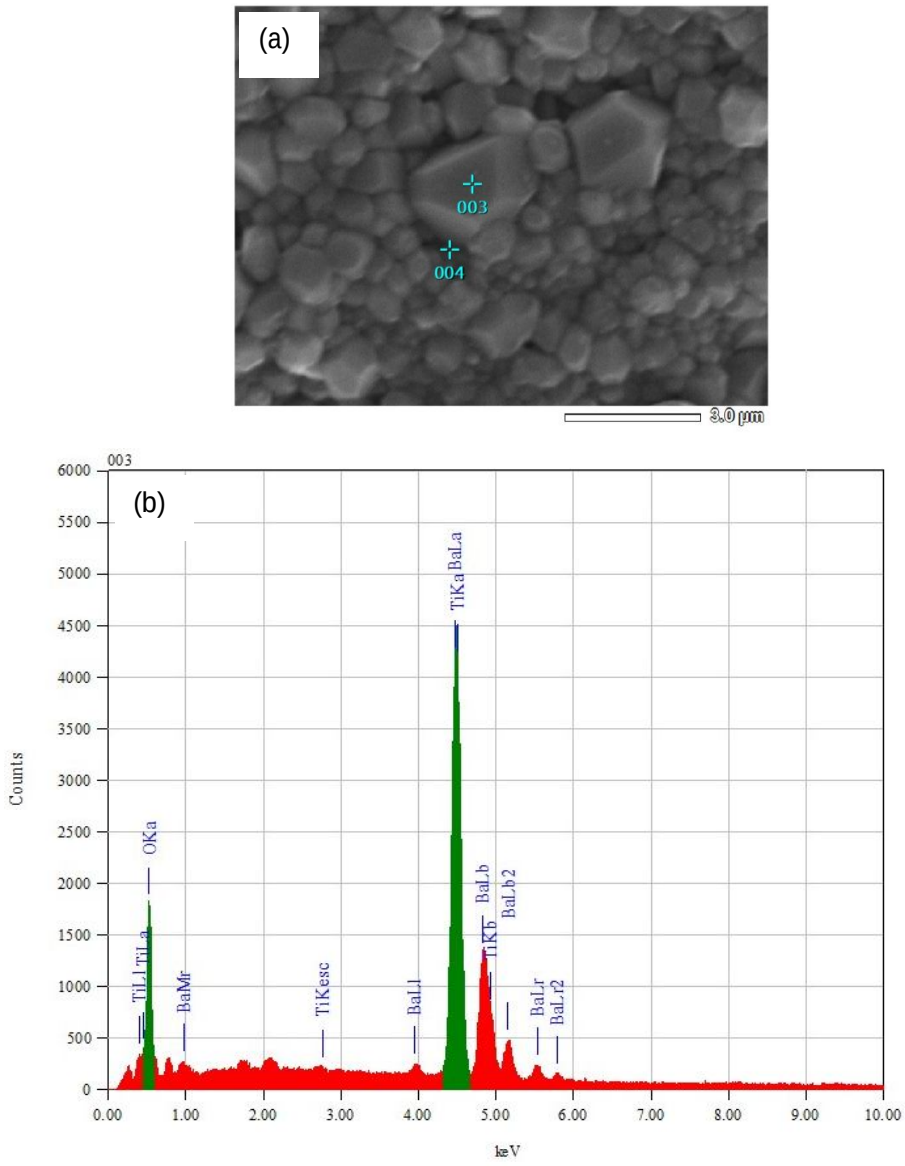

Fig. 4.28: (a) (X 10,000) SEM image of the microstructure and (b) EDX pattern of0.5 mole% Ta_2O_5 doped $BaTiO_3$ samplessintered at 1310^0C for 0hrs and 1280^0C for 6hrs[point 03]

Figure4.29 also shows the EDX analysis of0.5 mole% Ta_2O_5 doped $BaTiO_3$ samplessintered at 1310^0C for 0hours and 1280^0C for 6hours. The EDX pattern of Figure 4.29b shows the elemental analysis of spot 004 (Figure4.29a). From the pattern, it can be said the fine grains surrounding the large grains indicated the presence of Ta. So, it can be concluded that Ta_2O_5 does give pinning effect.

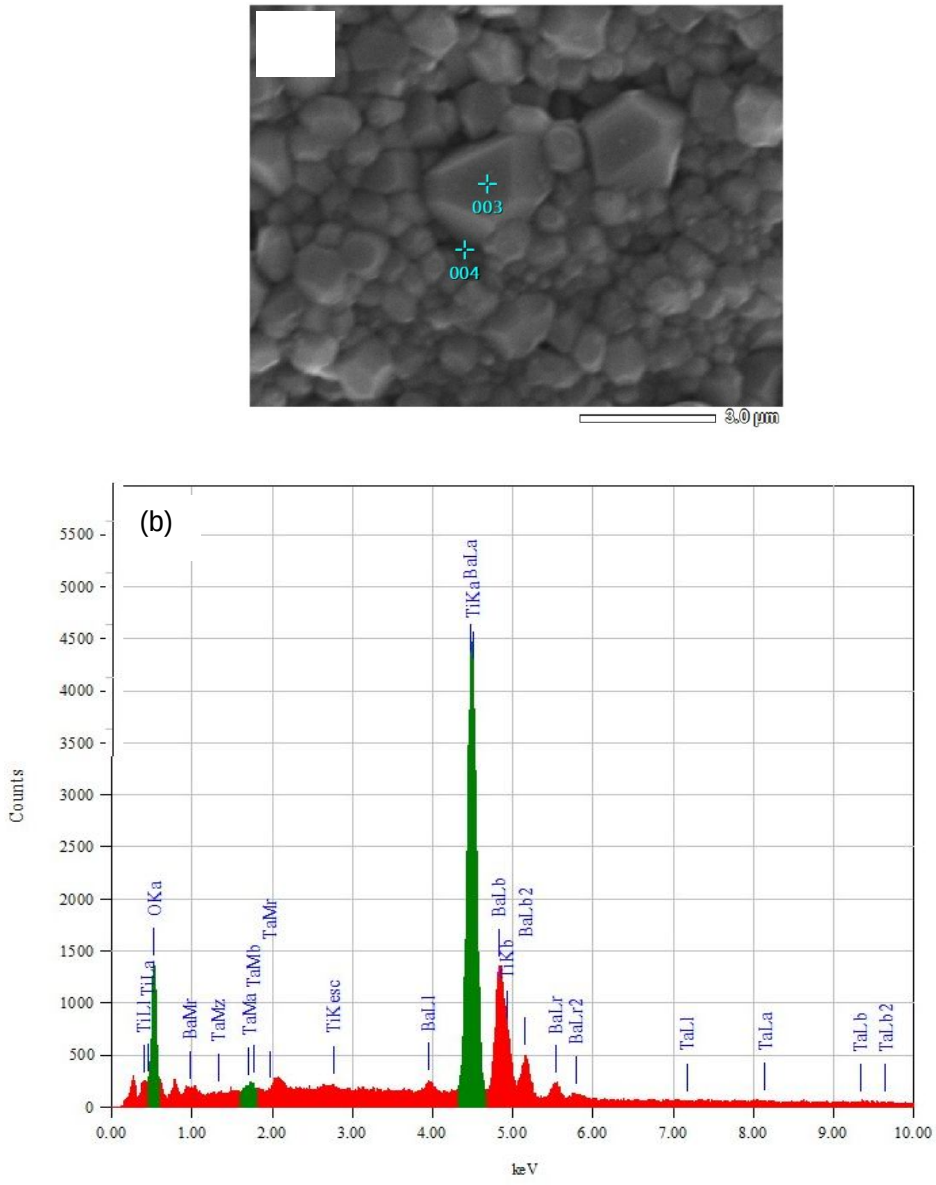

Fig. 4.29: EDX analysis of0.5 mole% Ta_2O_5 doped $BaTiO_3$ samplessintered at 1310^0C for 0hrs and 1280^0C for 6hrs[point 004]

Figure.4.30 shows the EDX analysis of1.5 mole% Ta_2O_5 doped $BaTiO_3$ samplessintered at 1310^0C for 0hours and 1280^0C for 6hours. The EDX pattern of Figure 4.30b shows the elemental analysis of spot 008 (Figure 4.30a). Unlike Figure 4.28b, Figure4.27b showed presence of Ta in the large grains. So, it can be said that Ta^{5+} ion might have substituted Ti^{4+} ion during the sintering process. So, it can be concluded that, 1.5mole% Ta_2O_5 enhances the chance for substitution of Ti^{4+} ion and improvement of dielectric constants.

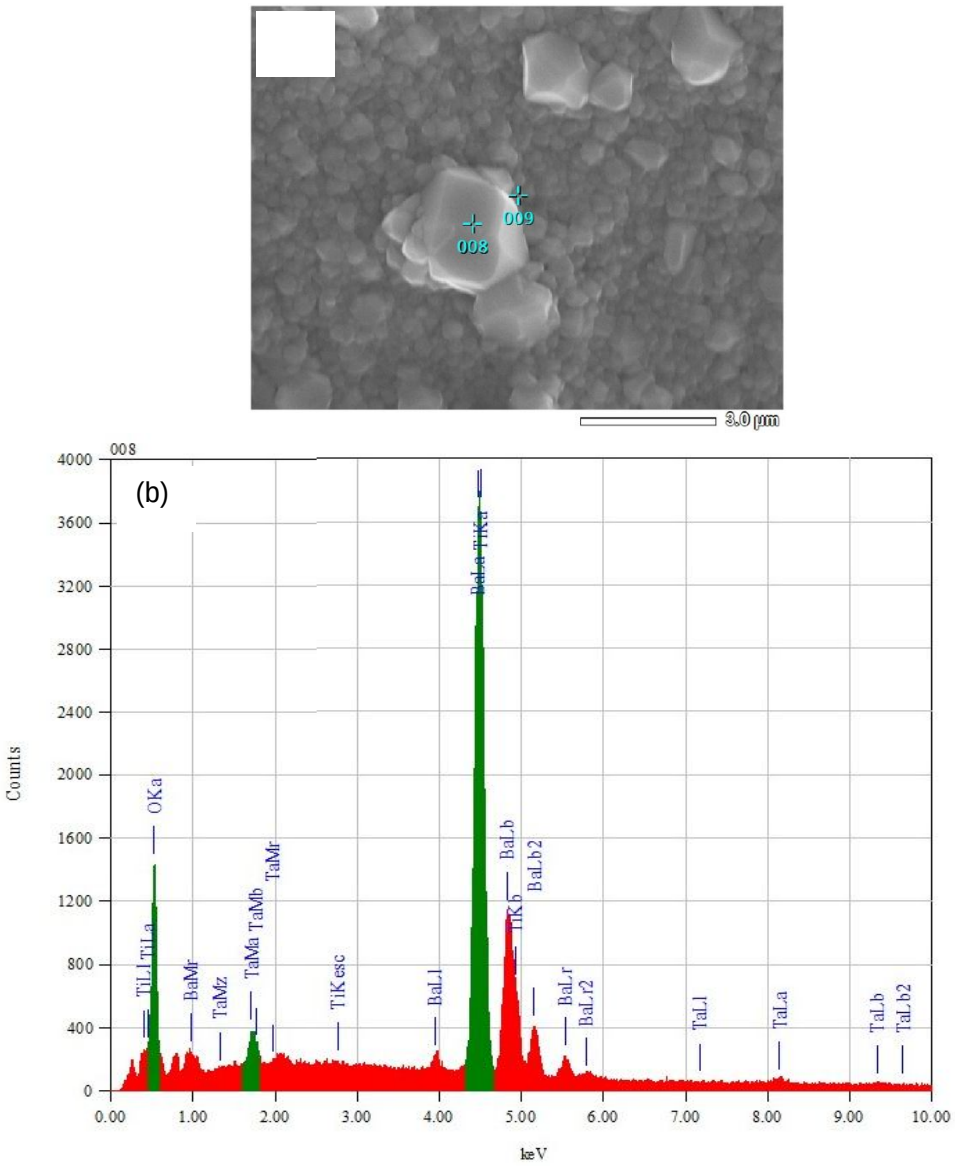

Fig. 4.30: EDX analysis of 1.5 mole % Ta_2O_5 doped $BaTiO_3$ samplessintered at 1310^0C for 0hrs and 1280^0C for 6hrs [point 008]

Figure4.31 also shows the EDX analysis of1.5 mole% Ta_2O_5 doped $BaTiO_3$ samplessintered at 1310^0C for 0hours and 1280^0C for 6hours. Similar to Figure4.29b, the EDX pattern of Figure 4.31b shows the elemental analysis of spot 008 (Figure 4.31a). From the pattern, it can be said the fine grains surrounding the large grains indicated the presence of Ta. So, it can be concluded that Ta_2O_5 does give pinning effect.

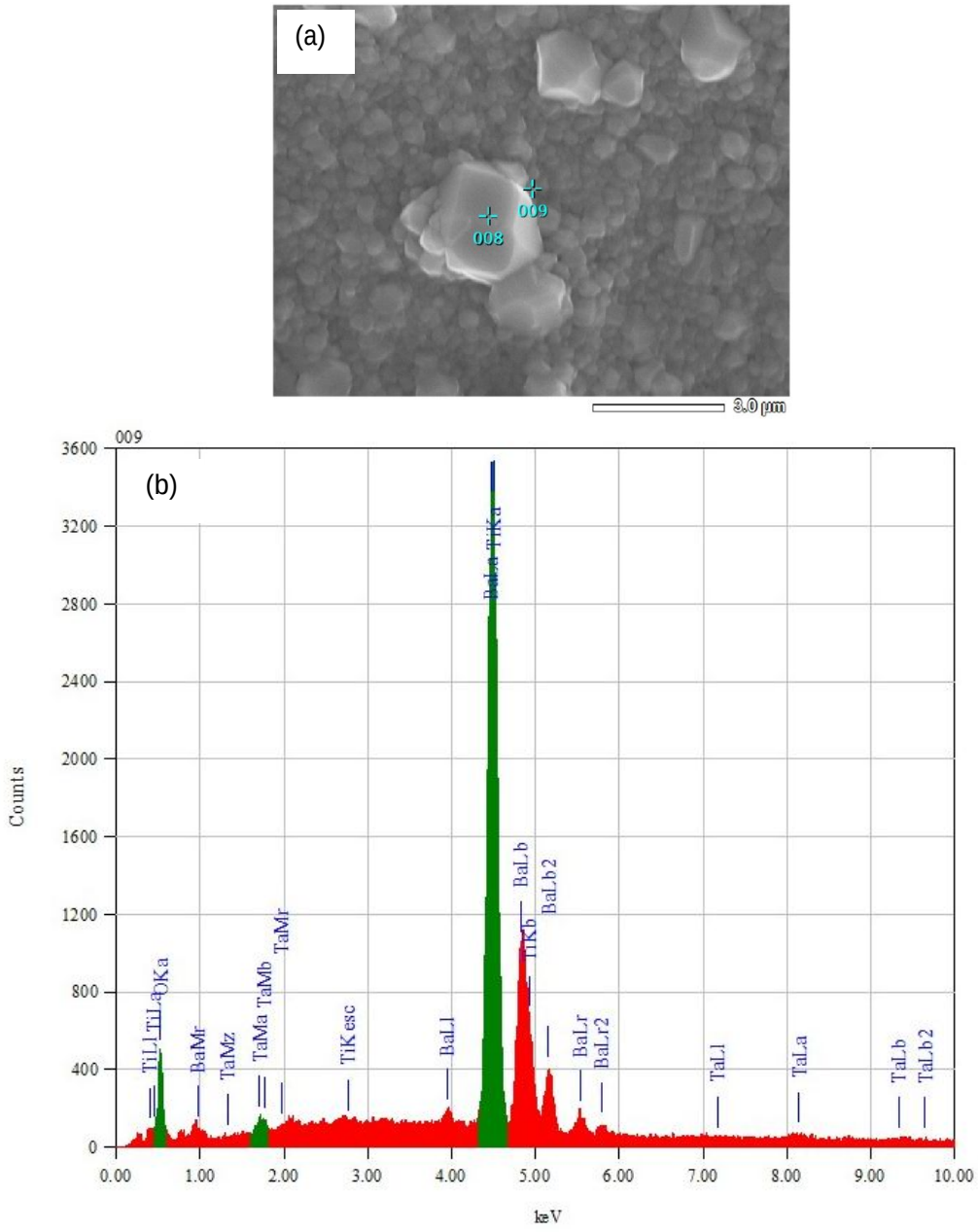

Fig. 4.31: EDX analysis of 1.5 mole % Ta_2O_5 doped $BaTiO_3$ samplessintered at 1310^0C for 0hrs and 1280^0C for 6hrs [point 009]

Conclusion

The project was undertaken to explore the effects of sintering parameters and compositional variation on dielectric properties of Ta_2O_5doped barium titanate. The findings of the research are as follows-

- Average grain size of around 1 µm normally provides a good condition for dielectric properties for doped $BaTiO_3$. In this research, grain sizes in the range of 0.8-1.2 µm showed high values of dielectric constant, while further increase in grain size deteriorated its property.
- At 0.5 mole% Ta_2O_5 doping, improvement of dielectric properties was mainly caused by grain size refinement.
- At 1.5 mole%Ta_2O_5 doping, dielectric properties were enhanced by the combination of grain size refinement and substitution of Ta^{5+}into the $BaTiO_3$lattice.
- Highest room temperature dielectric constant in the range of 22000-23000 was recorded for 1.5 mole % Ta_2O_5 doped $BaTiO_3$ samplessintered at 1310^0C (0hrs) and 1280^0C (6hrs) due to the combination of high %theoretical density and optimum average grain size of near 1 micron.
- This combination of doping level and sintering condition also produced the best stable value of dielectric constant as a function of temperature of around 21000.
- According to XRD patterns, at all sintering conditions, 1.0-1.5mole% Ta_2O_5 stabilized the cubic phase of $BaTiO_3$at room temperature. At certain sintering condition; even 0.5mole% Ta_2O_5 stabilized the cubic phase of $BaTiO_3$.
- However, results of the variation of dielectric constant with temperature revealed that Ta_2O_5doping lowered Curie temperature to lower temperature in the range of 80-100^0C. So, these results contradict the findingsof the XRD patterns.

Suggestion for future work

- After conducting the research, it has been realized that there are still lots of scope for further research withTa_2O_5 doped $BaTiO_3$ samples. In the current research, best combination of %theoretical density, microstructure and dielectric properties were achieved for 1.5 mole % Ta_2O_5 doped $BaTiO_3$ samplessintered at 1310^0C (0hrs) and 1280^0C (6hrs). But, the sintering condition by any means is not an energy efficient one. So, further research can be done by altering the conditions of double stage sintering in pursuit of developing energy efficient sintering conditions which will still produce high quality dielectric properties.
- Other dopants can be incorporated alongside doping with Ta_2O_5, to see how they modify the properties of doped$BaTiO_3$.

Bibliography

1. A. Moulson, J. Herbert: Electroceramics Material, Properties & Application., Chap-man&Hall, 1990.

2. W. Callister: Material Science and Enginering: An Introduction, J. Willey&Sons Inc. Chichester, 1994.

3. G. Arlt, D. Hennings, and G. De With, "Dielectric Properties of Fine-Grained Barium Titanate Ceramics," J. Appl. Phys. 58 [41], 1619-1625, 1985.

4. H. Kniekamp, and W. Heywang, "Depolarization effects in polycrystalline $BaTi0_3$", Z. Angew. Phys., 6[9], 385-390, 1954.

5. C. Miclea, C. Tanasoiu, I. Spanulescu, C. F. Miclea, A. Gheorghiu, L. Amarande, M. Cioangher, C. T. Miclea, "Microstructure and Properties of Barium Titanate Ceramics Prepared by Mechanochemical Synthesis", Romanian Journal of Information Science and Technology, 10 [4], 335-345, 2007.

6. L. Weiling, G. Lian, and G. Jingkun, "Sintering and Dielectric Properties of Fine-Grained $BaTi0_3$ ceramics", Science in China (Series E), 42 [5], 554-560, 1999.

7. K. Kinoshinta and A. Yamaji, "Grain-Size Effects on Dielectric Properties in Barium Titanate", J. Appl. Phys. 47 [I], 371-374, 1976.

8. H. T. Martirena and J. C. Burfoot, "Grain-Size Effects on Properties of Some Ferroelectrics Ceramics," J. Phys. Soc. C, 7, 3182-3192, 1974.

9. B. D. Stojanović, V. R. Mastelaro, C.O.P. Santos and J. A. Varela, "Structure Study of Donor Doped Barium Titanate Prepared from Citrate Solutions", Science of Sintering, 36, 179-188, 2004.

10. T. Nagai, K. Iijima, H. J. Hwang, M. Sando, T. Sekinoand, K. Niihara, "Effect of MgO Doping on The Phase Transformations of $BaTi0_3$", J. Am. Ceram. Soc., 83 [1], 107–112, 2000.

11. T. R. Armstrong, L. E. Morgens, A. K. Maurice, and R. C. Buchanan, "Effects of Zirconia on Microstructure and Dielectric Properties of Barium Titanate Ceramics", J. Am. Ceram. Soc., 72 [4], 605-611, 1989.

12. Y. Yuan, S. R. Zhang, X. H. Zhou, and B. Tang, "Effects of Nb_2O_5 doping on the microstructure and the dielectric temperature characteristics of barium titanate ceramics", J. Mat. Sci., 44, 3751-3757, 2009.

13. H. M. Chan, M. P. harmer, and D. M. Smyth, "Compensating Defects in Highly Donor-Doped $BaTi0_3$", J. Am. Ceram. Soc., 69 [6], 507-510, 1986.

14. Y. J. Kim, J. W. Hyun, H. S. Kim, J. H. Lee, M. Y. Yun, S. J. Noh, and Y. H. Ahn, "Microstructural Characterization and Dielectric Properties of Barium Titanate Solid Solutions with Donor Dopants", Bull. Korean Chem. Soc., 30 [6], 1267-1273, 2009.

15. G. H. Jonker, and W. Noorlander, Science of Ceramics, 1, 255-264, 1962.

16. M.N. Rahaman, R. Manalert, "Grain boundary mobility of $BaTi0_3$ doped with aliovalentcations". Journal of the European Ceramic Society, 18 [8], 1063-107, 1998.

17. C. B. Carter, M. G. Norton: Ceramic Materials Science and Engineering, Springer, New York, 2007.

18. D. W. Richerson: Modern Ceramic Engineering, Marcel Dekker, New York, 1992.

19. S.O. Kasp, Principals of Electronic Materials and Devices, 3rd edition, 2006.

20. W. D. Kingery, H. K. Bowen, D. R. Uhlman: Introduction to Ceramics, John Willey & Sons, 2nd edition, Singapore, 1976.

21. K. Uchino, E. Sadanaga, T. Hirose, J. Am. Ceram. Soc., 72[8], 1555-1558, 1989.

22. Y.I. Jung, S.Y. Choi "grain growth behavior during stepwise sintering of barium titanate in hydrogen gas and air", J. of Am. Ceram. Soc., 86 [12], 2228 –2230, 2003.

23. W.J. Merz, "The electric and optical behavior of BaTiO3 single-domain crystals", Phys. Rev. 76, 1221–1225, 1949.

24. W.J. Merz, "The effect of hydrostatic pressure on the Curie point of barium titanate single crystals", Phys. Rev., 77, 52–54, 1950.

25. W.J. Merz, "Domain properties in $BaTiO_3$". Phys. Rev., 88, 421–422, 1952.

26. W.J. Merz, "Double hysteresis loop of $BaTiO_3$ at the Curie point", Phys. Rev., 91, 513-517, 1953.

27. W.J. Merz, "Domain formation and domain wall motions in ferroelectric $BaTiO_3$ single crystals" Phys. Rev., 95, 690–698, 1954.

28. Y. Su, G.J. Weng, "The shift of Curie temperature and evolution of ferroelectric domain in ferroelectric crystals", Journal of the Mechanics and Physics of Solids, 53, 2071–2099, 2005.

29. B.W. Lee, K.H. Auh, "Effect of grain size and mechanical processing on the dielectric properties of $BaTiO_3$", J. Mater. Res., 10[6], 1995

30. X. Wang, R. Chen, Z. Gui, L. Li, "The grain size effect on dielectric properties of $BaTiO_3$ based ceramics", Materials Science and Engineering, B99, 199-202 (2003)

31. T. Hoshina, K. Takizawa, J. li, T. Kasama, H. Kafemoto, T. Tsurumi, "Domain size effect on dielectric properties of Barium titanate ceramics", Japanese Journal of Applied Physics, 47[9], 7607-7611, 2008.

32. L. A. Xue and R. J. Brook, “Promotion of Densification by Grain Growth,” J. Am. Ceram. Soc., 72 [2], 341–44, 1989.
33. M. Drofenik, “Origin of the Grain Growth Anomaly in Donor-Doped Barium Titanate,” J. Am. Ceram. Soc., 76 [1], 123–28, 1993.
34. J. S. Choi and H. G. Kim, “Influence of Stoichiometry and Impurity on the Sintering Behaviour of Barium Titanate Ceramics,” J. Mater. Sci., 27, 1285– 90, 1992.
35. F. Chaput and J. Boillot, “Sintering and Dielectric Properties of Sol–Gel Ba/SrTitanate Ceramics,” Sci. Ceram., 14, 133–38, 1988.
36. T. R. Armstrong, K. A. Young, and R. C. Buchanan, “Dielectric Properties of Fluxed Barium Titanate Ceramics with Zirconia Additions,” J. Am. Ceram. Soc., 73, 700–705, 1990.
37. T. Ohno, D. Suzuki, H Suzuki, T. Ida, “Size Effect for Barium Titanate Nano-particles”, J. Soc. Powder Technology, Japan, 41[2], 86-91, 2004.
38. L. Mitoseriu, “The role of internal stress on the size-dependent ferro-para phase transition in $BaTi0_3$ ceramics”, FizicaSolidelor - FizicăTeoretică, 69-76, 1997-1998.